Parametric Contrast Enhanced Ultrasound Evaluation of Transarterial Chemoembolization

A Thesis

Submitted to the Faculty

Of

Drexel University

By

Minakshi Mohanty

in partial fulfillment of the

requirements for the

degree of

Master of Science in Biomedical Engineering

June 2015.

Dedications

To Dad, Mom, and Tuhin, for their endless love, support and encouragement

-Minakshi

Acknowledgements

This thesis would not have been possible without the help and guidance of many people. First and foremost, I am extremely thankful and fortunate to work under the guidance of Dr. Flemming Forsberg. I would be forever grateful to him for him unwavering support, optimism and encouragement throughout the duration of the thesis work.

I would like to thank Dr. Peter Lewin and Dr. Andres Kriete for being on my thesis committee, and for their valuable inputs. I heartily thank John Eisenbrey and Jaydev Dave for helping me in understanding different ways to processes ultrasound data. I would like to acknowledge the contributions of Dr. Colette Shaw and Dr. Dan Brown in selecting subjects eligible for study enrollment from their patient population and Priscilla Machado for scanning the patients and acquiring the data successfully. I would also like to thank A. Lyshchik, J. Weinstein, D.A. Merton and L. Pino. A special thanks to Maria Stanczak for helping me identify region of interest in the ultrasound scan data.

Last but not the least, I would like to thank my parents, my brothers, Tuhin and Ankan, and my friends Prasidhi, Supreet, Kartikeya, and Hansa for consistently motivating and cheering me.

Table of Contents

Appendices

List of Tables

List of Figures

List of Abbreviations

ANOVA: Analysis of Variance

AUC: Area under Curve

CEUS: Contrast Enhanced Ultrasound

CT: Computed Tomography

CPS: Cadence Pulse Sequencing

HCC: Hepatocellular Carcinoma

HIFU: High-intensity Focused Ultrasound

MAX: Maximum Signal Intensity

MIP: Maximum Intensity Projection

MRI: Magnetic Resonance Imaging

PER: Perfusion

RF: Radiofrequency

ROI: Region of Interest

SAD: Sum of Absolute Difference

TACE: Transarterial Chemoembolization

TTP: Time to Peak

UCA: Ultrasound Contrast Agent

Abstract

Parametric Contrast Enhanced Ultrasound Evaluation of Transarterial Chemoembolization

Minakshi Mohanty

Flemming Forsberg, PhD and Peter Lewin, PhD

This work investigates quantitative contrast enhanced ultrasound (CEUS) derived blood flow parameters for evaluating chemoembolization of hepatocellular carcinoma. Hepatocellular carcinoma (HCC) is the third leading cause of cancer mortality worldwide and is becoming increasingly common. Liver transplant is the only cure with 70 percent 5 year survival rate. However, transplant requires the tumor to fall under the Milan criteria (less than 5cm or up to 3 nodules each less than 1cm) and the technique is limited by the availability of donors. Transarterial chemoembolization (TACE), currently, is a treatment option for non-resectable tumors. It involves the administration of drug eluting beads via catheter into the branch of the hepatic artery that feeds the tumor. These beads occlude the blood supply to the tumor and at the same time release chemotherapy, leading to necrosis of the tumor and reduction in its size. Presently, the effectiveness of TACE procedure is determined one month post embolization through the use of contrast enhanced magnetic resonance imaging (MRI) or computed tomography (CT) scans, by evaluating blood flow within the tumor. Early screening for effective chemoembolization with contrast-enhanced MRI has been proven ineffective due to an inability to adequately visualize the vasculature. An earlier estimation of treatment efficacy would provide clinicians more time and options for re-treatment. Additionally, a number of patients may have morbidities including renal insufficiency. These patients may develop nephrogenic systemic fibrosis, which is the

necrosis of skin and the internal organs, on exposure to gadolinium (present in MRI contrast agents).

This project proposes the use of contrast enhanced ultrasound (CEUS) for monitoring the effectiveness of transarterial chemoembolization. Ultrasound contrast agents are gas filled microbubbles, which are encapsulated within a thin elastic shell made of lipids. They have a diameter of 1-10μm. Due to their restriction to the vasculature, an absence of contrast within the tumor is expected in cases where complete embolization has been achieved. Earlier studies have shown that lack of detected agents as little as 2 days post procedure correlated with effective procedure. However, currently there is no established standard as to how many days post treatment should the follow up be conducted, or which contrast agent to use.

Fourteen patients with 16 lesions scheduled for transarterial chemoembolization (TACE) of HCC using drug eluting beads provided informed consent to undergo CEUS exam prior to treatment, 2 weeks post treatment, and the morning of follow up (contrast enhanced MRI 1 month post TACE). Ultrasound was performed using a Sequoia 512 scanner with 4C1 probe (Siemens Medical Solutions, Mountain View, CA). CEUS data was acquired using Cadence Pulse Sequencing (Siemens) during bolus injection of 0.6-0.7 ml of Definity (Lantheus Medical Imaging, N. Billerica, MA). Motion compensation was performed and time intensity curves were generated on a pixel-by-pixel basis to create parametric images showing maximum signal intensity (MAX), time to peak intensity (TTP), perfusion (PER), and area under curve (AUC). These values were averaged over the tumor and expressed

normalized relative to baseline. Results were then grouped by clinical diagnosis (fully treated (n=5), partially treated (n=5) or no change (n=6)) and compared at each time point.

Parametric imaging was successfully performed on 10 lesions, while six were excluded due to inability to identify tumor. Significant difference was observed in the time to peak dataset 2 weeks post TACE between complete response and no response group (p=0.018). No significance was observed in maximum intensity, perfusion and area under curve dataset. In the time intensity parameters obtained 4 weeks post TACE, no significant difference was observed.

In conclusion, time to peak currently appears to be a good quantitative CEUS parameter for evaluating the effectiveness of TACE treatment 2 weeks post treatment.

1. INTRODUCTION

1.1 An Overview

Liver is a vital organ of the human body. It is located in the upper right quadrant of the abdomen, below the diaphragm [1]. The liver consists of four lobes and receives its blood supply from hepatic artery and portal vein. The hepatic artery supplies the liver with oxygenated blood from the heart and the portal vein brings in nutrient rich blood from the intestines [2]. Liver is made up of two kinds of cells: parenchymal cells and non-parenchymal cells. Parenchymal hepatocytes constitute about 75% of the liver volume. Non-parenchymal cells occupy about 6.5% of the liver volume [1].

The functions of the liver include:

- Breaking down and storage of nutrients absorbed form the intestines. Many nutrients need to be broken down into simpler forms by the liver before they can be used by the rest of the body.
- Liver secretes bile into the intestines that help in the absorption of nutrients.
- Detoxify or excrete drugs such as penicillin, ampicillin and erythromycin.
- Forms blood substances, fibrinogen, prothrombin, accelerator globulin, factor VII, used in coagulation.
- Storage site for vitamin A, d and B_{12} and iron in the form of ferritin [3].

Hepatocelluar carcinoma is the most common form of liver cancer. It begins in the liver cells, called hepatocytes. In about 70-90% of cases, hepatocellular carcinoma develops as a result of chronic liver disease [4]. These may include infection from Hepatitis B or

Hepatitis C virus, cirrhosis of the liver and excessive alcoholism. It is the third leading cause of cancer mortality worldwide. The survival rate one year after diagnosis is less than 50% [5]. Liver transplantation is the only cure for HCC with 70% 5 year survival rate [6]. Liver transplant is possible only for tumors that fall under the Milan criteria (1 lesion less 5cm or up to 3 nodules less than 3cm) [7]. Liver transplantation is limited by the availability of donors [8]. About 30% of referred patients are eligible for surgical resection. The 5 year recurrence rates for this group is higher than 50% [9].

In patients with non-resectable tumors, chemoembolization has shown to be an effective measure to reduce tumor progression. In the process, anti-cancer drugs are administered directly to the tumor via catheter and the blood supply to the tumor is subsequently obstructed using embolization materials such as gelfoam [10]. Drug eluding beads are being used by many clinicians to provide gradual and sustained delivery of chemotherapeutic after embolization. Currently, the effectiveness of this procedure is determined, by evaluating the blood flow within the tumor, one month post treatment through the use of contrast enhanced MRI scans. An earlier method to evaluate the efficacy of the treatment would provide increased treatment options, in turn better patient outcomes. Additionally, a number of patients who have morbidities including renal insufficiency,

This study proposes the use of contrast enhanced ultrasound as a follow up method to evaluate the efficacy of TACE treatment at an earlier timeframe. Ultrasound contrast agents are gas filled microbubbles that are encapsulated by a lipid shell to provide stability. The diameter of these bubbles lie in the range of 1-10 μm [11]. Because of their small size, they are capable of passing through the pulmonary capillaries, and at the same time be restricted to the vascular system [11]. These microbubbles have been approved for the purpose of

echocardiography in the United States and also for the characterization of liver lesions throughout Europe and Asia [12].

1.2 Thesis Objective

Primary Aim: *To investigate quantitative contrast enhanced ultrasound (CEUS) derived blood flow parameters for evaluating chemoembolization of hepatocellular carcinoma (HCC).*

Transarterial chemoembolization procedure aims at blocking the tumor vascularity, and providing gradual and steady dose of chemotherapy to induce tumor necrosis. The efficacy of this procedure is monitored using contrast enhanced MRI scan 4 weeks post TACE. The aim of this study is investigate if CEUS derived blood flow parameters can be used as a follow up method to evaluated TACE, instead of MRI. Parametric images are generated to show maximum intensity, time to peak, perfusion and area under curve for each pixel in the image throughout the time sequence. These parameters are analyzed to determine if they correlate with effective chemoembolization.

2. BACKGROUND AND LITERATURE REVIEW

This chapter presents the background information and literature review related to liver anatomy, hepatocellular carcinoma, its treatment using transarterial chemoembolization and the follow up procedure. This chapter also discusses the potential use of contrast enhanced ultrasound to predict the efficacy of the treatment and compare it to the current clinical imaging choices.

2.1 Liver Anatomy

The liver is the second largest organ in the human body [2]. It is located in the upper right quadrant of the abdomen, below the diaphragm [1]. It is a solid organ weighing about 1.5 kg [13]. The liver consists of four lobes, left, right, caudate and quadrate lobe [3]. The liver has dual blood supply. It receives about 25% of the total blood supply from the hepatic artery and the rest 75% from the portal vein. The hepatic artery supplies oxygenated blood directly from the systemic arterial system whereas, the portal vein provides partially deoxygenated blood via the bowel, spleen and other viscera [3].

The liver performs different types of functions. These include metabolism of carbohydrates, fats and proteins, maintaining blood glucose level, filtering out toxins and regulating hormonal balance. The liver acts as a storage site for vitamins A, B_{12}, and D. It stores iron in the form of ferritin. The liver forms the blood substances used in coagulation [3].

2.2 Hepatocellular Carcinoma

Hepatocellular carcinoma is the most common type of liver cancer. It develops in the liver cells called hepatocytes. HCC is the third leading cause of cancer mortality worldwide [5]. American Cancer Society estimates 35,660 new cases of liver cancer in USA in 2015, three-fourths of which will be HCC [1].The primary risk factors of HCC are Hepatitis B virus, Hepatitis C virus and cirrhosis of the liver. The underlying cause of HCC cases differs from one geographical location to another. Eastern Asia and sub- Saharan Africa have the most cases of hepatocellular carcinoma, where the leading risk factor is chronic infection with hepatitis B virus, along with exposure to aflatoxin B [7]. In North America, Europe and Japan, the dominant risk factor is hepatitis C virus, together with alcoholism [7].

The symptoms of HCC include jaundice, fatigue, upper abdominal pain, nausea, and vomiting, unintentional weight loss, loss of appetite and abdominal swelling [15].

2.3 Treatment Methods

Treatment of HCC depends on the stage of the disease, along with the patient's age, and overall health. The Barcelona Clinic Liver Cancer (BCLC), the four stages of the disease are:

- Early stage (A): It is also known as the Milan criteria. Asymptomatic single tumor 5cm or 3 nodules, each less than or equal to 3cm

- Intermediate stage (B): these include patients with tumors that exceed early criteria but do not show cancer related symptoms, vascular invasion or metastases.
- Advanced stage (C): patients with mild cancer-related symptoms, vascular invasion or extrahepatic spread.
- End- stage (D): patients with advanced, symptomatic disease [16].

The treatment methods include surgical resection, liver transplantation, and image-guided tumor ablation.

2.3.1 Surgical Resection

Surgical resection involves removal of all or a part of the liver. This procedure is mostly restricted to patients with solitary HCC without vascular invasion or extra hepatic spread. It is more favorable for patients without cirrhosis, as they are capable of tolerable major resections with low rates of complications [7]. A tumor diameter of ≤ 5cm is used as a cut off limit for surgical resection. Larger tumors will have more nodules, making incomplete resection or early recurrence of disease more likely [17]. High serum bilirubin level and significant portal hypertension (≥ 10 mm Hg) is an indication of hepatic decompensation [17]. Therefore, only patients with normal bilirubin level and no portal hypertension should be considered for resection, as they will not present relevant functional impairment. Only 30% of the referred patients are eligible for surgical resection and this group is still plagued by 5 year recurrence rates higher than 70% [9].

2.3.2 Liver Transplantation

Theoretically, a liver transplantation can cure both the cancer as well as the underlying cirrhosis simultaneously. The success of the treatment will not depend on the extent of liver function impairment [7]. Patients with cirrhosis are selected for liver transplant based on the Milan criteria. The Milan criteria includes HCC of 5cm or less, or up to three nodules of 3cm of less, without vascular invasion or extra hepatic spread [7]. A study conducted by Mazzaferro and colleagues showed that patient who met the Milan criteria had a 4-year survival of 75% with a recurrence rate of less than 15% [7]. These results were feasible in an era with quick availability of donor organs. The shortage of donor imposes a delay in the treatment, during which the tumor may progress, reducing the effectiveness of a liver transplant. If the waiting period exceeds six months, treatments such as ablation, or chemoembolization may be performed to delay tumor progression. Transplantation policies may vary from country to country, but generally are implemented to give priority to the sickest patients. Live donations have shown similar results to that of cadaveric donations, but its application is limited due to societal constraints and thus, a scarcity of appropriate donors [7].

2.3.3 Image guided tumor ablation

Image guided tumor ablation is a treatment option for patient with early stage (stage A) HCC. Ablation is the process of inducing tumor necrosis using chemicals, such as ethanol,

acetic acid, or by modifying the temperature using radiofrequency, microwave, laser, high-intensity focused ultrasound or cryoablation [7, 18].

The principle of radiofrequency ablation involves conversion of electromagnetic energy into heat. The equipment used consists of a generator that converts energy produced by alternating current of 90Hz in to radiofrequency band of 500 kHz [19]. The current is linked to an active electrode in the form of a needle that is inserted into the tumor. The current is dispersed with a passive electrode in the form of a plate, placed on the skin of the patient. The tissue surrounding the needle opposes the flow of current. This resistance generates heat causing tumor tissue necrosis [19].

In case of tumor size less than 2cm, both radiofrequency ablation and ethanol injection achieve almost complete necrosis. However, the efficacy of treatment with ethanol injection decreases in large tumors. Radiofrequency ablation may still be effective in larger tumors. Ablation is not recommended if the tumor size exceeds 5cm [7].

High-intensity focused ultrasound (HIFU) is also an ablation technique for treatment of liver cancers. The primary therapeutic mechanism of this technique is the deposition of thermal energy by a focused ultrasound beam. A high power transducer generates the ultrasound beam. The transducer employed is phased array and bowl- shaped. This helps achieve focalization of the ultrasound beam. The HIFU beam is focused onto the tissue that needs to be ablated. The beam passes through the skin and other soft tissues without causing any damage. But, the tissue present in the focal region of the HIFU beam absorbs significantly more acoustic energy, in comparison to its surrounding area. This results in an increase in temperature which causes localized coagulation necrosis. The adjacent areas remain unharmed in this procedure. Image guidance is provided by magnetic resonance

imaging. Thus this technique is referred to as magnetic resonance guided high-intensity focused ultrasound (MR-HIFU). Unlike ablation using RF, MR- HIFU does not require insertion of probe into the body. Thus, it is a completely non-invasive technique. MR-HIFU also does not rely much on thermal conduction, as the entire ablation volume is directly heated by the deposited ultrasound energy [18].

2.3.4 Transarterial Chemoembolization

Transarterial chemoembolization (TACE) is typically used to treat patients with non-resectable tumors. A normal liver has dual blood supply, 75% by the portal vein and 25% by the hepatic artery. Liver tumors are predominantly supplied by hepatic artery. This feature makes it possible to deliver localized treatment to tumors and at the same time limit the toxicity to uninvolved adjacent parenchyma [20]. Chemoembolization involves the direct infusion of anti-cancer drugs followed by occlusion of tumor vasculature using an embolization material [10]. In this process the tumor vasculature is accessed using a catheter through the hepatic artery. A catheter is inserted into the femoral artery and advanced until it reaches the common hepatic artery. Once the catheter is accurately positioned, the tumor is visualized by performing an angiogram. Beads containing chemotherapy drug are injected into the catheter and released inside the feeder vessel. These beads block the blood supply to the tumor and also begin a controlled release of chemotherapy causing shrinkage and necrosis of the tumor. It has been shown that patients with stage 3 or stage 4 HCC can be down staged using chemoembolization to a point where chemoembolization can take place [21]. TACE has shown to be an effective measure not just to slow down tumor progression but also improve patient response with less toxicity

[22, 23]. LC beads (Biocompatibles UK Ltd) consists of poly-vinyl alcohol hydrogel with modified sulfonate groups for attachment of anthracycline drugs (doxorubicin). Embolization using LC beads result in obstruction of the tumor vasculature as well as gradual, sustained and intratumoral release of chemotherapy [24].

Currently, the effectiveness of the TACE procedure is decided four weeks post embolization by evaluating blood flow inside the tumor using contrast- enhanced MRI [25]. Contrast enhanced MRI has been established as the clinical standard imaging modality in these patients. Early screening of the tumor to predict the efficacy of the treatment has been proven ineffective, due to an inability to visualize the vasculature [26]. Additionally, a number of patients have morbidities including renal insufficiency. These patients may develop nephrogenic systemic fibrosis, which is the necrosis of skin and the internal organs, on exposure to gadolinium (present in MRI contrast agents).

Thus, an alternative technique that does not use metallic contrast and can also access the effectiveness of the treatment in less than one month would greatly benefit this patient population. The use of contrast enhanced ultrasound for the purpose of evaluation of TACE effectiveness is proposed in this study.

2.4 Ultrasound contrast agents

Ultrasound contrast agents are made up of high molecular weight gas-filled microbubbles. They have a diameter of 1-10μm. They are encapsulated within a thin elastic shell which is made up by lipid, fatty acid, protein, or polymers helps to maintain the stability of the microbubbles in the human body. Due to their small size, they can mimic the red blood cells and enter the capillary network [11]. Ultrasound contrast agents can be injected

intravenously as a bolus or as a constant infusion by using a pump. These contrast agents have approximately 17,000-fold more compressibility than water, and hence they can strongly scatter ultrasound waves. An improvement of about 15-25 dB can be achieved in the signal-to-noise (SNR) ratio of the ultrasound image, thus increasing the sensitivity of this imaging mode [27, 28].

A microbubble undergoes alternate phases of compression and rarefaction when insonified by an ultrasound wave. This brings about a change in the size of the microbubble. In the positive half of the cycle, the size of the microbubble decreases and in the negative half, it increases. This behavior of microbubbles depends on the frequency of the incident ultrasound wave and the acoustic pressure amplitude [29]. The compression and expansion of the microbubbles are however not exactly equal. This results in asymmetrical and nonlinear bubble oscillations [30].

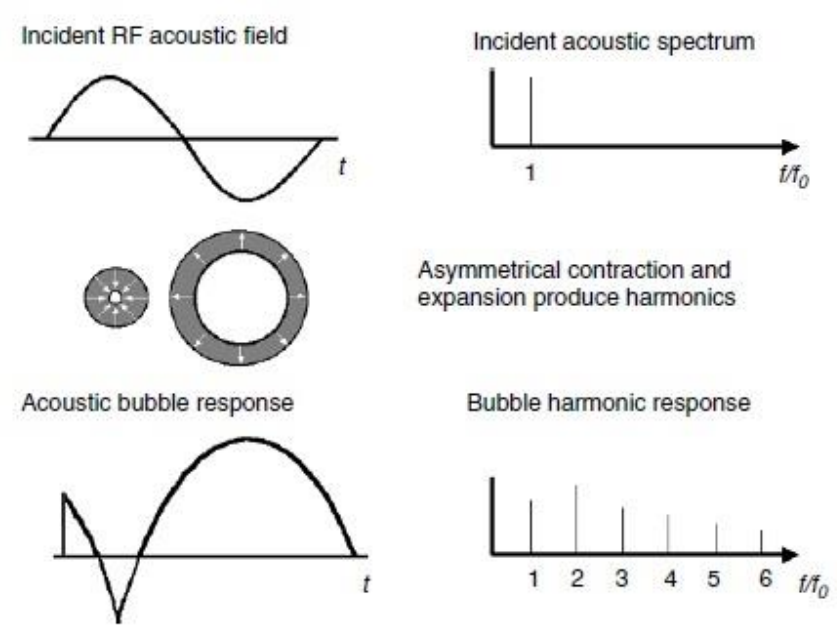

Figure 2.1: Acoustic nonlinear response of contrast agent microbubbles. Reproduced from [31]

There are a number of ultrasound contrast agents that are available in the market. Table 2.1 summarizes a list of ultrasound contrast agents, their composition and their availability.

Table 2.1: List of Commercially Available Ultrasound Contrast Agents. Reproduced from [32]

Name	**Manufacturer**	**Year**	**Gas**	Co**ating**	**Availability**
Echovist	Schering AG	1991	Air	Galactose	Off market
Albunex	Molecular Biosystems	1994	Air	Human Albumin	Off market
Levovist	Bayer Shering Pharma AG	1996	Air	Galactose	Off market
Optison	GE Healthcare	1997	C_3F_8	Human Albumin	EU, USA

Definity	Lantheus Medical Imaging	2001	C_3F_8	Phospholipids	Worldwide
Sono-Vue or Lumason	Bracco SpA	2011	SF_6	Phospholipids	Europe, South Korea, China, India, Hong Kong, Singapore, USA
Imagent	Alliance Pharmaceutical	2002	C_6F_{14}	Phospholipids	Off market
Sonazoid	GE Healthcare	2006	C_4F_{10}		Japan, South Korea, Norway and China

As discussed in section 1.2, the aim of the study is not only to evaluate if CEUS of HCC at one to two weeks and one month post TACE, correlate with the clinical evaluation standard of a contrast-enhanced MRI at one month, but also, to establish whether changes in blood flow parameters relative to baseline correlate with effective embolization. For the purpose of this evaluation, the CEUS data is subjected to motion compensation. Motion

compensation is based on Maximum Intensity Projection (MIP) algorithm which is discussed in section 2.5.

2.5 Maximum Intensity Projection (MIP) Algorithm

MIP algorithm is a reconstruction technique that performs one-to-one mapping of the pixels with maximum intensity from corresponding locations in all frames onto the final reconstructed image [33]. Figure 2.2 shows a schematic of MIP algorithm to produce MIP images. In the figure, the three dimensional structure can be considered as the object to be scanned. During scanning, the contrast agent flows through the two blood vessels in the object. The direction of flow is indicated by white dash lines. The scan data contain frames from the 1^{st} to the n^{th} frame. To produce the final image, show at the bottom of figure, the MIP algorithm uses the following equation.

$$Final\ image\ (i\ ,\ j) = max(Frame_1(i, j), Frame_2(i, j), \ldots\ldots Frame_n(i, j))\ ;\ \vee(i=1{:}a, j=1{:}b) \quad (2.1)$$

Where,

a: number of rows in each frame

b: number of columns in each frame

(i, j): pixel location

N: total number of frames [34]

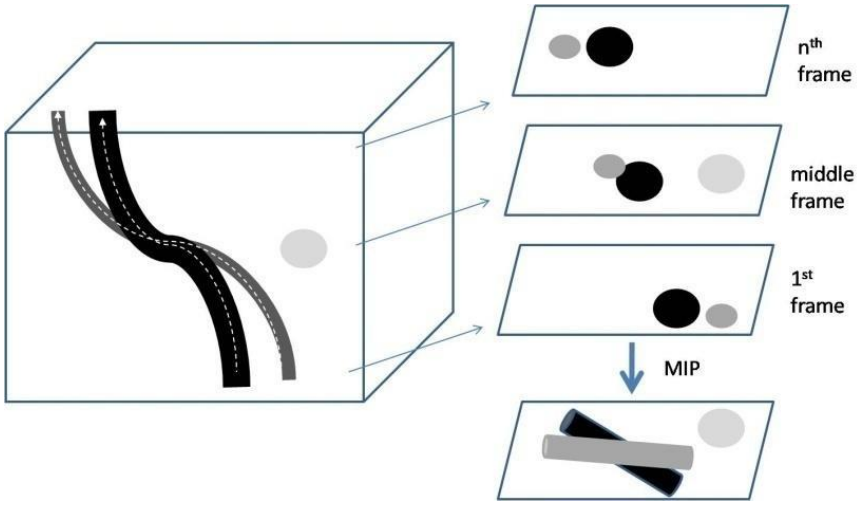

Figure 2.2: Schematic of MIP to produce MIP images. Reproduced from [34]

Post motion compensation, the CEUS data is subjected to parametric imaging, where the time-intensity curve parameters are extracted. Section 2.6 discusses time-intensity curve and parameters in details.

2.6 Time – Intensity curve

The time intensity curve is a plot of signal intensity over time after the administration of contrast agent. Arrival time (AT) is the first point of the curve clearly above the baseline intensity, which is followed by further rise in the intensity. Time to peak (TTP) is the time from the contrast agent injection to the point at which maximum intensity is reached for each individual pixel. Perfusion (PER) is defined as the slope of the rise of the curve from 10% to 30% of the maximum. This not an accurate representation of the perfusion on pixel level due to the presence of noise. A modified definition of perfusion is defined as the slope of the curve from the time of contrast arrival to the peak intensity. Area under curve (AUC)

is defined as the area under the time – intensity curve from contrast arrival to peak intensity [35].

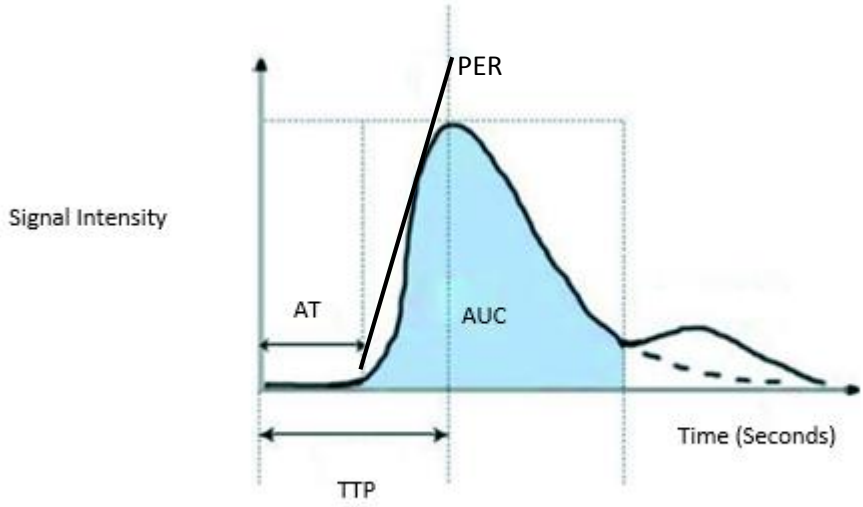

Figure 2.3: Time-intensity curve and the parameters Arrival time (AT), time to peak (TTP), perfusion (PER) and area under curve (AUC). Reproduced from [35]

3. MATERIALS AND METHOD

Fourteen patients with 16 lesions scheduled for transarterial chemoembolization (TACE) of hepatocellular carcinoma using drug eluding beads signed informed consent to undergo contrast enhanced ultrasound (CEUS) exam prior to treatment, 2 weeks post treatment and one month post treatment (on the day of contrast enhanced MRI). The ultrasound exam was performed using a Sequoia 512 scanner with 4C1 probe (Siemens Medical Solutions, Mountain View, CA). CEUS data was acquired using Cadence Pulse Sequencing (Siemens) during bolus injection of 0.6-0.7ml of Definity (Lantheus Medical Imaging, N. Billerica, MA). Motion compensation and parametric imaging was performed on the CEUS data. Time –intensity curves were generated on a pixel-by-pixel basis to create parametric images that show maximum signal intensity (MIP), time to peak intensity (TTP), perfusion (PER) and area under curve (AUC). Results were grouped based on MRI findings and were compared using ANOVAs.

3.1 Materials

3.1.1 Ultrasound Contrast Agent

The ultrasound contrast agent Definity (Lantheus Medical Imaging, N Billerica, MA) was used for all imaging procedures throughout the study. Definity is a sterile non-pyrogenic suspension of liposome-encaspsulated perfluoropropane microbubbles [28, 36]. The contrast is composed of three phospholipids contained in a matrix of sodium chloride, propylene glycol and glycerine in water. Definity is supplied in a vial that contains

phospholipids and perfluoropropane gas. Table 3.1 gives a summary of the microsphere size distribution.

Table 3.1: Microsphere size distribution [37]

	Microsphere particle size parameters
Mean diameter range	1.1 µm – 3.3 µm (*in vitro* measurement)
Percent less than 10 µm	98%
Maximum diameter	20 µm

The contrast agent is available as a single use in 2ml glass vial containing clear liquid. It is activated by allowing it to warm up to room temperature and then by shaking the vial with the aid of shaking device (Vialmix : ESPE, Seefeld, Germany). This provides an opaque, homogeneous, milky suspension of liquid microspheres (1.2×10^{10} microspheres/ml and 150µl octofluoropropane/ml) that can be injected intravenously [37]. Definity is FDA-approved in the United States of America for use with echocardiography.

3.1.2 Imaging Equipment

Ultrasound scans were performed using Sequoia 512 scanner with a 4C1 probe. (Siemens Medical Solutions, Mountain View, CA). The 4C1 transducer has a frequency bandwidth of 1-4MHz [38]. CEUS data was acquired using Cadence™ Pulse Sequencing (Siemens). It is a low-power multipulse technique where three pulses with varied phase and amplitude are transmitted and the resulting echoes are summed. CPS imaging results in considerable

tissue suppression, allowing for better detection of the contrast microbubbles. CPS should be used at low mechanical index in order to prevent bubble destruction [39].

3.2 Data Acquisition from Patients

14 patients with 16 lesions participated in the study. The participants signed a written consent and were approved to take part in the study by the Thomas Jefferson University Hospital's Institutional Review Board. The enrolled patients were scheduled for transarterial chemoembolization with drug eluding beads for the treatment of hepatocellular carcinoma. These patients first received a CEUS exam prior to treatment. Post treatment, CEUS exams were conducted 2 weeks post TACE and one month post TACE during MRI follow up. During each exam, grayscale B-mode, power Doppler and CEUS of the tumor were performed. At first, a standard ultrasound examination (without contrast) was performed to locate the liver mass and obtain information regarding its shape, shape and ultrasound characteristics. On completion of the standard exam, the patient received a bolus injection of 0.6-0.7ml of Definity through an IV catheter (typically in the antecubital vein), followed with a slow flush of 10ml of normal saline. CEUS exam was performed for 1 minute following the injection of Definity. The scan data contains the grayscale image on the right hand side and the contrast enhanced image on the left side, as shown in figure below. The HCC is marked using a red circle in figures 3.1, 3.2 and 3.3.

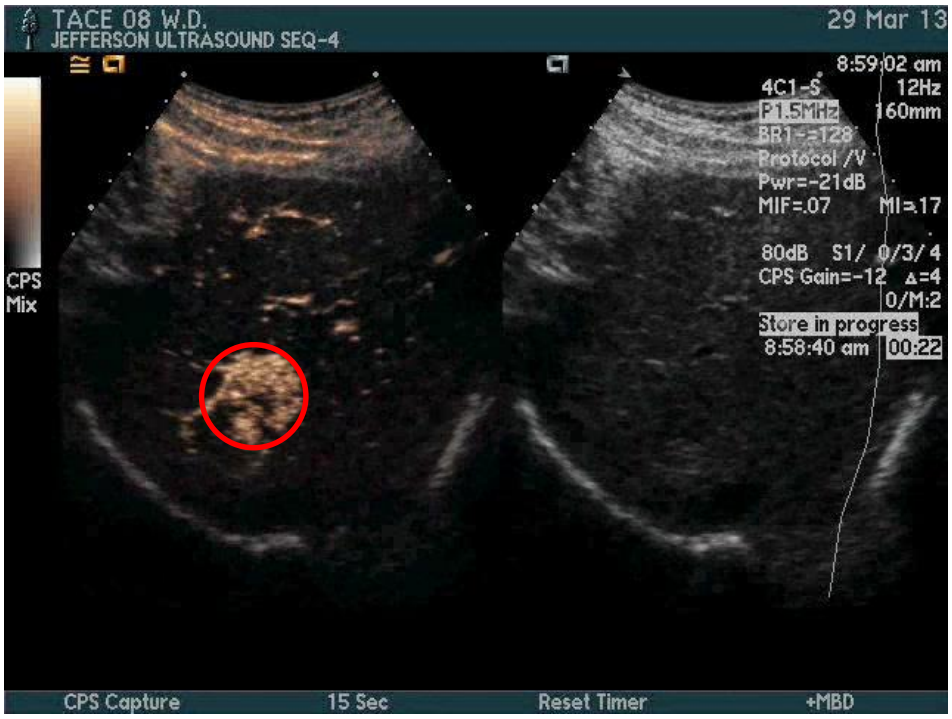

Figure 3.1: CEUS scan data of a patient prior to TACE procedure.

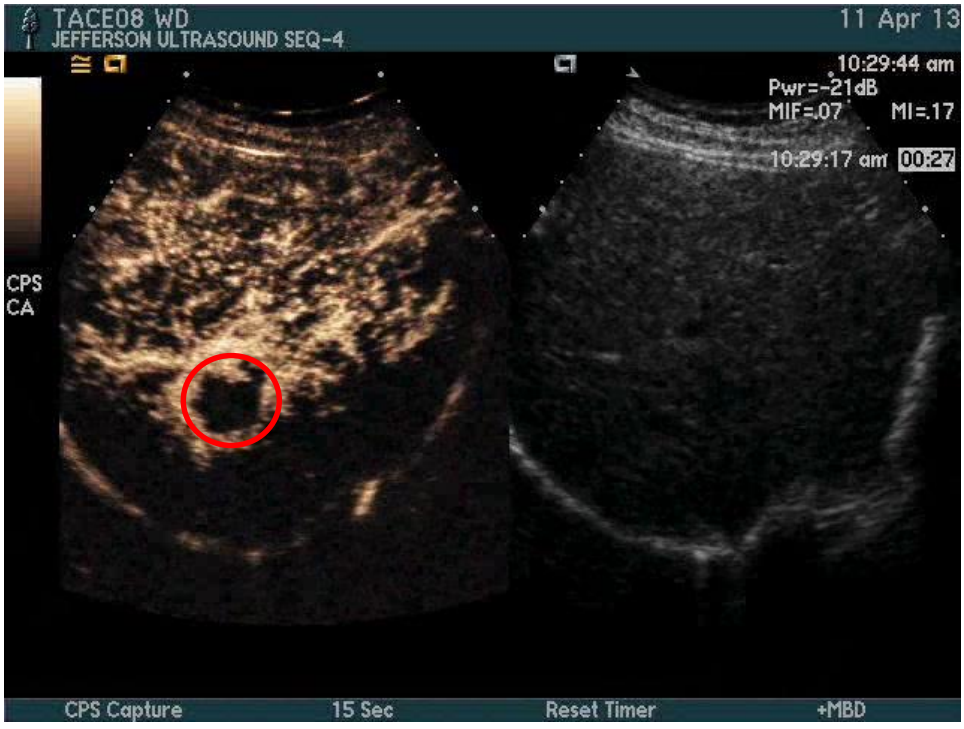

Figure 3.2: CEUS scan data of a patient 2 weeks post TACE procedure.

Figure 3.3: CEUS scan data of a patient 4 weeks post TACE procedure.

3.3 CEUS Data Analysis

The offline processing of the CEUS data was performed using MATLAB (Version R2013a, Mathworks Inc.) license obtained via Drexel University. The CEUS data processing may be divided into two parts:

1. Motion Compensation
2. Parametric Imaging

3.3.1 Motion Compensation

The CEUS scans performed on the patients suffer from motion artifacts due to respiration, movement of the patient as well as the transducer. Performing motion compensation on the data will not only reduce motion artifacts, but also aid in better visualization of the tumor. Maximum intensity projection algorithm was used to develop an automated technique for motion compensation. For implementation of the motion compensation, an algorithm was developed in MATLAB (R2013a, The Mathworks Inc., Natick, MA) in the ultrasound research laboratory of Thomas Jefferson University Hospital by Dr. Jaydev K. Dave and his team. The working of this algorithm is described in the following sections.

3.3.1.1 Creating a database of individual frames

The scan data is available in Windows media audio/video (.wmv) file format. The data is first organized into a suitable format in order to process it. This is done by splitting the video data into individual JPEG (.jpg) frames (US scanner sampling rate = 9Hz, 10Hz, 11Hz, 12Hz, 14Hz) using a free Video to JPG Converter v.5.0.23 build 320, an open source software developed by DVDVideoSoft Ltd. Certain frames were eliminated from the processing. These include the scout frames. Scout frames are the initial frames acquired by US technologist while trying to locate the liver mass. These frames may not be present in the later part of the scan. Thus, if a kernel is selected in any of these frames, there would be no region that corresponds to the kernel in the successive frames.

During an ultrasound scan, the sonographer may move the transducer back and forth to obtain a better visualization of the structures in the scanned area. This fluctuation in

position of the transducer may cause frames from different scan angles and position to be present in the scan data. Such frames, if used, to generate final image may lead to misdiagnosis. These frames are identified and removed from the final dataset [34]. The final set of frames are numbered starting from 0, for processing convenience using Advanced Renamer Version 3.66 an open source software developed by Kim Jensen (Denmark).

3.3.1.2 Kernel Selection

To select the kernel, the first frame from the in-flow of contrast agent is presented to the user. The kernel is a group of pixel that is analyzed as a single unit. It would be used to track the motion that may produce misalignment in the final image. The kernel selected should not coincide with the image borders. It should neither be too large nor too small. Very small kernels may result in multiple matches, whereas, very large kernels may affect the activity of the motion compensation in consecutive frames [34]. Figure 3.4 shows selection of the kernel from the first frame in the contrast inflow period.

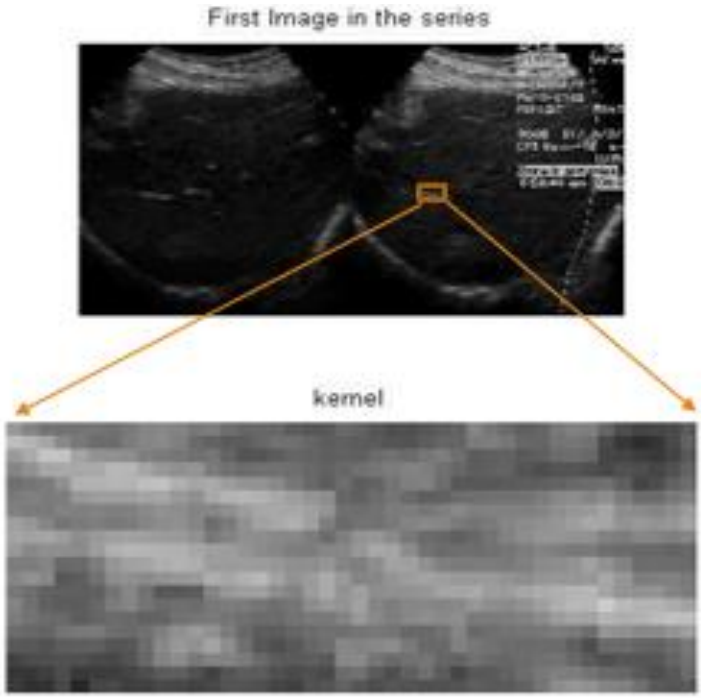

Figure 3.4: Selection of kernel from the first frame in the contrast inflow period.

3.3.1.3 Calculating the number of iterative steps for each frame

The algorithm computes the number of iterative steps. It is based on the size of the selected kernel, size of individual frames and the overlap percentage, "p", specified by the user. Consider an image with "m" pixel columns and "n" pixel rows. Let "a" and "b", respectively, be the rows and columns of the selected kernel. After completing an iteration, the kernel would have moved through "x" pixel columns or "y" pixel rows to its new location corresponding to next iteration. Based on the overlap percentage 'p', the total number of iterations (N) is given by:

$$N=\frac{1}{1-\frac{p}{100}} * \left(\frac{mn}{ab}\right) \quad \text{..... (3.1)}$$

Since ‘”p” represents the percentage of overlap of the kernel in between iterations, a 100% overlap value indicates no motion of the kernel from its previous iteration to the new position for the next iteration [34].

3.3.1.4 Scanning successive frames

In each successive frame, the algorithm scans from left to right and top to bottom to identify the best match for the selected kernel. Sum of absolute difference (SAD) is used to calculate the best match for the kernel. For a kernel with “m” rows and “n” columns, SAD is calculated by equation

$$\text{SAD} = \sum_{i=1}^{m} \sum_{j=1}^{n} | krn(i,j) - img(i,j) | \quad \text{(3.2)}$$

where, *krn (i, j)* and *img (i, j)* are respectively the pixel values of the kernel and the portion of image being scanned during a particular iteration, at location *(i, j)*. SAD values are computed for every iteration in each frame and stored in an array. The minimum value of the SAD values corresponds to the best match to the selected kernel. The coordinates of the best match in the particular frame is selected and the process is repeated for all the frames [34].

3.3.1.5 Calculating the displacement to evaluate the motion in successive frames with respect to the first frame

The co-ordinates of the best match obtained are compared to the original kernel co-ordinates. The displacement is calculated using equation

$$D = \sqrt{(y2 - y1)^2 + (x2 - x1)^2}$$

Where,

(x1, y1) = co-ordinates of the kernel in the first frame

(x2, y2) = co-ordinates of the best match to the kernel

The displacement as well as the co-ordinates of the best match are saved for further processing [34].

3.3.1.6 Decision-making criteria

This step is to identify the noisy frames and eliminate them from further processing. This is achieved by calculating the reliability parameter (RP) for every frame.

$$RP = \frac{|E[SAD] - SAD_i|}{E[SAD]} \quad \text{..... (3.3)}$$

Where E[SAD] is the mean of all SAD values and "*i*" denotes the SAD value of the i^{th} frame. In certain frames, the region of interest that was supposed the match the kernel may extend beyond the image boundaries as seen in Figure 3.5.

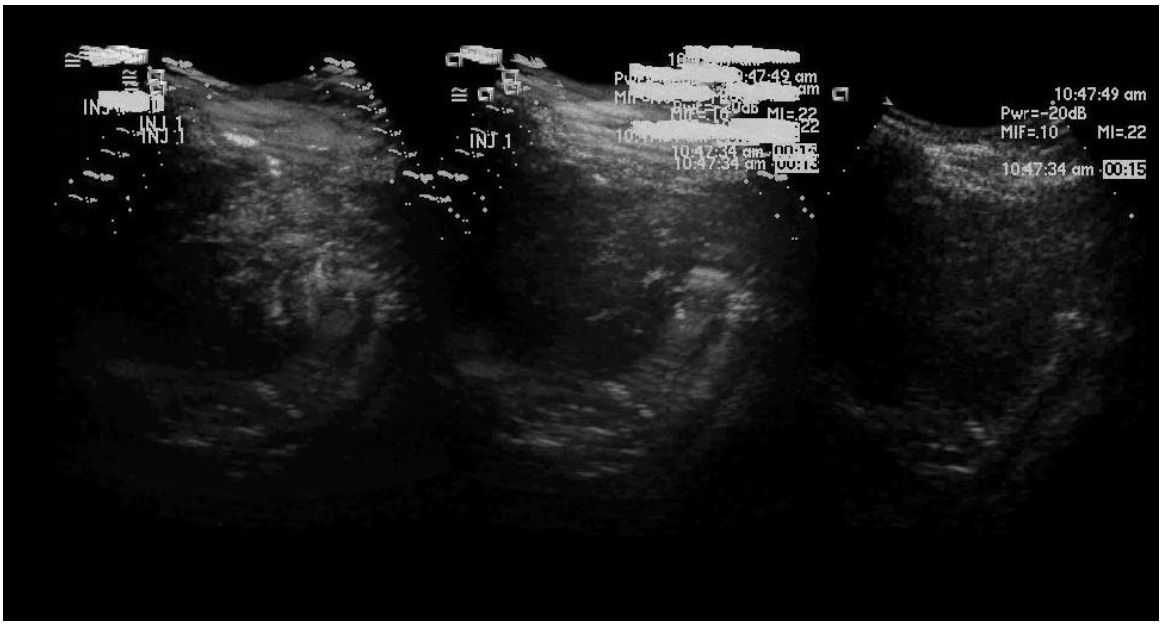

Figure 3.5: Example showing kernel match extending beyond image borders.

The RP, in such cases, is a useful parameter to identify as well as eliminate these frames. Higher RP values would indicate good match (low SAD values) and vice versa [34].

A threshold RP value is set for each case that helps decide whether to accept or reject the frame under consideration. Figure 3.6 shows box plot of RP values of the 16 CEUS scans.

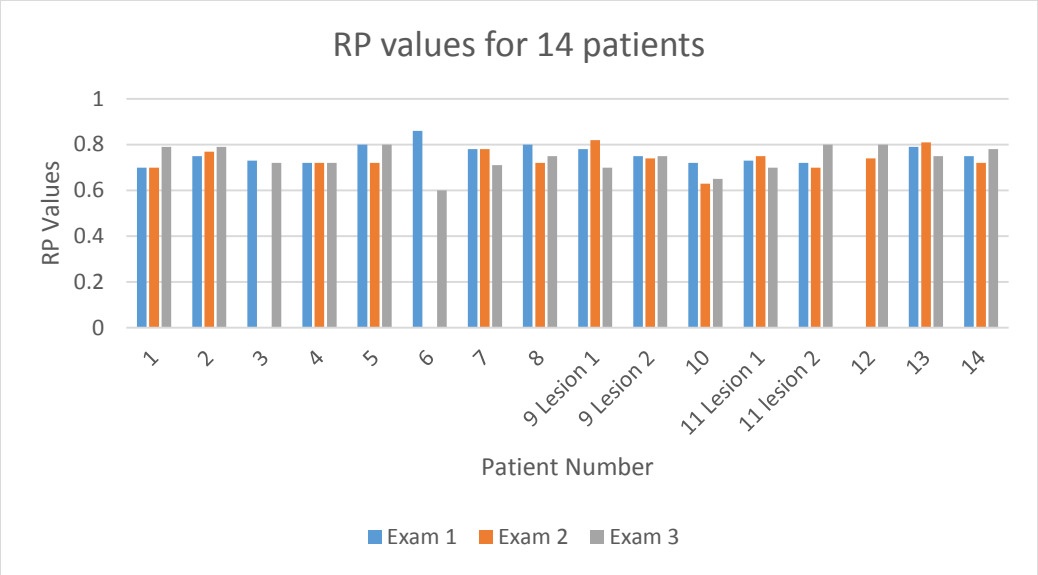

Figure 3.6: Reliability Parameters for 14 Patients

3.3.1.7 Final image reconstruction

The frames that have RP values greater than the threshold are selected and retained for the image construction process. Starting from the second frame, each successive frame is aligned with respect to the first frame. The alignment is based on the displacement calculated by the algorithm in section 3.3.1.5. The stored co-ordinates of the kernel matches in each frame is compared with the kernel co-ordinates in the first frame, and is then superimposed onto the first frame. The final image is then displayed after processing all the selected frames [34]. Figure shows the complete flowchart of the motion compensation algorithm.

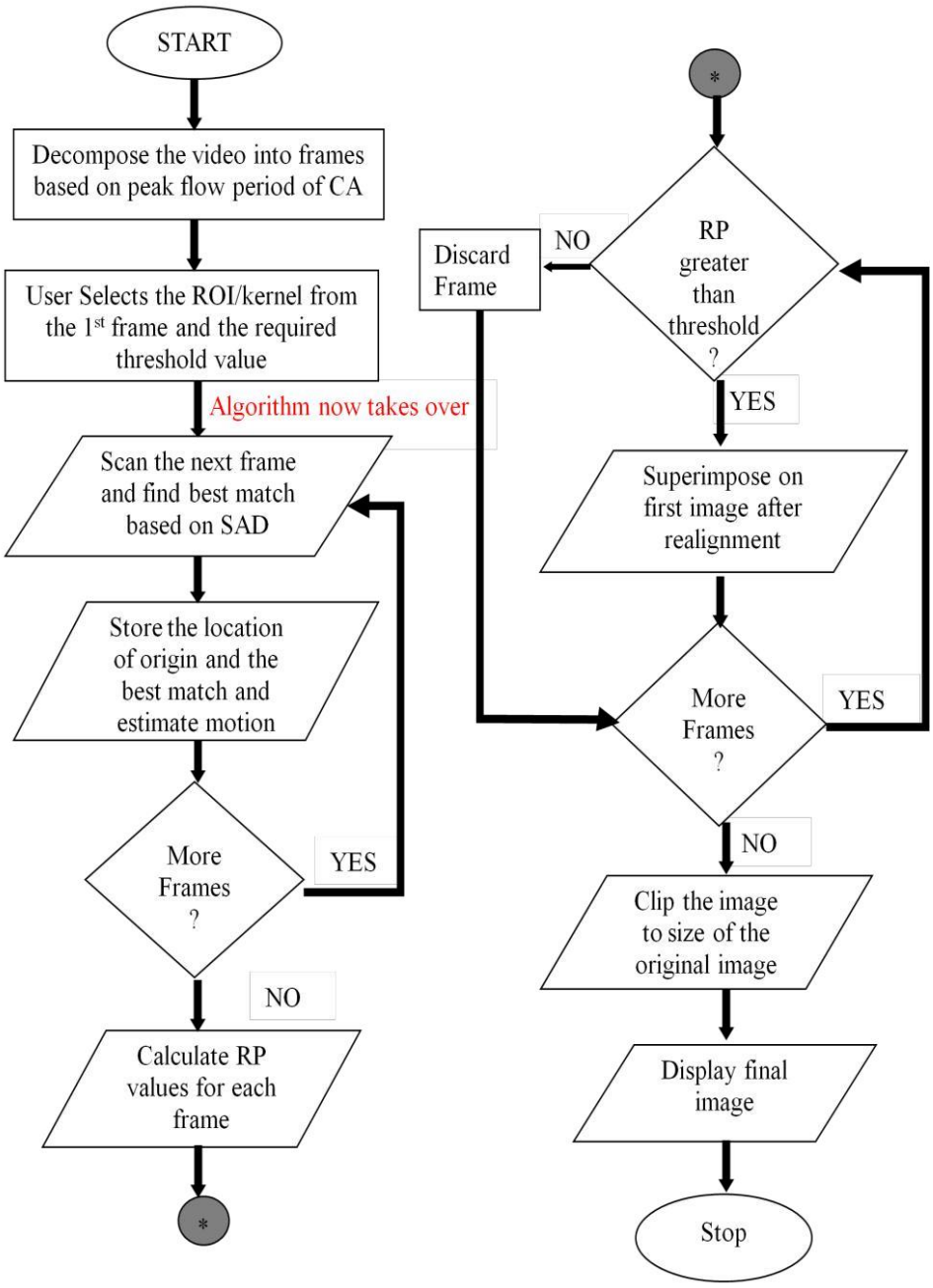

Figure 3.7: Motion Compensation Algorithm Flowchart. Reproduced from [34]

Figures 3.8, 3.9 and 3.10 show the final motion compensated image. The red circle indicates the tumor location.

Figure 3.8: Final reconstructed image (Prior to TACE)

Figure 3.9: Final reconstructed image (2 weeks post TACE)

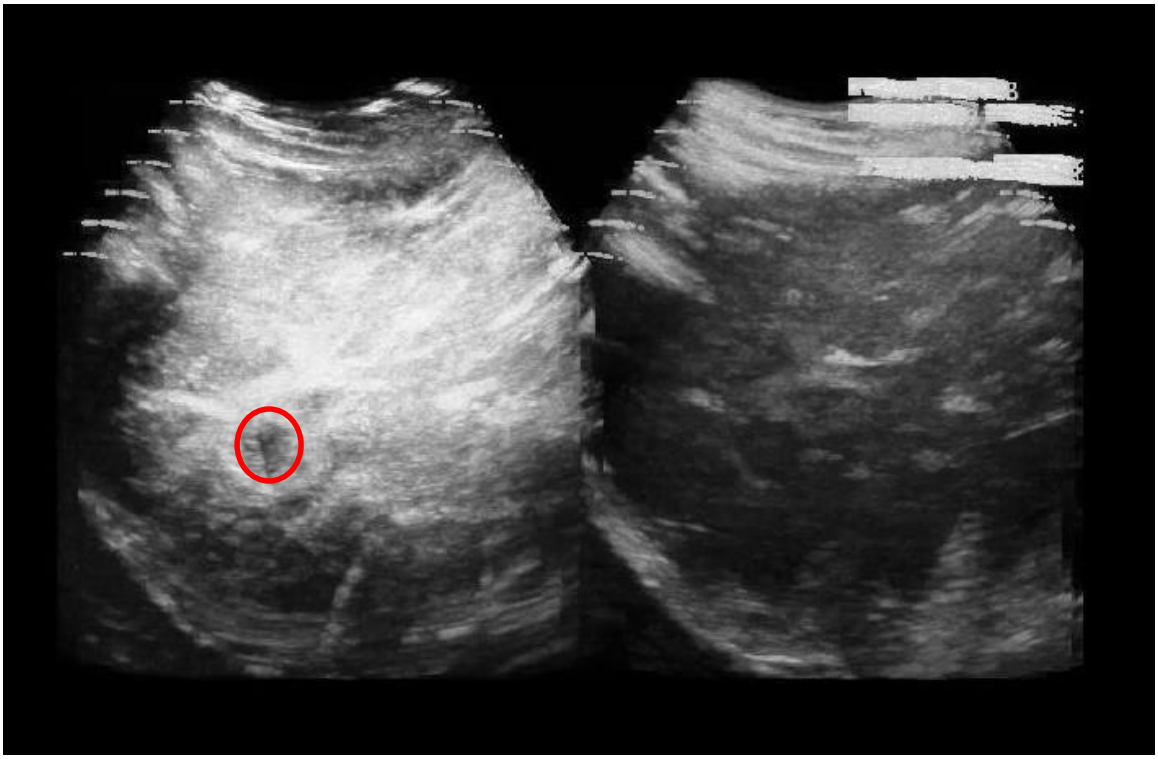

Figure 3.10: Final reconstructed image (4 weeks post TACE)

The image sequence produced during motion compensation were saved and numbered according to their original frame number. This helps to keep record of the images that were discarded due to presence of excessive noise.

3.3.2 Parametric Imaging

Parametric imaging was performed on the motion compensated sequences of each lesion. Time intensity curves were generated on a pixel-by-pixel basis to create parametric images showing maximum signal intensity (MAX), time to peak (TTP), Perfusion (PER) and area under curve (AUC). Parametric imaging was performed using MATLAB (R2013a,

Mathworks Inc., Natick, MA). The algorithm of parametric imaging is explained in the following sections.

3.3.2.1 Creating a file list

The sequence of the motion compensated images are imported into MATLAB and converted to gray scale. During motion compensation, these images were saved and numbered according to their frame number. The frame number was extracted from the file name and saved into a matrix. The image sequences were all saved into a single array.

3.3.2.2. Calculating the parameters

The array containing the image sequence is scanned one pixel at a time to determine when the peak intensity occurs. The maximal intensity is calculated and the frame number (3^{rd} dimension of the array) is determined. This frame number is then divided by the US scanner sampling frequency to compute the time of peak intensity.

Maximum intensity, time to peak, perfusion and area under curve are computed and parametric images are generated as shown in the figures below.

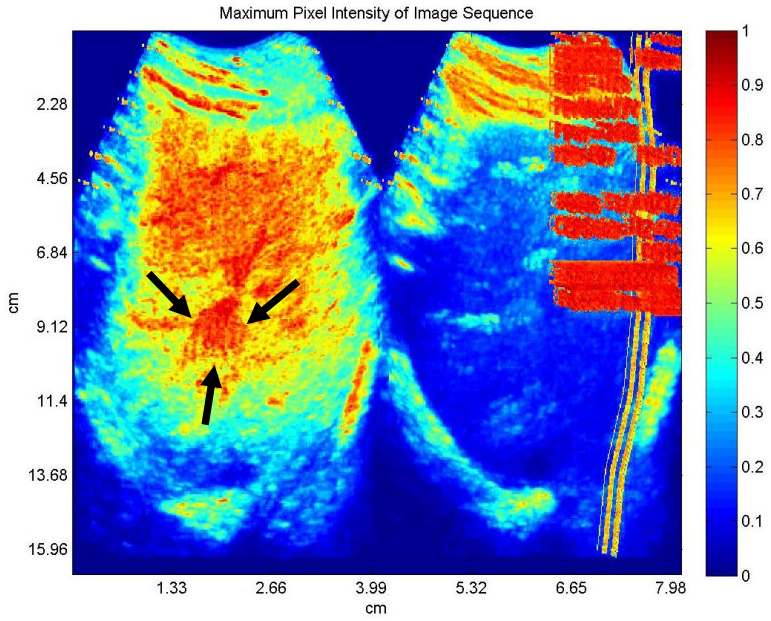

Figure 3.11: Parametric image showing the maximum intensity

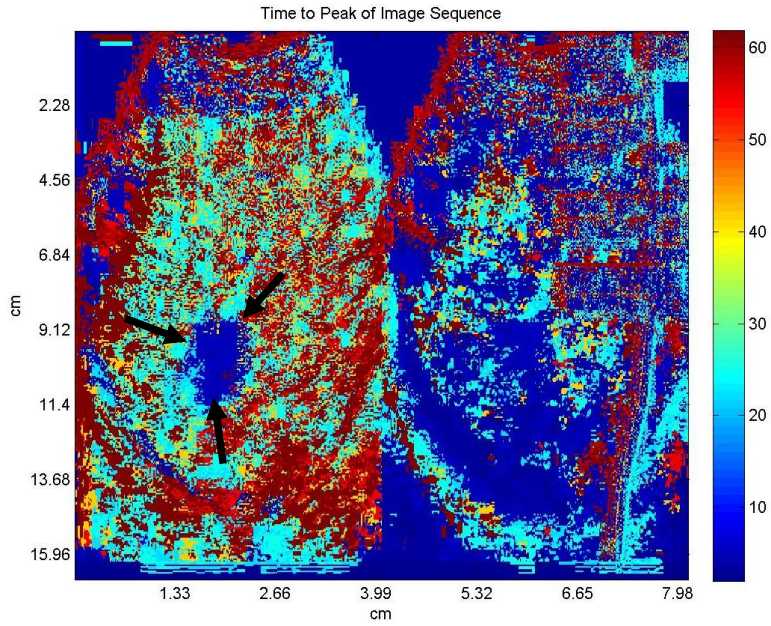

Figure 3.12: Parametric image showing the time to peak

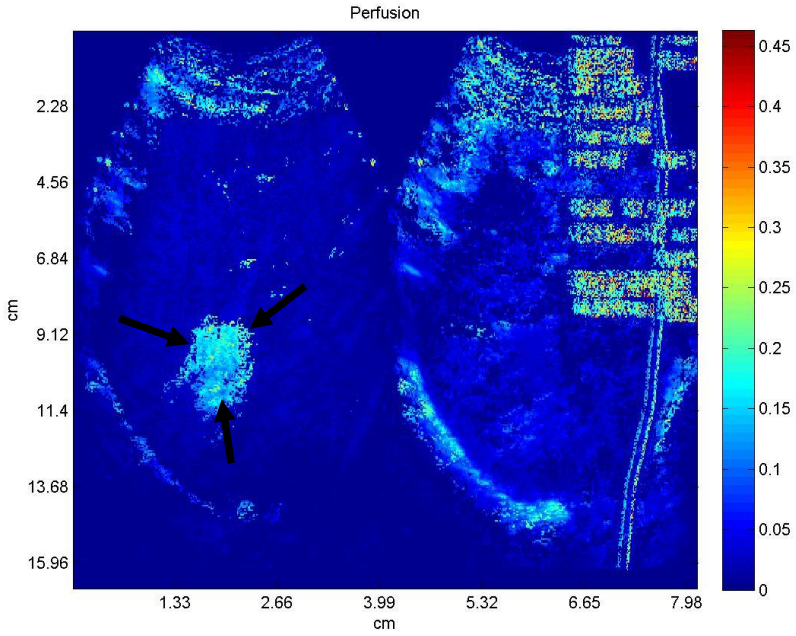

Figure 3.13: Parametric image showing Perfusion

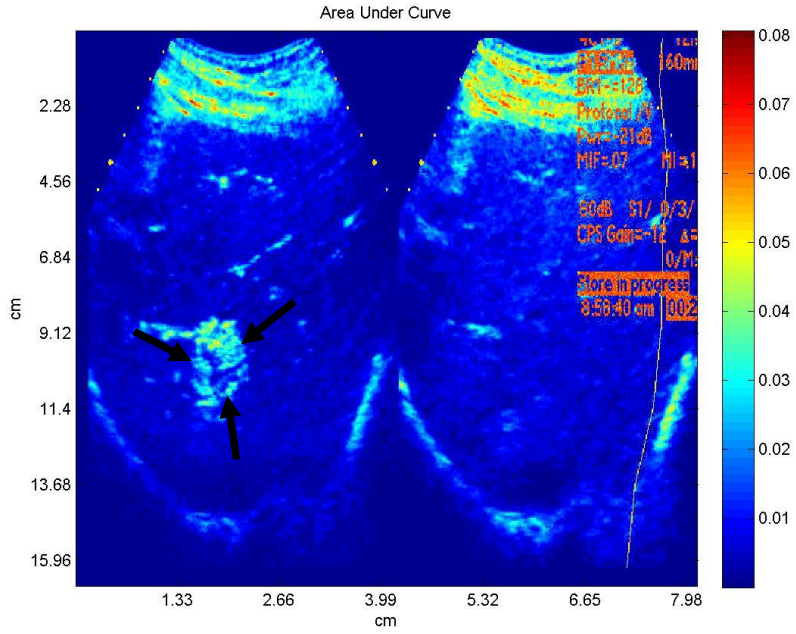

Figure 3.14: Parametric image showing area under curve

3.3.2.3 Evaluate the four parameters in selected region of interest (ROI)

The user is presented with an image to select the tumor on the B-mode side of the image. This ROI is then translated onto the contrast enhanced side of the image. The time intensity parameters of the ROI are saved.

Figure 3.15: User selected ROI in B-mode

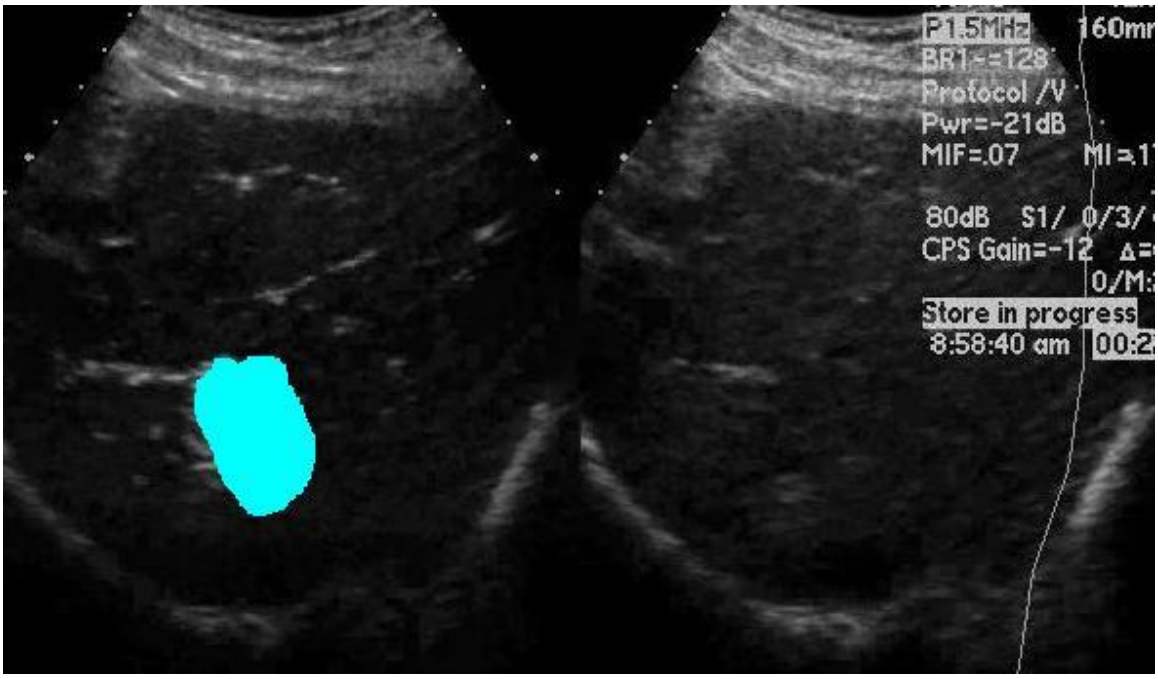

Figure 3.16: Translated ROI from B-mode to contrast enhanced mode

Parametric imaging was performed on the entire dataset. The values are average over tumor and expressed normalized relative to baseline. Results were then grouped by MRI findings and compared at each time point. The statistical analysis was performed using SPSS Statistics 23 (IBM, Armonk, NY).

4. RESULTS

Twenty one patients scheduled for transarterial chemoembolization using drug-eluting beads were approached for this study. Fourteen patients (11 males and 3 females) with 16 lesions were enrolled in the study. Six lesions were excluded due to excessive motion making it difficult to identify the tumor ROI. A total of three CEUS scans, pre TACE procedure, 2weeks post TACE and 4 weeks post TACE, were performed on each lesion. One lesion had two scans, as the patient was unable to attend the follow up 2 weeks post TACE. Thus, this study involved analysis of 10 lesions, 29 CEUS scans for analysis. The flow diagram below summarizes the patient enrollment as well as the data processing for the study.

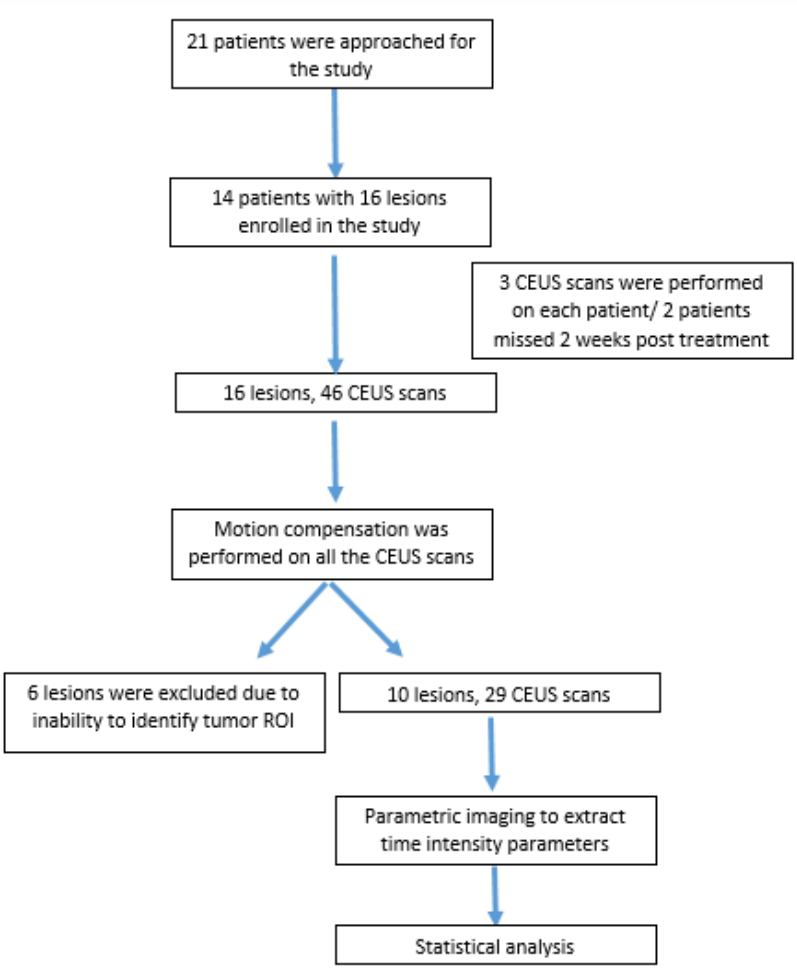

Figure 4.1: Flow diagram showing patient enrollment and data processing for the study.

4.1 Motion Compensation

Motion compensation was successfully performed on the CEUS data. The new sequence of images were saved and numbered according to their initial frame number. This was done to maintain a track of the timeline of the frame while generating time-intensity curves.

The figures below show selected frames from a sequence of motion compensated images. The outcomes of the patients were divided into three groups: 1=complete response, 2=partial response and 3= no response.

4.1.1 Complete Response

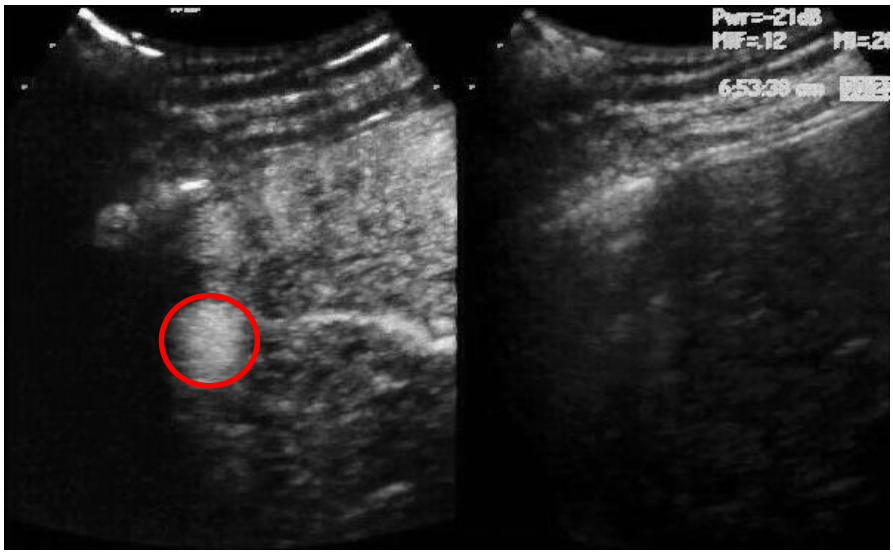

Figure 4.2: Image after motion compensation, pre-treatment scan

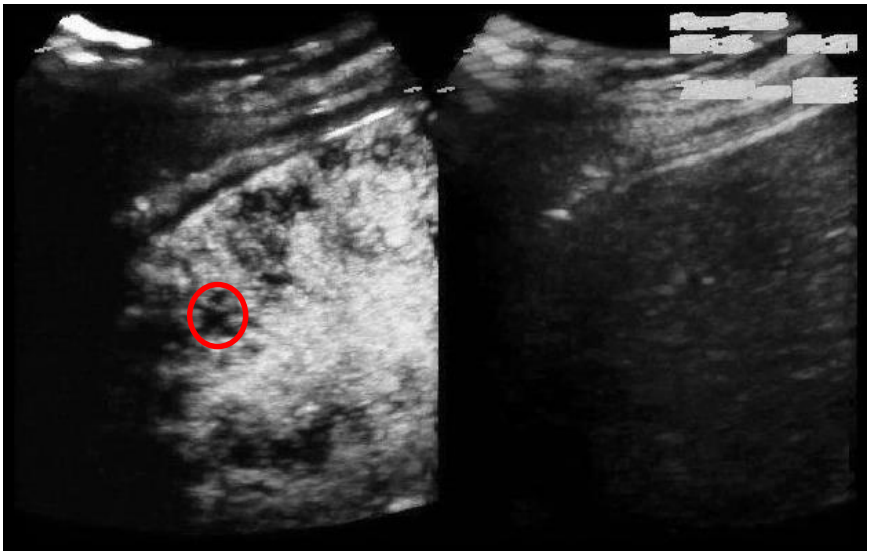

Figure 4.3: Image after motion compensation, 2 weeks post treatment scan

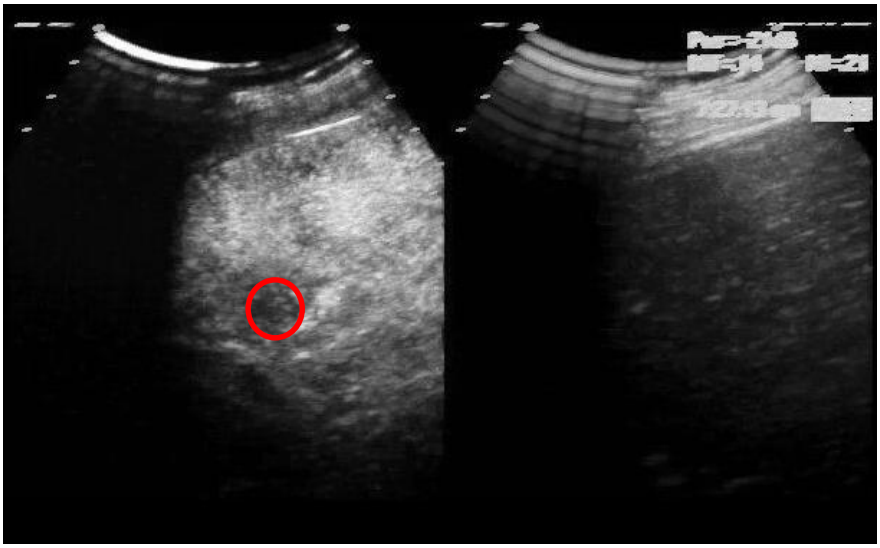

Figure 4.4: Image after motion compensation, 4 weeks post treatment scan

4.1.2 Partial Response

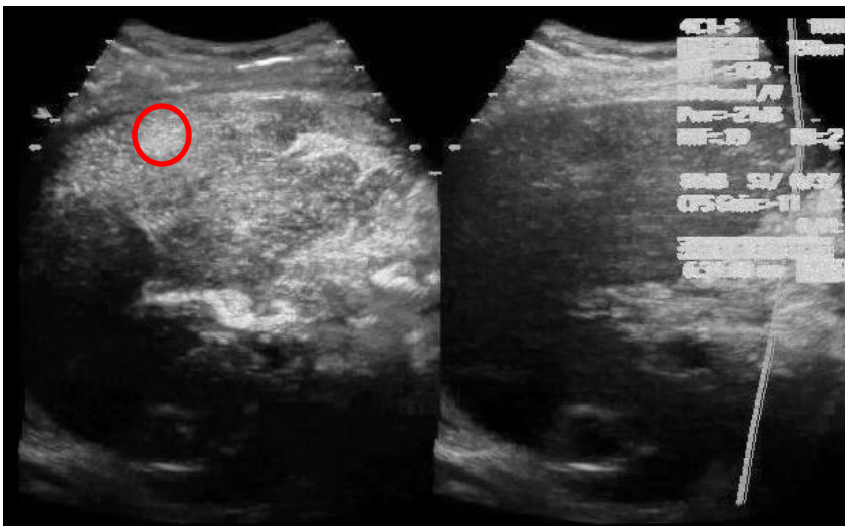

Figure 4.5: Image after motion compensation, pre-treatment scan

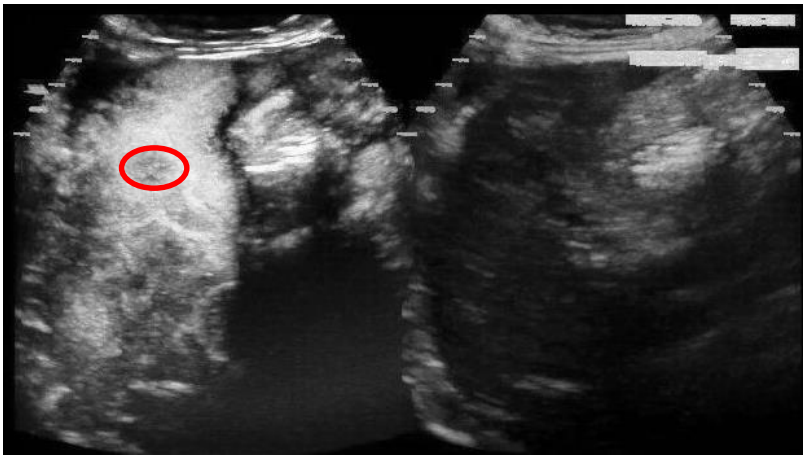

Figure 4.6: Image after motion compensation, 2 weeks post treatment scan

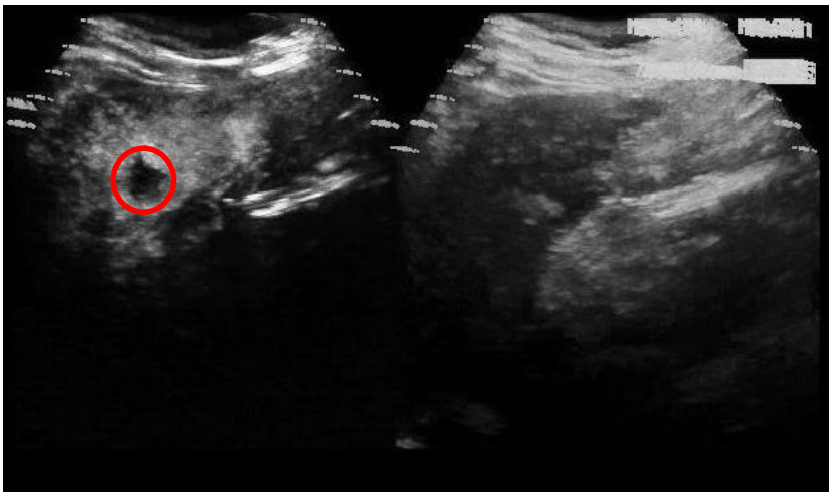

Figure 4.7: Image after motion compensation, 4 weeks post treatment scan

4.1.3 No Response

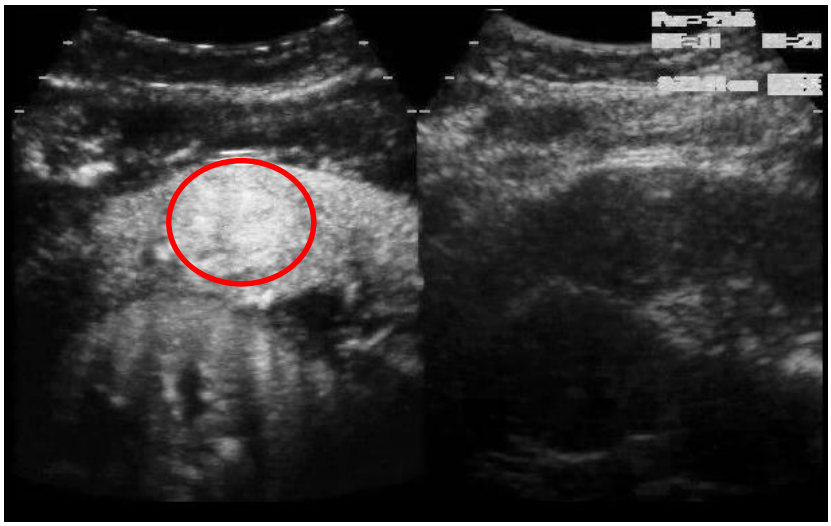

Figure 4.8: Image after motion compensation, pre-treatment scan

Figure 4.9: Image after motion compensation, 2 weeks post treatment scan

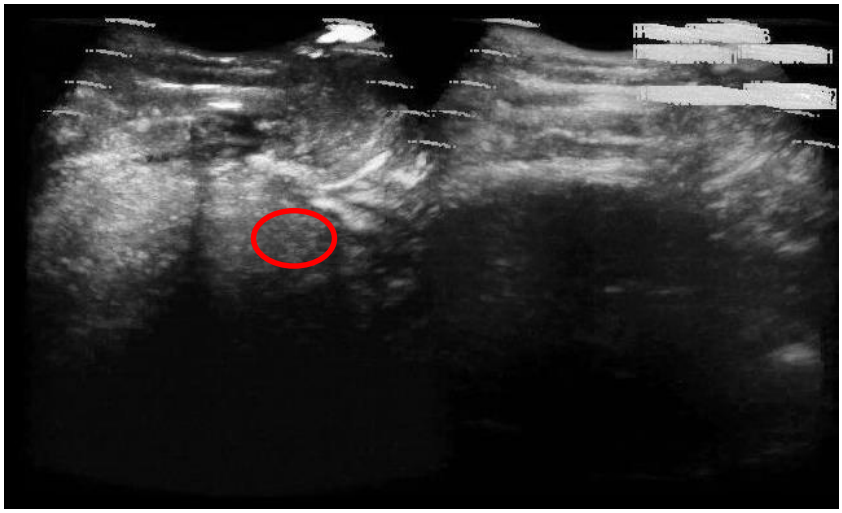

Figure 4.10: Image after motion compensation, 4 weeks post treatment scan

4.2 Parametric Imaging

Parametric Imaging was successfully performed in 10 the lesions. The tumor ROIs were marked and the parameters maximum intensity (MAX), time to peak (TTP), perfusion (PER) and area under curve (AUC) were extracted from the generated time-intensity curves. Figures below show parametric images from the three groups: complete response, partial response and no response.

4.2.1 Parametric Images of a complete response case

4.2.1.1 Complete Response- Maximum Intensity

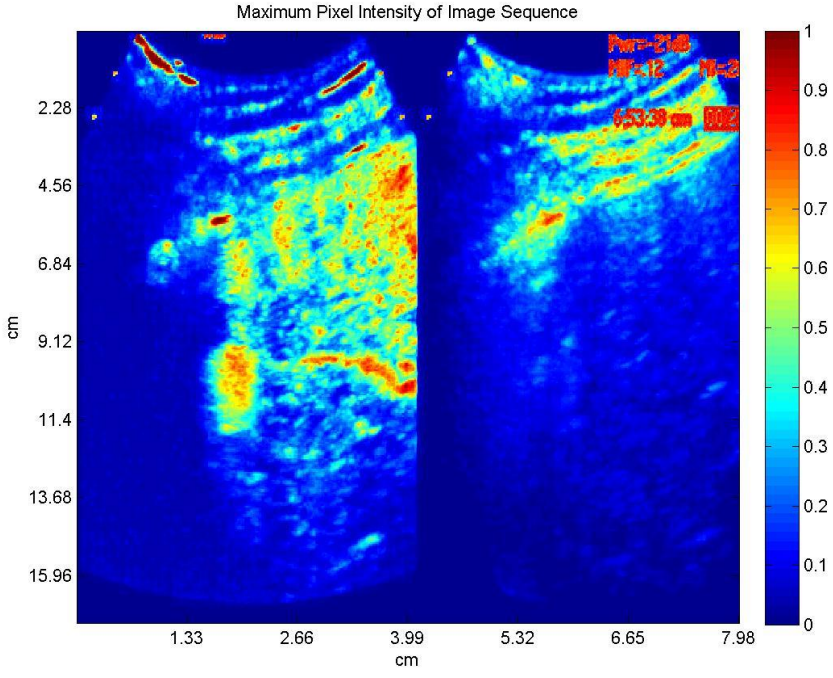

Figure 4.11: Maximum Intensity of Image Sequence – pre treatment

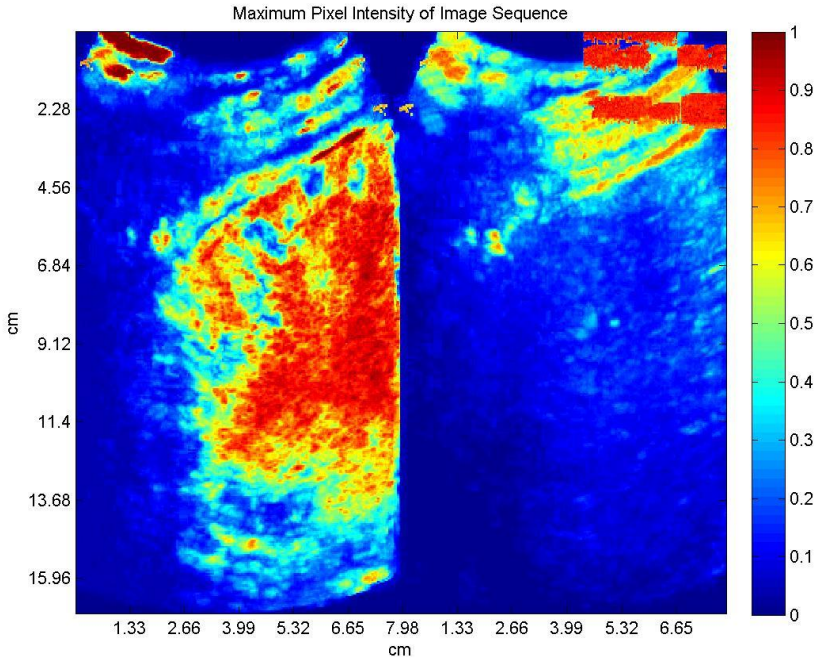

Figure 4.12: Maximum Intensity of Image Sequence – 2 weeks post treatment

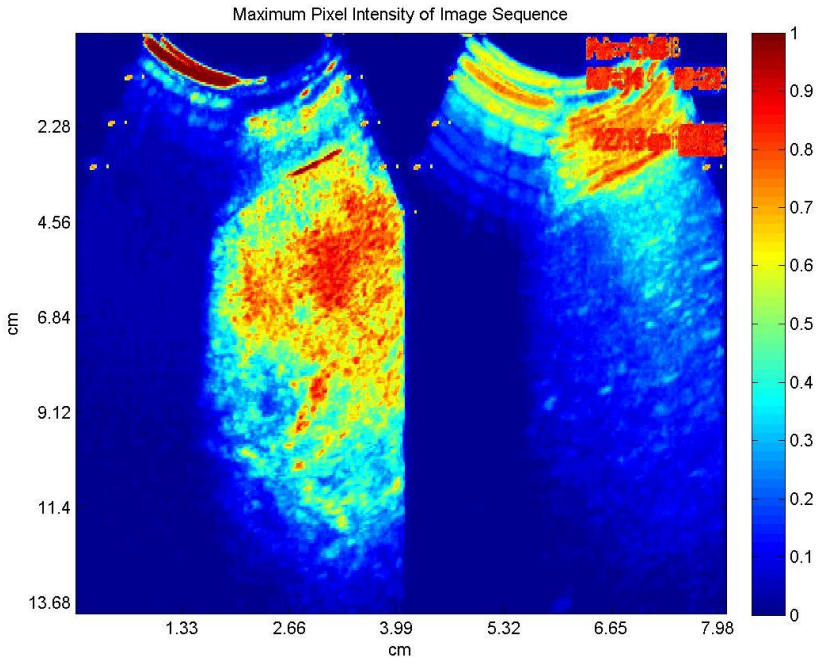

Figure 4.13: Maximum Intensity of Image Sequence – 4 weeks post treatment

4.2.1.2 Complete Response- Time to peak

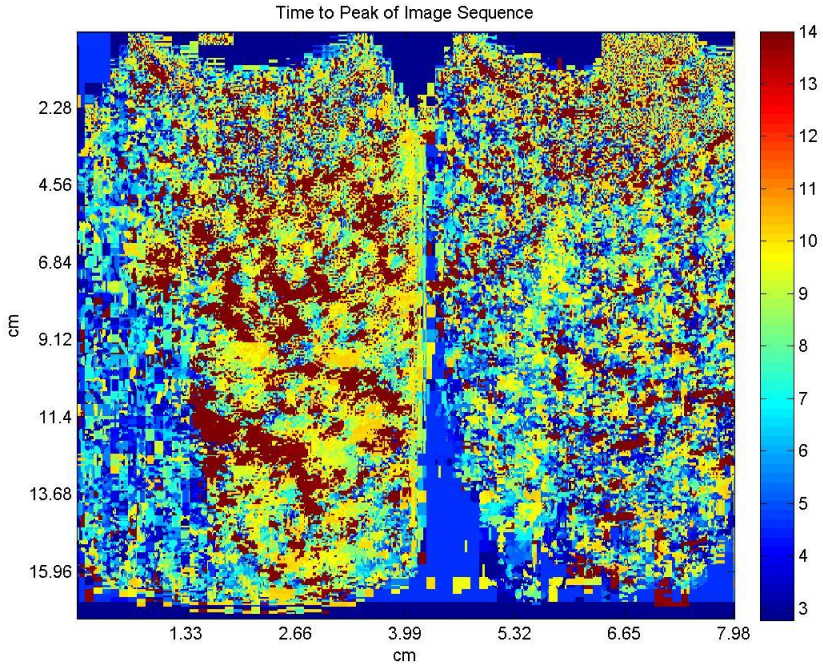

Figure 4.14: Time to peak of Image Sequence – pre treatment

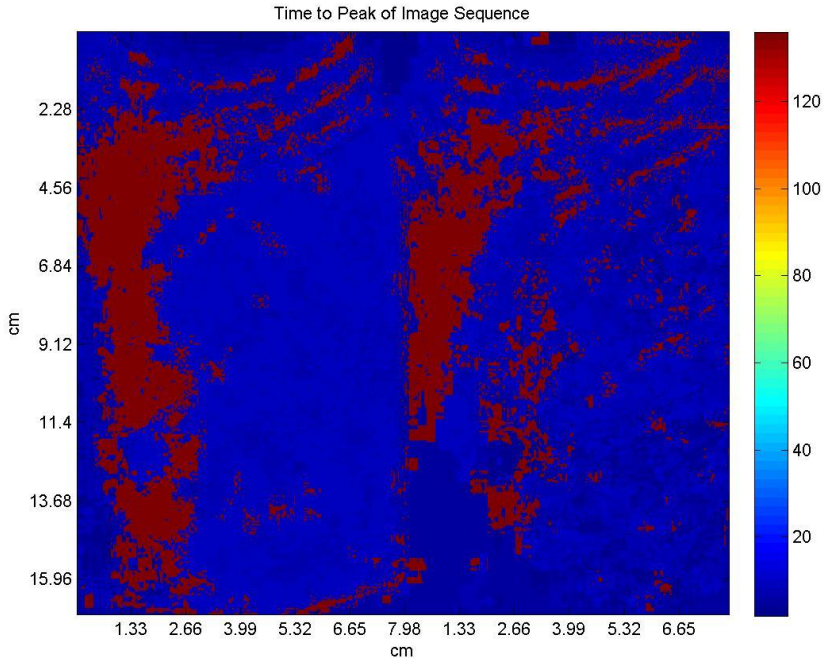

Figure 4.15: Time to peak of Image Sequence – 2 weeks post treatment

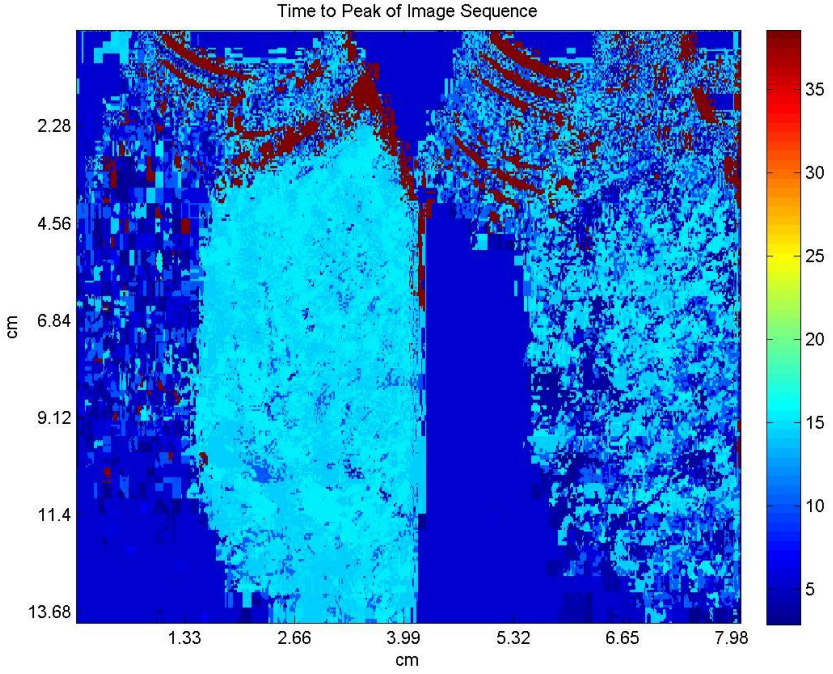

Figure 4.16: Time to peak of Image Sequence – 4 weeks post treatment

4.2.1.3 Complete Response- Perfusion

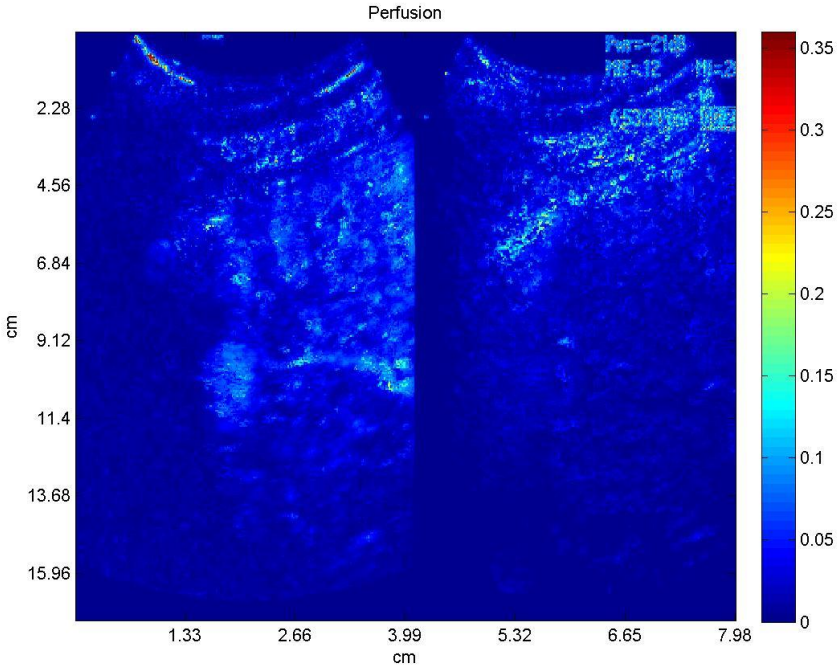

Figure 4.17: Perfusion– pre treatment

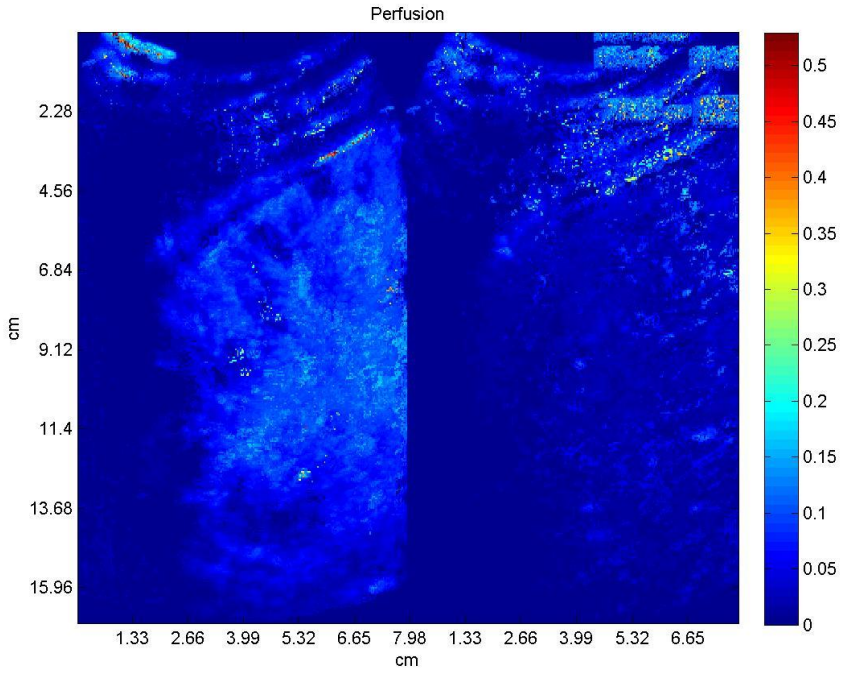

Figure 4.18: Perfusion– 2 weeks post treatment

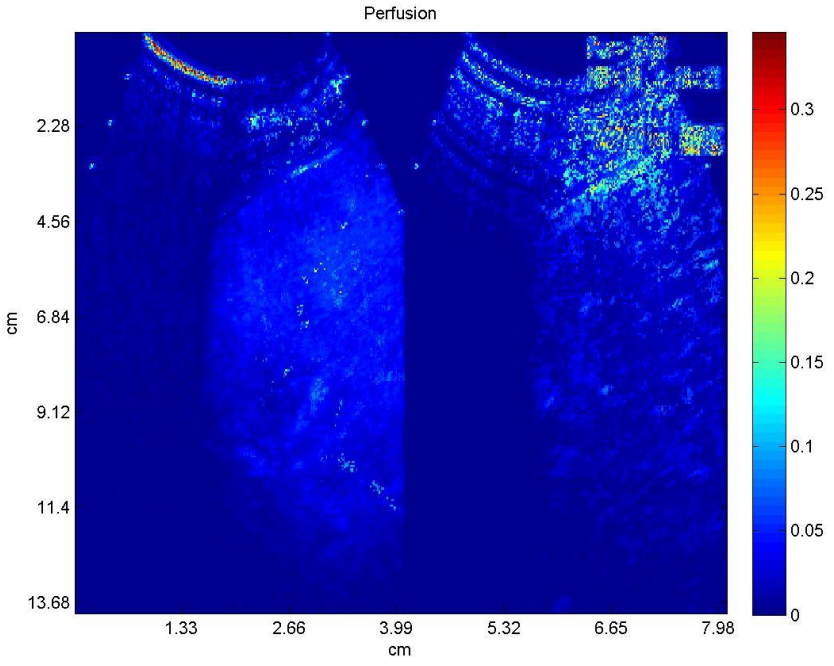

Figure 4.19: Perfusion– 4 weeks post treatment

4.2.1.4 Complete Response- Area under curve

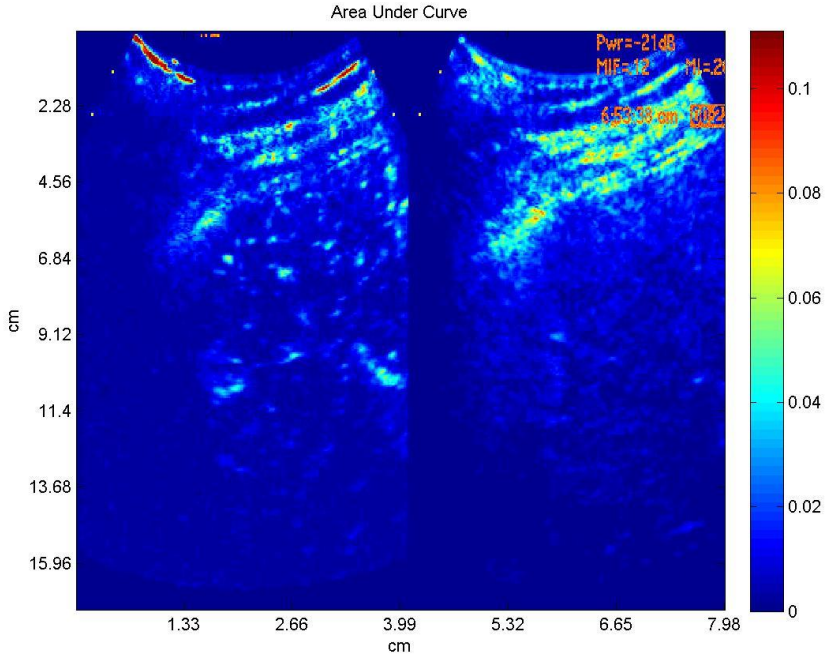

Figure 4.20: Area under curve – pre treatment

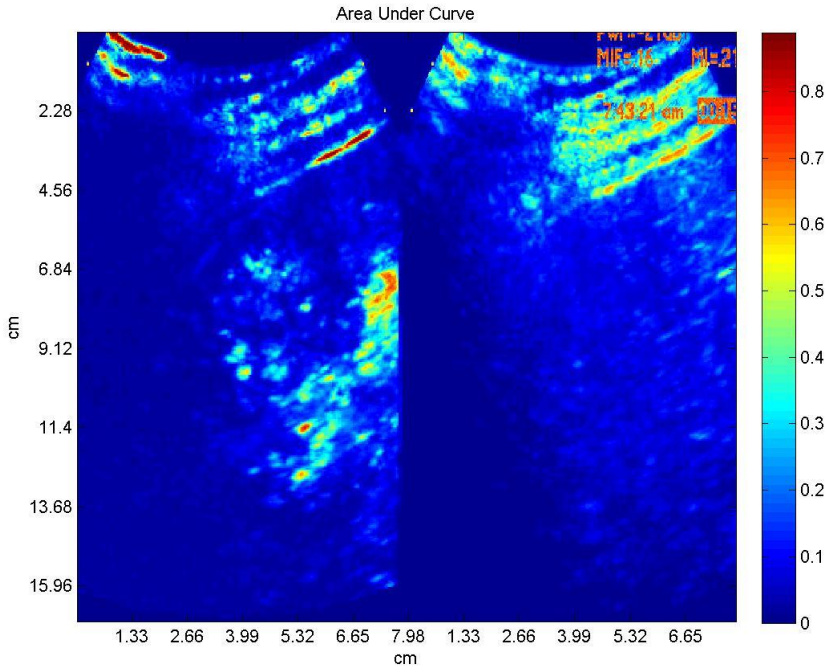

Figure 4.21: Area under curve – 2 weeks post treatment

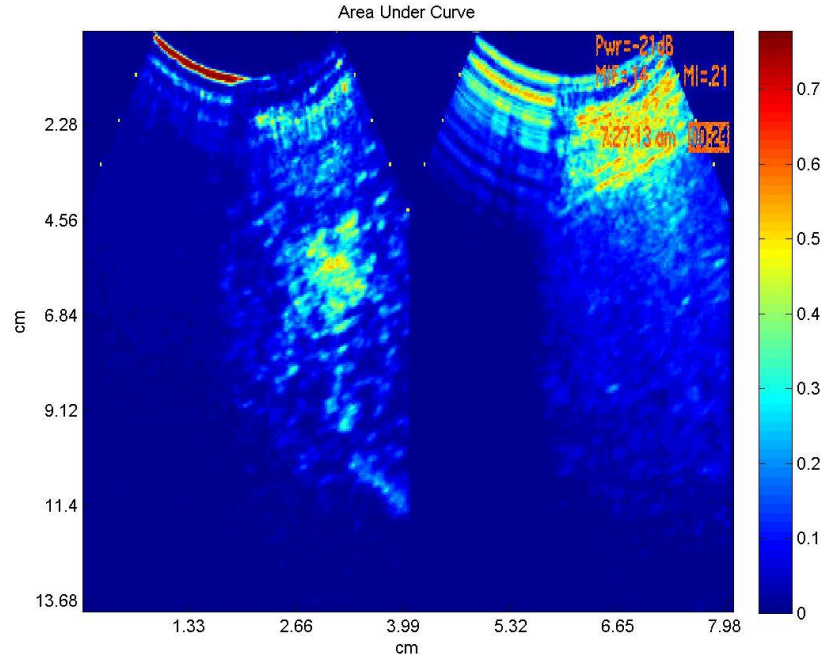

Figure 4.22: Area under curve – 4 weeks post treatment

4.2.2 Parametric Images of a partial response case

4.2.2.1 Partial Response- Maximum Intensity

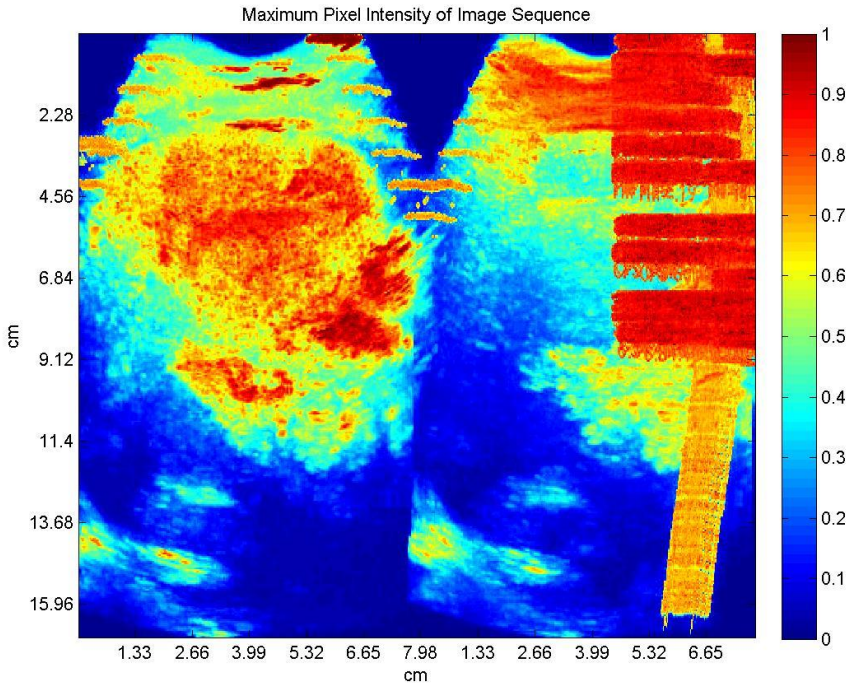

Figure 4.23: Maximum Pixel Intensity of image sequence – pre treatment

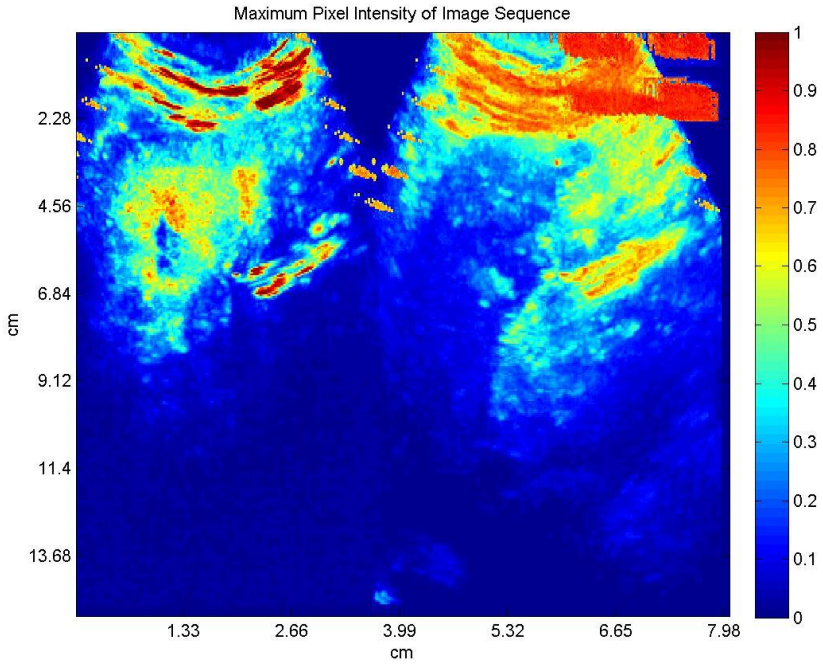

Figure 4.24: Maximum Pixel Intensity of image sequence – 2 weeks post treatment

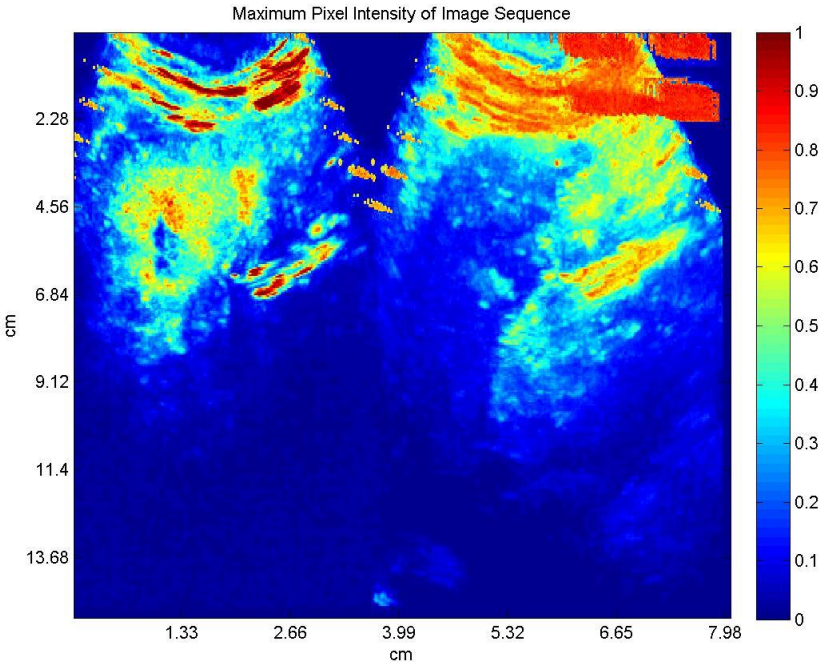

Figure 4.25: Maximum Pixel Intensity of image sequence – 4 weeks post treatment

4.2.2.2 Partial Response- Time to peak

Figure 4.26: Time to peak of image sequence – pre treatment

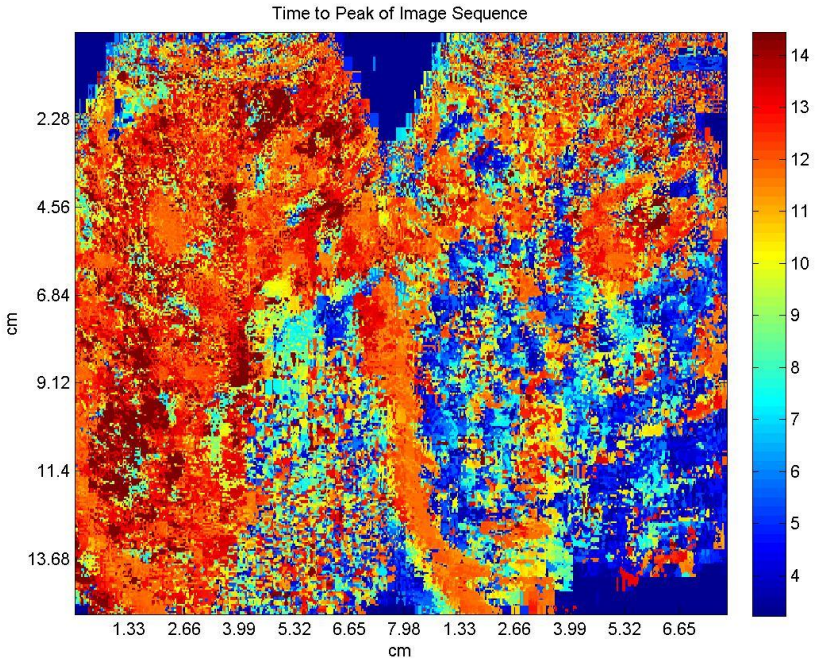

Figure 4.27: Time to peak of image sequence – 2 weeks post treatment

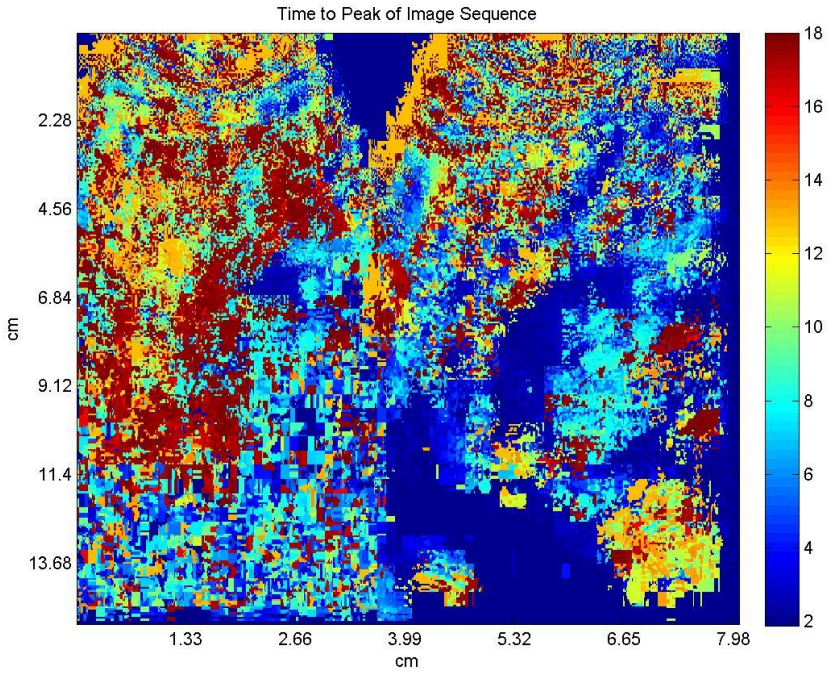

Figure 4.28: Time to peak of image sequence – 4 weeks post treatment

4.2.2.3 Partial Response- Perfusion

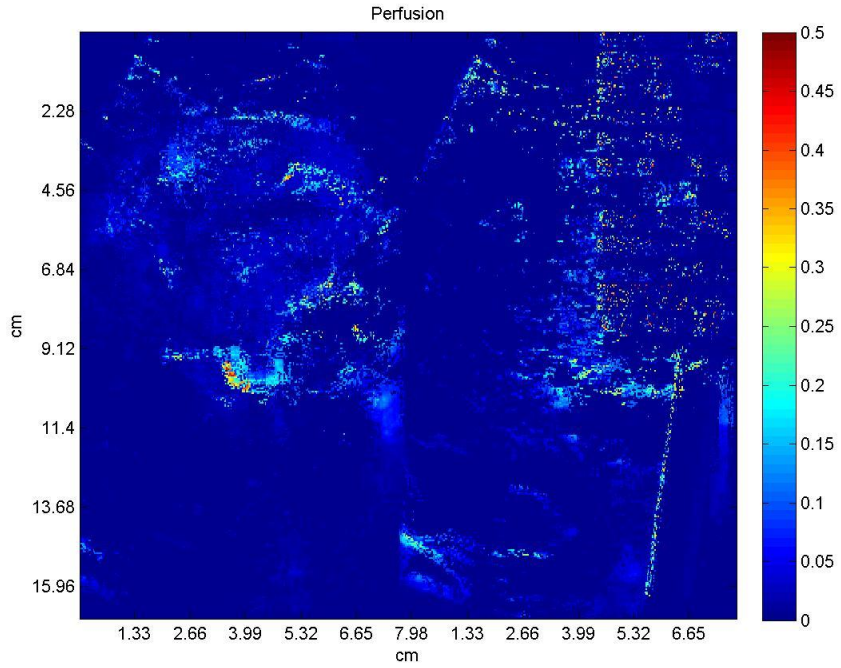

Figure 4.29: Perfusion – pre treatment

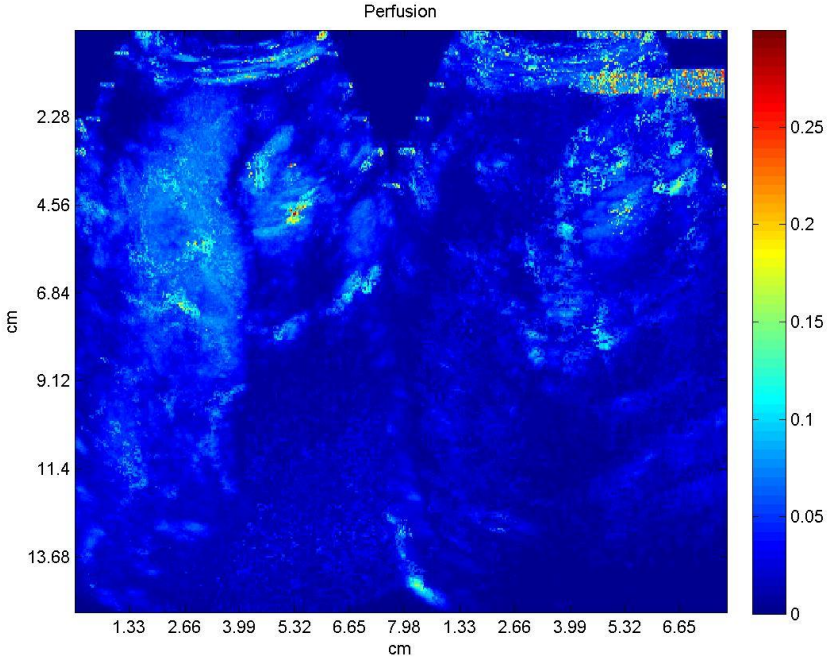

Figure 4.30: Perfusion – 2 weeks post treatment

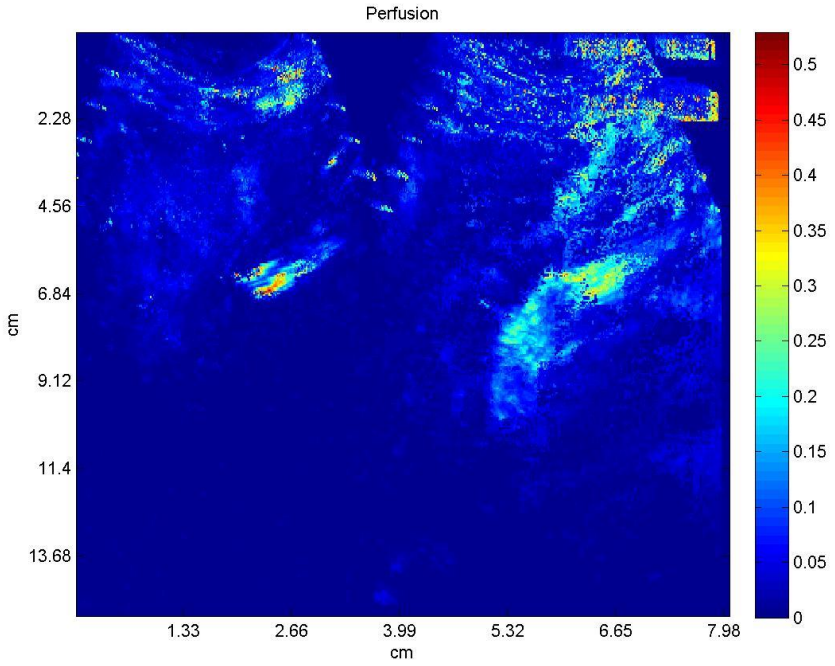

Figure 4.31: Perfusion – 4 weeks post treatment

4.2.2.4 Partial Response- Area under curve

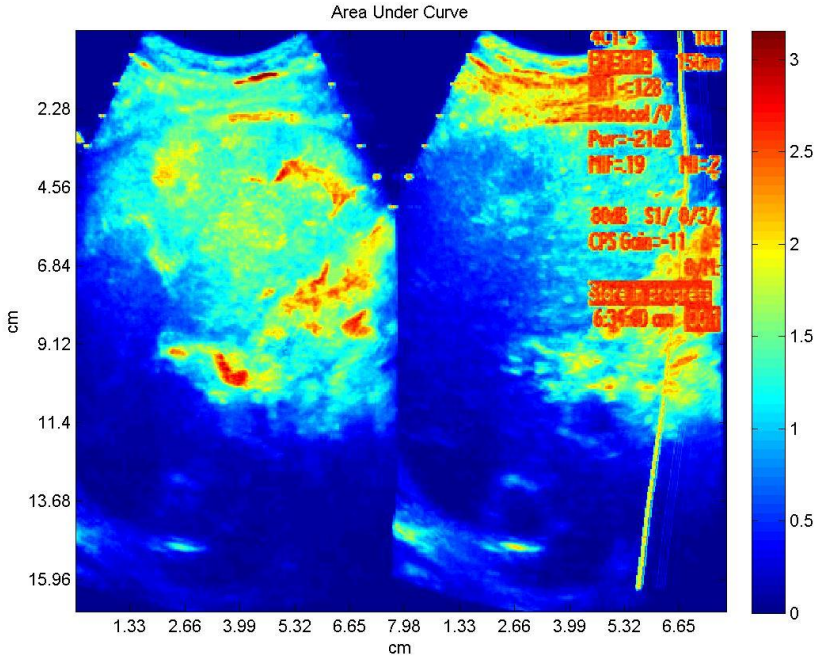

Figure 4.32: Area under curve – pre treatment

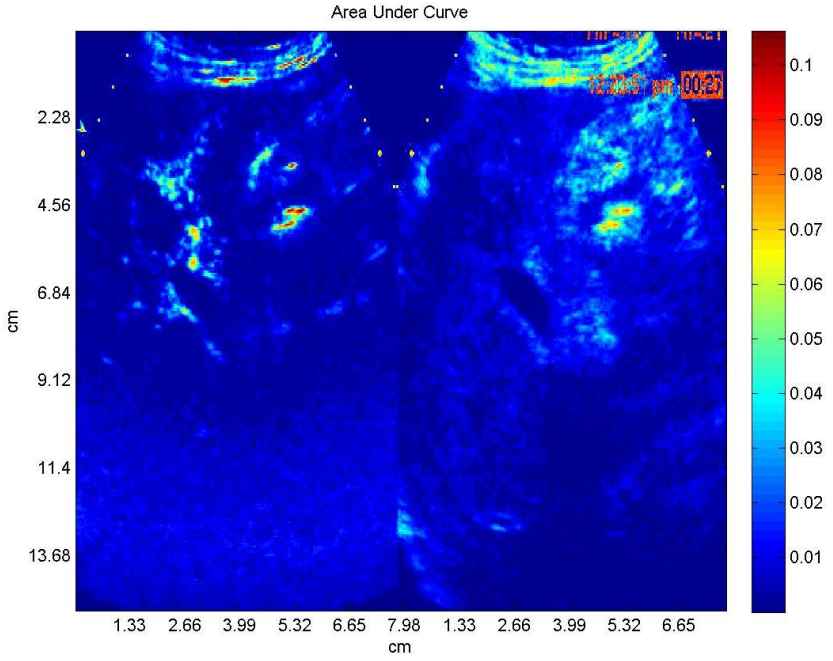

Figure 4.33: Area under curve – 2 weeks post treatment

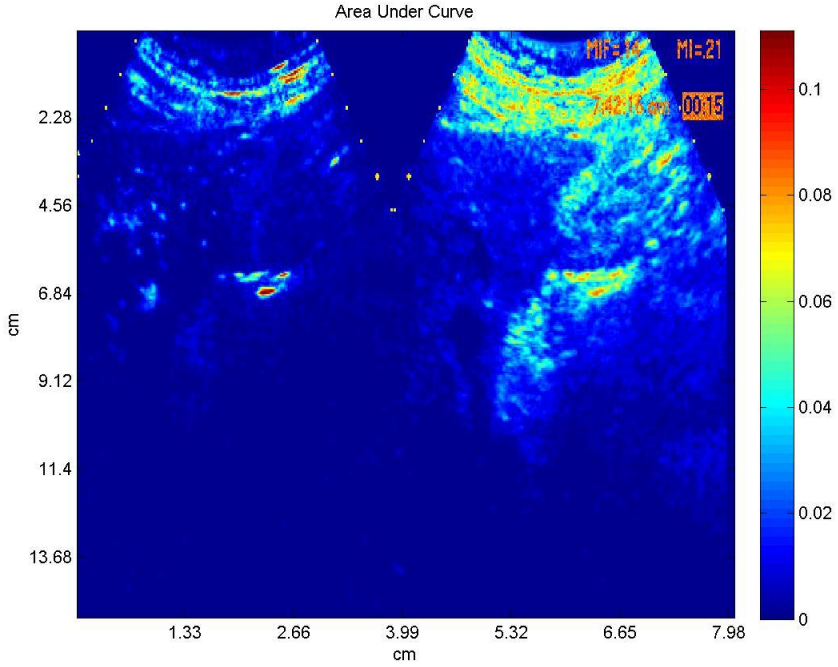

Figure 4.34: Area under curve – 4 weeks post treatment

4.2.3 Parametric Images of a no response case

4.2.3.1 No Response- Maximum Intensity

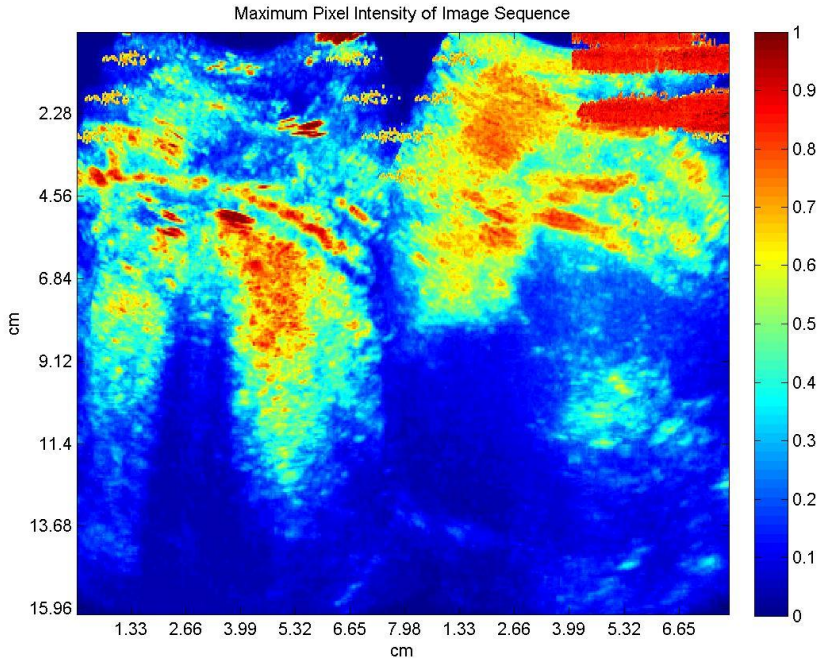

Figure 4.35: Maximum pixel intensity of image sequence– pre treatment

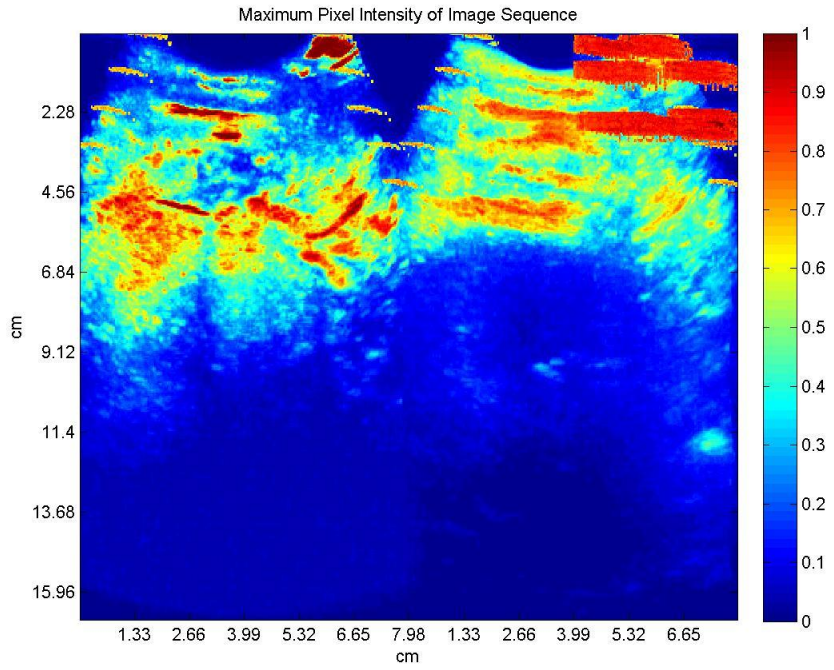

Figure 4.36: Maximum pixel intensity of image sequence– 2 weeks post treatment

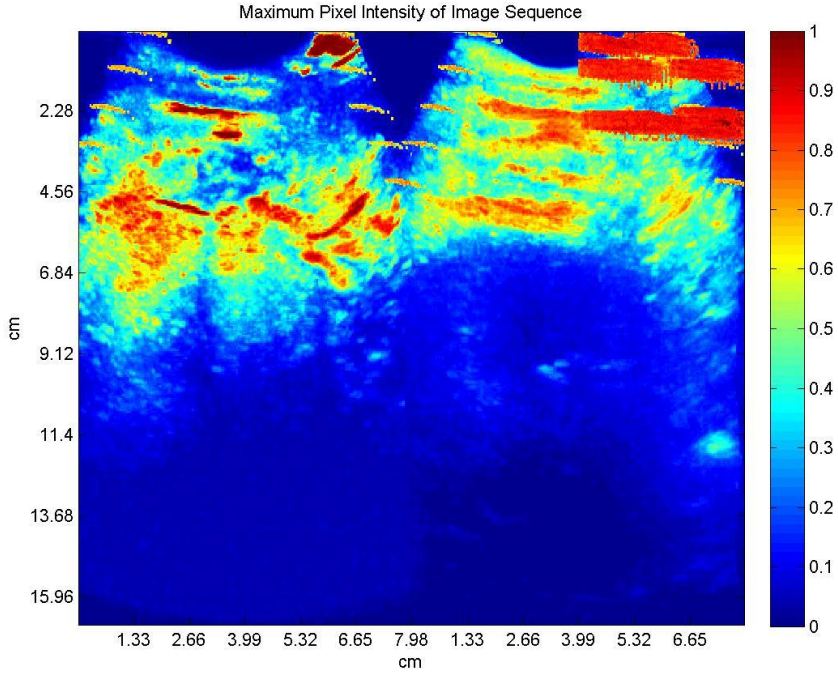

Figure 4.37: Maximum pixel intensity of image sequence– 4 weeks post treatment

4.2.3.2 No Response- Time to peak

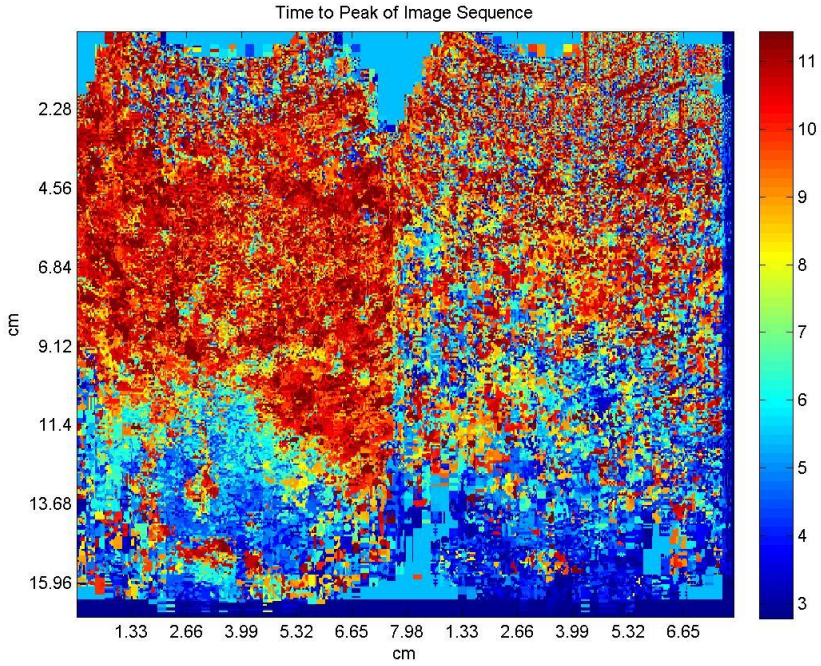

Figure 4.38: Time to peak of image sequence– pre treatment

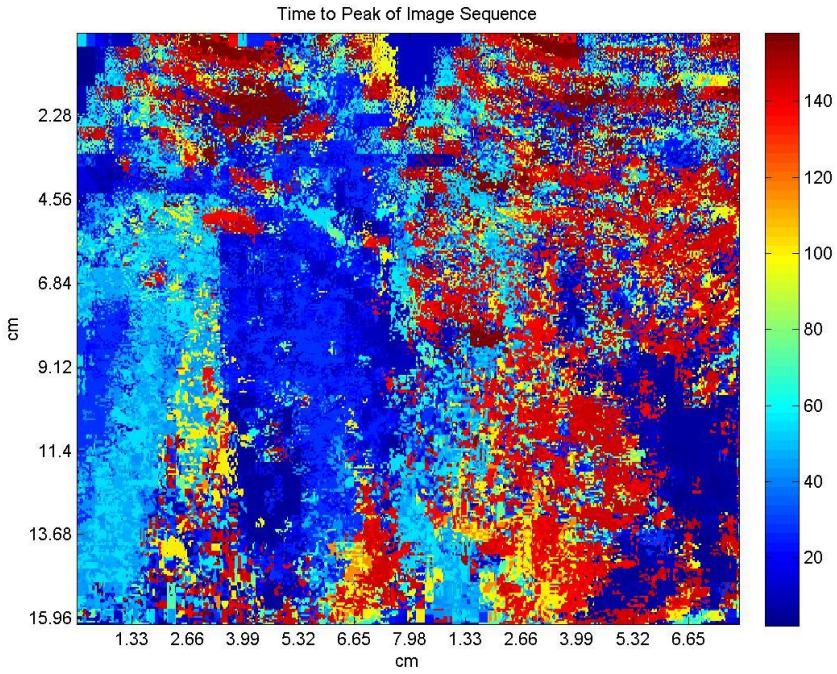

Figure 4.39: Time to peak of image sequence– 2 weeks post treatment

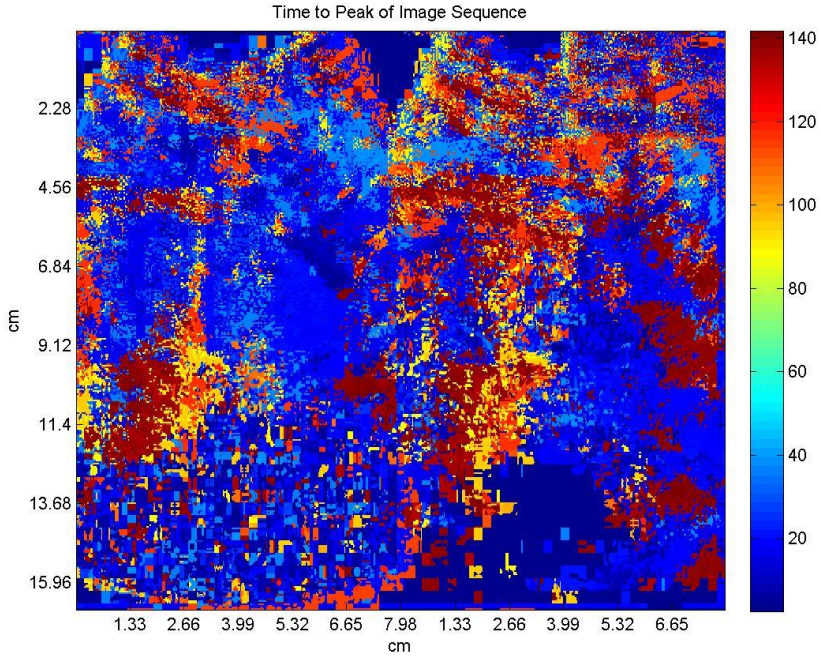

Figure 4.40: Time to peak of image sequence– 4 weeks treatment

4.2.3.3 No Response- Perfusion

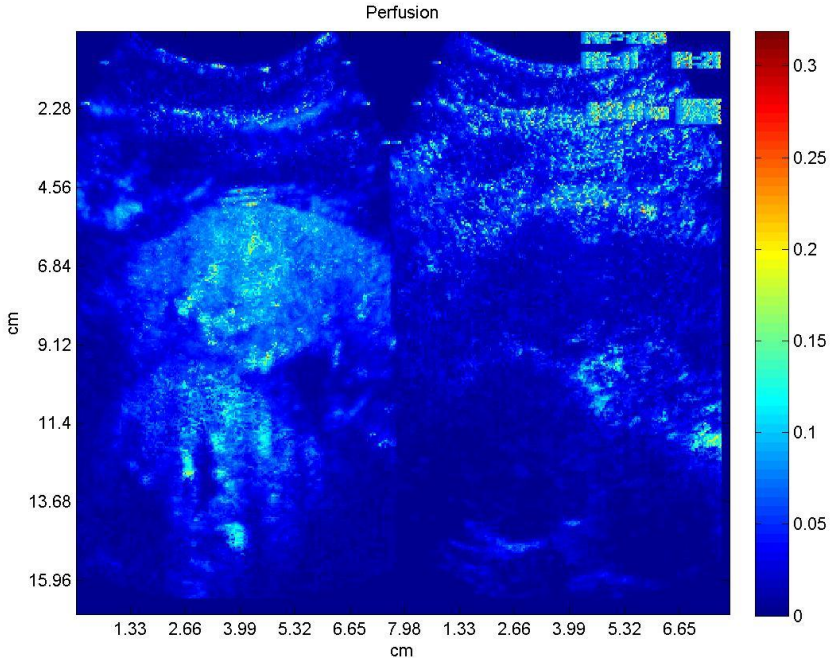

Figure 4.41: Perfusion– pre treatment

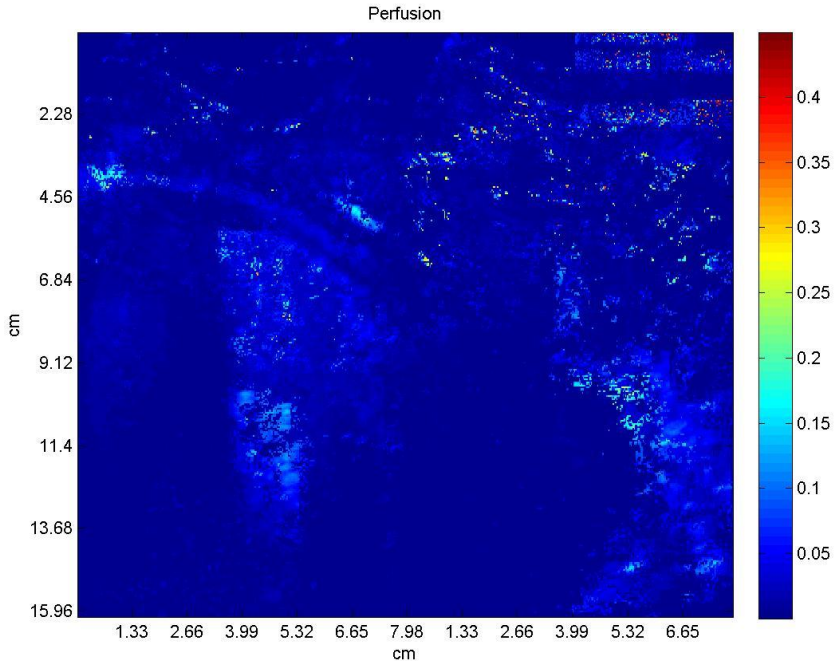

Figure 4.42: Perfusion– 2 weeks post treatment

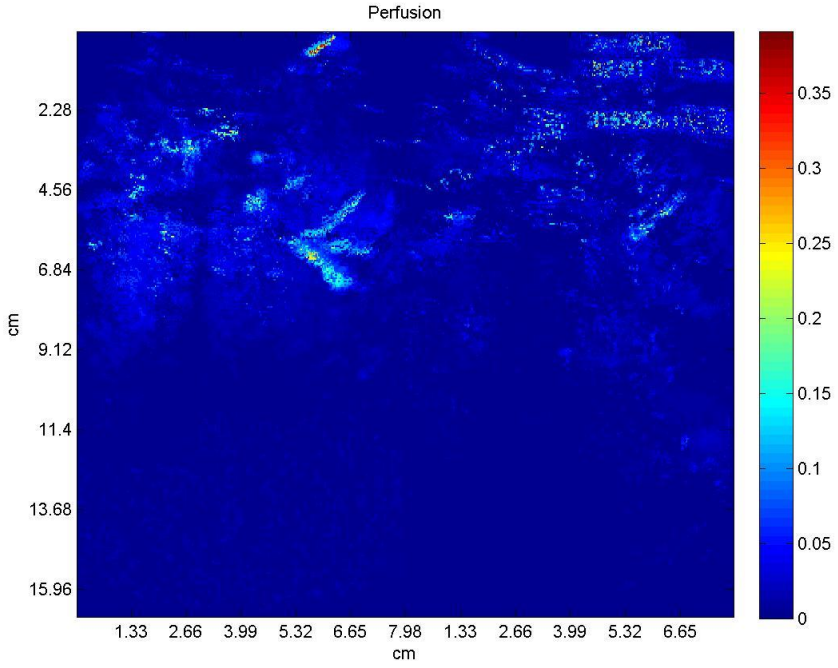

Figure 4.43: Perfusion- 4 weeks post treatment

4.2.3.4 No Response- Area under curve

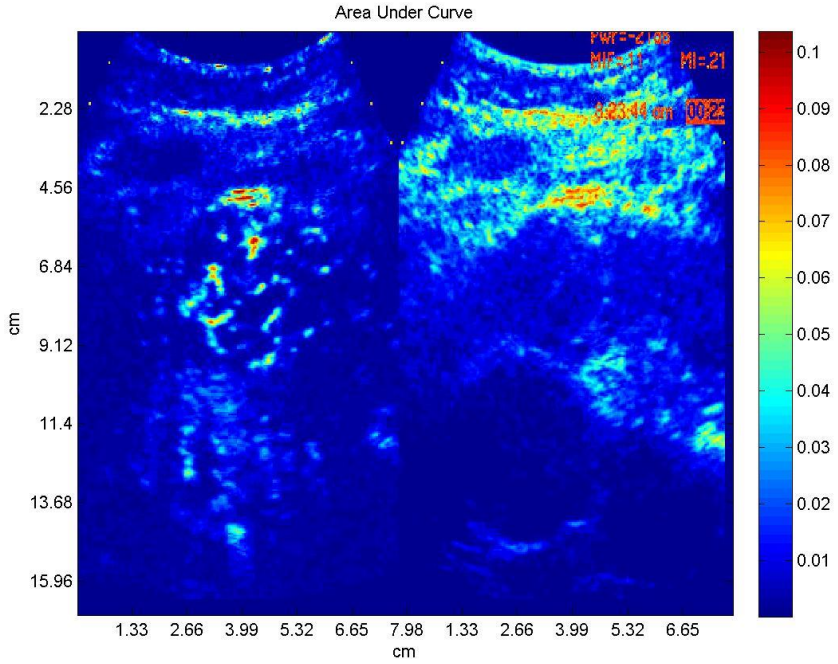

Figure 4.44: Area under curve– pre treatment

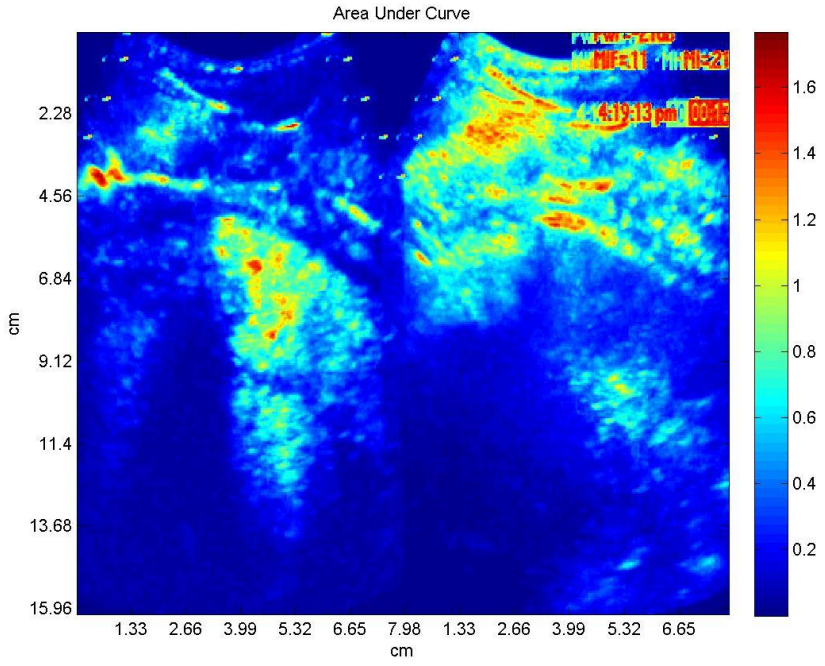

Figure 4.45: Area under curve– 2 weeks post treatment

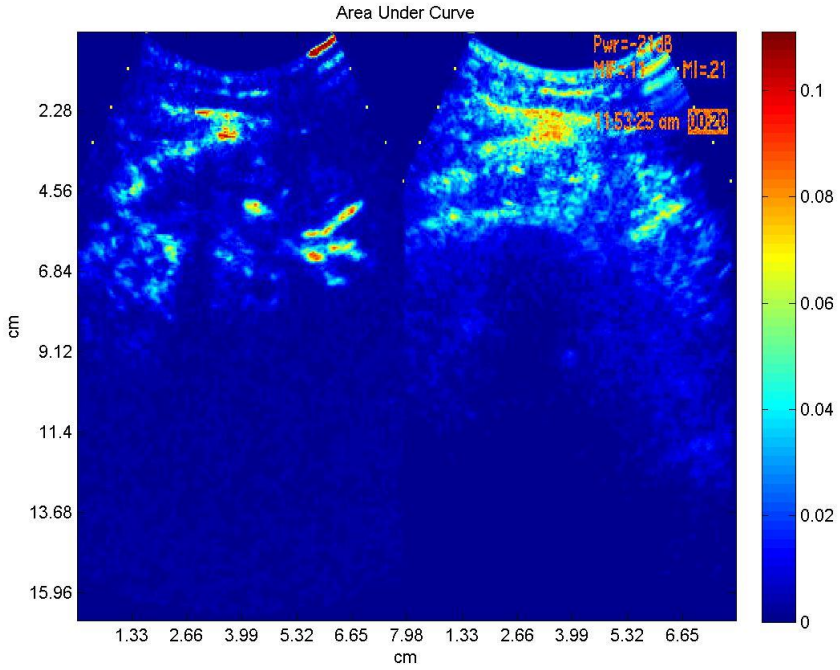

Figure 4.46: Area under curve– 4 weeks post treatment

4.3 Parametric Data of the ROI

The parametric data of all the patients were tabulated and normalized relative to baseline. Table 4.1, 4.2 and 4.3 show the extracted parametric values as well as the normalized values.

Table 4.1: Parametric values of patients with complete response

	MAX	TTP	PER	AUC	NMAX	NTTP	NPER	NAUC
Complete Response								
TACE01								
Pre TACE	0.435	22.793	0.036	0.004	1.000	1.000	1.000	1.000
After 2weeks	0.326	6.559	0.072	0.436	0.749	0.288	2.003	121.139
After 4weeks	0.666	7.825	0.101	0.008	1.531	0.343	2.809	2.250
TACE10								
Pre TACE	0.713	47.248	0.016	0.299	1.000	1.000	1.000	1.000
After 2weeks	0.312	13.904	0.032	0.007	0.438	0.294	2.071	0.022
After 4weeks	0.446	24.351	0.022	0.003	0.625	0.515	1.419	0.008
TACE11 Lesion 1								
Pre TACE	0.873	10.473	0.085	0.007	1.000	1.000	1.000	1.000
After 2weeks	0.683	14.174	0.051	0.004	0.782	1.353	0.601	0.600
After 4weeks	0.499	4.443	0.114	0.020	0.572	0.424	1.344	3.062
TACE11 Lesion 2								
Pre TACE	0.404	10.161	0.043	0.008	1.000	1.000	1.000	1.000
After 2weeks	0.662	9.418	0.086	0.063	1.637	0.927	1.977	7.911
After 4weeks	0.386	14.354	0.027	0.043	0.956	1.413	0.628	5.468

Table 4.2: Parametric values of patients with partial response

	MAX	TTP	PER	AUC	NMAX	NTTP	NPER	NAUC
Partial Response								
TACE02								
Pre TACE	0.720	7.339	0.101	0.015	1.000	1.000	1.000	1.000
After 2weeks	0.395	15.904	0.026	0.003	0.549	2.167	0.259	0.212
After 4weeks	0.288	36.847	0.008	0.224	0.401	5.021	0.078	14.821
TACE06								
Pre TACE	0.615	22.485	0.044	0.005	1.000	1.000	1.000	1.000
After 2weeks	-	-	-	-	-	-	-	
After 4weeks	0.057	3.245	0.017	0.002	0.092	0.144	0.397	0.444
TACE07								
Pre TACE	0.712	15.287	0.105	0.019	1.000	1.000	1.000	1.000
After 2weeks	0.692	41.037	0.028	0.486	0.972	2.685	0.264	25.595
After 4weeks	0.663	10.372	0.083	12.035	0.931	0.679	0.787	633.405
TACE08								
Pre TACE	0.707	49.124	0.031	1.490	1.000	1.000	1.000	1.000
After 2weeks	0.788	11.767	0.069	0.012	1.115	0.240	2.231	0.008
After 4weeks	0.453	12.536	0.039	0.003	0.640	0.255	1.269	0.002

Table 4.3: Parametric values of patients with no response

	MAX	TTP	PER	AUC	NMAX	NTTP	NPER	NAUC
No Response								
TACE05								
Pre TACE	0.209	7.556	0.028	0.003	1.000	1.000	1.000	1.000
After 2weeks	0.539	26.967	0.061	1.728	2.578	3.569	2.199	595.828
After 4weeks	0.365	33.282	0.019	0.006	1.748	4.404	0.679	2.138
TACE14								
Pre TACE	0.793	9.843	0.083	0.015	1.000	1.000	1.000	1.000
After 2weeks	0.544	26.819	0.035	0.610	0.687	2.725	0.418	41.463
After 4weeks	0.337	25.377	0.017	0.005	0.425	2.578	0.207	0.333

Average and standard deviation of the normalized values are computed. Table 4.4 and 4.5 show the calculated average and standard deviation of the three groups.

Table 4.4: Average of the normalized data

	Average MAX	Average TTP	Average PER	Average AUC
Complete Response				
Pre TACE	1.000	1.000	1.000	1.000
After 2weeks	0.902	0.716	1.663	32.418
After 4weeks	0.921	0.674	1.550	2.697
Partial Response				
Pre TACE	1.000	1.000	1.000	1.000
After 2weeks	0.879	1.697	0.918	8.605
After 4weeks	0.516	1.525	0.633	162.168

No Response				
Pre TACE	1.000	1.000	1.000	1.000
After 2weeks	1.632	3.147	1.308	318.645
After 4weeks	1.087	3.491	0.443	1.236

Table 4.5: Standard deviation of the normalized data

	Stdev MAX	Stdev TTP	Stdev PER	Stdev AUC
Complete Response				
Pre TACE	0.000	0.000	0.000	0.000
After 2weeks	0.618	0.533	0.823	4.398
After 4weeks	0.208	0.546	0.437	2.736
Partial Response				
Pre TACE	0.000	0.000	0.000	0.000
After 2weeks	0.294	1.288	1.137	14.714
After 4weeks	0.356	2.342	0.514	314.233
No response				
Pre TACE	0.000	0.000	0.000	0.000
After 2weeks	1.337	0.597	1.259	391.995
After 4weeks	0.936	1.291	0.334	1.276

4.4 Statistical Analysis

Statistical analysis of the data involved comparing three groups. The data obtained is tested for normal distribution. In case of normal distribution ANOVA is used to test significance.

In non-normal data, Kruskal-Wallis test is used. SPSS Statistics 23 (IBM, Armonk, NY) was used to perform statistical tests.

4.4.1 Two weeks post TACE

In the post 2 week dataset, it was seen that maximum intensity, perfusion and area under did not show normal distribution, whereas time to peak was normal distribution. Table 4.6 shows the p values for four parameters, maximum intensity, and time to peak, perfusion and area under curve, 2 weeks post TACE. The analysis performed showed a significant value in case of time to peak (p=0.047), but no significant value for maximum intensity, perfusion and area under curve.

Table 4.6: p-values for parameters, 2 weeks post TACE

Parameter	p value
MAX	0.844
TTP	0.047
PER	0.794
AUC	0.184

The ANOVA for time to peak results do not provide information about the significance among the groups. Thus, pairwise comparison, Fisher's LSD test was performed. Table 4.7 show the result of the LSD test performed on the post 4 week time to peak data.

Table 4.7: LSD comparison of TTP data 2 weeks post treatment

Response Type	p-value
Complete response vs Partial Response	0.188
Complete response vs No Response	0.018
Partial response vs No Response	0.116

4.4.2 Four weeks post TACE

Table 4.8 shows the p values for four parameters, maximum intensity, and time to peak, perfusion and area under curve, 4 weeks post TACE. The analysis performed showed significant value no significant value for any of the four parameters.

Table 4.8: p-values for parameters, 4 weeks post TACE

Parameter	p value
MAX	0.403
TTP	0.338
PER	0.158
AUC	0.779

Significant difference was observed only in time to peak, 2 weeks post TACE (p=0.047). On performing pairwise comparison, significant difference is observed between complete response and no response groups (p=0.018).

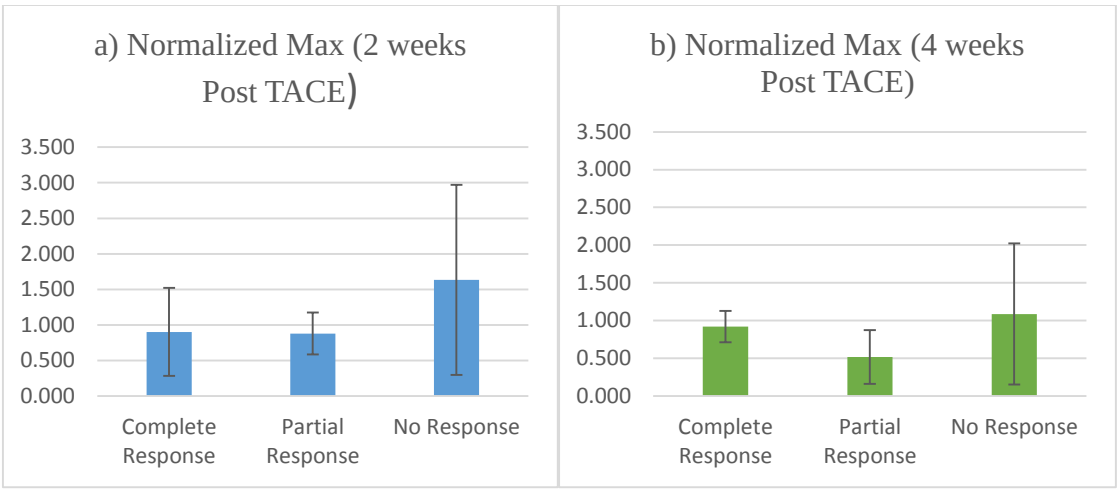

Figure 4.47: Average of normalized maximum intensity a) 2 weeks post TACE, b) 4 weeks post TACE

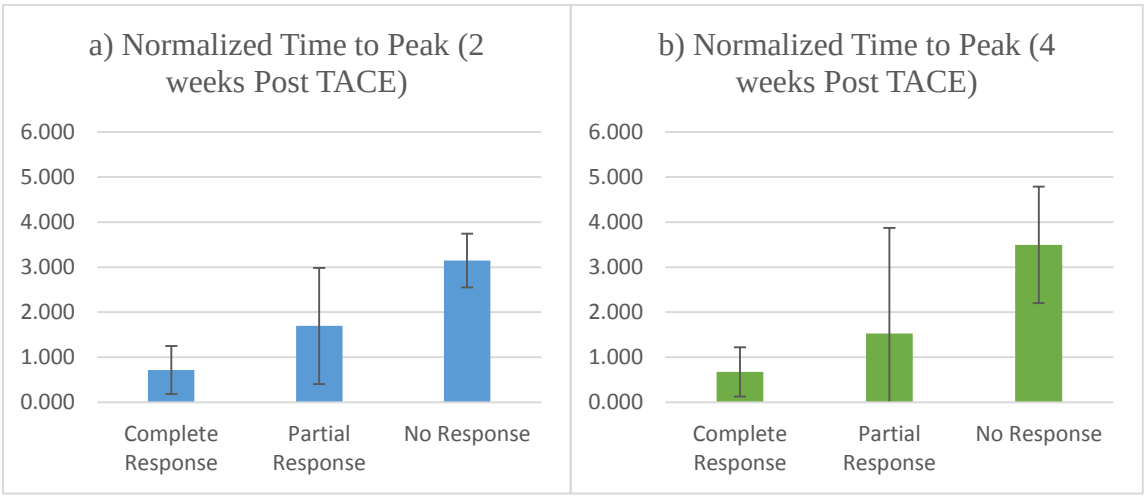

Figure 4.48: Average of normalized time to peak a) 2 weeks post TACE, b) 4 weeks post TACE

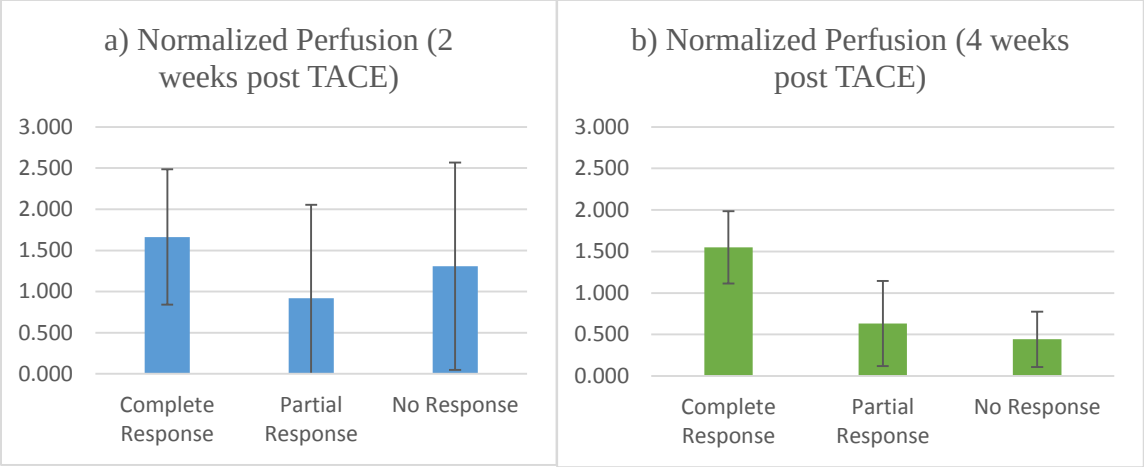

Figure 4.49: Average of normalized perfusion a) 2 weeks post TACE, b) 4 weeks post TACE

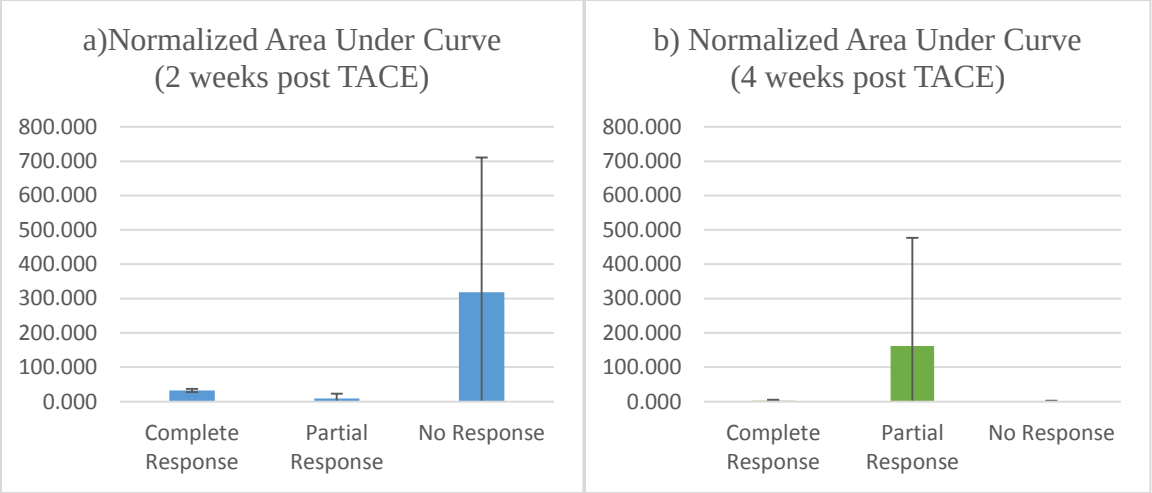

Figure 4.50: Average of normalized area under curve a) 2 weeks post TACE, b) 4 weeks post TACE

It can be noted from the graphs above, that there is a decrease in the perfusion as well as area under the curve value 2 weeks and 4 weeks post treatment in the case of complete response. However, on performing statistical analysis, these datasets do not show

significant difference. This may be due to small sample size used for the study, which is resulting in low statistical power.

5. DISCUSSION

Fourteen patients with 16 lesions were scanned. Out of these 16 lesions, 6 lesions were excluded inability to identify tumor. Motion compensation and parametric imaging were successfully performed in the 10 lesions. Statistical analysis performed on the parameters 2 weeks post TACE showed a significant value in case of time to peak ($p=0.047$), but no significant difference in case of MAX, PER and AUC. No significant difference was seen in any of the four parameters 4 weeks post TACE. On performing pairwise comparison between the three outcome groups, significant difference was seen between complete response and no response ($p=0.018$) in time to peak 2 weeks post TACE. However, there was no significant difference between the complete and partial response group ($p=0.188$) and between partial response and no response ($p=0.116$). Thus, contrast enhanced evaluation of transarterial chemoembolization does appear to be an effective follow up method 2 weeks post TACE.

Studies conducted by Kono et al. showed lack of detected contrast agent 2 days post TACE. The study was performed on 29 patients who were scheduled for a TACE procedure. The authors report that if CEUS performed within days after TACE is as sensitive as they had reported in their study, it would prove to be an attractive alternative to contrast enhanced CT/MRI [40]. This is because sonography is inexpensive, assessable, and can be performed repeatedly at the bedside.

In the case of TACE, it is not clear whether residual tumor blood flow detected shortly after TACE is an indication of treatment failure, as the chemotherapy in the beads still continue to treat residual tumor tissue.

There were a number of limitations to this study. Firstly, only 10 lesions were used for the study. A small sample size results in low statistical power. The statistical power of this study was calculated to be 60.23%. This in turn reduces the chances of detecting the true effect. Excessive motion artifacts and noise made identification of tumor difficult even after motion compensation was performed on the CEUS scans.

6. CONCLUSION AND FUTURE WORK

The overall objective of this thesis was to determine the feasibility of using contrast enhanced ultrasound for the evaluation of transarterial chemoembolization with drug eluting beads. The purpose of the study is to establish whether changes in blood flow parameters relative to baseline correlate with effective chemoembolization.

Performing motion compensation on the CEUS data helps remove the motion artifacts and frames plagued with noise. The time intensity curve parameters considered for the study were maximum pixel intensity, time to peak, perfusion and area under curve. These parameters were averaged over the tumor and expresses normalized relative to baseline. Statistical analysis was performed on these datasets and significant difference was observed only in the time to peak dataset 2 weeks post TACE procedure. Time to peak currently appears to be a good quantitative CEUS parameter to evaluate TACE effectiveness.

The results presented in this study are based on a limited sample size (10 lesions). As this was a pilot study, no sample size assessment could be made a priori. The number of subjects selected was based on the investigators experience and the norms associated with pilot studies conducted in radiology. A similar study conducted on a larger scale with more number of patients would increase the statistical power of the study.

List of References

[1] Simon Elliott,"Liver" Clinical Ultrasound, Chapter 7, 93-103, Third Edition, Elsevier Limited

[2] Vikramjit Mitra, Jane Metcalf, "Functional Anatomy and Blood Supply of the Liver", Anaesthesia and intensive care medicine, Volume 13, Issue 2,2011

[3] John E. Hall, "The Liver as an Organ",Guyton and Hall textbook of Medical Physiology, Twelfth edition.

[4] Sherman M.," Hepatocellular Carcinoma: epidemiology, surveillance, And diagnosis." Semin Liver Dis 2010; 30: 3–16

[5] Alterkruse SF, McGlynn KA, Reichman ME, "Hepatocellular Carcinoma Incidence, Mortality, and Survival Trends in the United States from 1975 to 2005", J. Clinical Oncology., 27:1485-1492,2009

[6] Mazzaferro V, Regalia E, Doci R, et al. "Liver Transplantation for the Treatment of Small Hepatocellular Carcinomas in Patients with Cirrhosis". N. Engl. J. Med., 334:693-699, 1996.

[7] Alejandro Forner, Josep M Llovet, Jordi Bruix, "Hepatocellular Carcinoma" The Lancet, vol 379, 2012

[8] Llovet JM, Fuster J, Bruix J. "Intention-to-treat Analysis of Surgical Treatment for Early Hepatocellular Carcinoma: Resection versus Transplantation." Hepatology, 39:1434-1440, 1999.

[9] Llovet JM, Bruix J. "Systematic Review of randomized trials for unresectrable hepatocellular carcinoma: Chemoembolization improves survival". Hepatology, 37:429-442, 2003.

[10] Yamada R, Kishi K, Sato M, et al. Transcatheter arterial chemoembolization (TACE) in the treatment of unresectable liver cancer. World J. Surg., 19:795-800, 1995.

[11] Wheatley, MARGARET A. "Composition of contrast microbubbles: Basic chemistry of encapsulated and surfactant-coated bubbles." Ultrasound Contrast Agents: Basic principles and clinical applications. 2nd ed. London: Martin Dunitz (2001): 3.

[12] Bouakaz A, de Jong N. WFUMB Safety Symposium on Echo-Contrast Agents: nature and types of ultrasound contrast agents. Ultrasound Med Biol., 33:187-196, 2007.

[13] Gelfand DW: "Anatomy of the liver". Radiol Clin North Am 1980; 18: pp. 187-194

[14] "Cancer Facts & Figures 2015", American Cancer Society,Inc.

[15] Sun et. al, "Symptom Management in Heptocellular Carcinoma", Clinical Journal of Oncology Nursing, 12.5: 759-66, 2008

[16] "Hepatocellular Carcinoma", Ferri's Clinical Advisor, 2015

[17] Jordi Bruix, "Treatment of Hepatocellular Carcinoma", Hepatology, vol 25, No.2, 1997

[18] Wijlemans J. W, Bartels L.W, et al. :Magnetic resonance-guided high-intensity focused ultrasound (MR-HIFU) ablation of liver tumors", Cancer Imaging, 387-394, 2012

[19] Tito Livraghi, "Radio Frequency Ablation of Hepatocellular Carcinoma", Surg Oncol Clin N Am 20, 281-299, 2011

[20] Carin F. Gonsalves, Daniel B. Brown, "Chemoembolization of hepatic malignancy", Abdominal Imaging, 34:557-565, 2009

[21] Chapman WC, Majella Doyle MB, Stuart JE, et al. "Outcomes of neoadjuvant transarterial chemoembolization to downstage hepatocellular carcinoma before liver transplantation". Ann. Surg., 248:617-625, 2008.

[22] Vogl TJ, Lemmer J, Lencioni R, et al., "Liver, gastrointestinal, and cardiac toxicity in intermediate hepatocellular carcinoma treated with PRECISION TACE with drug-eluting beads: results from the PRECISION V randomized trial''. AJR Am. J. Roentgenol., 197:W562-570, 2011.

[23] Lammer J, Malagrari K, Vogl T, et al. "Prospective randomized study of doxorubicin-eluting-bead embolizaion in the treatment of hepatocellular carcinoma: results of the PRECISION V study". Cardiovasc. Intervent. Radiol. 33:41-52, 2010.

[24] Lewis AL, Gonzalez MV, Lloyd AW, et al. "DC Bead: In Vitro characterization of a drug-delivery device for transarterial chemoembolization". J. Vasc. Interv. Radiol., 17:335-342, 2006.

[25] Brown DB, Nickolic B, Covey AM, et al. “Quality improvement guidelines for transhepatic arterial chemoembolization, embolization, and chemotherapeutic infusion for hepatic malignancy”, J. Vasc. Interv. Radiol. In Press

[26] Yan FH, Zhou KR, Cheng JM, et al. “Role and limitation of FMPSPGR dynamic contrast scanning in the follow-up of patients with hepatocellular carcinoma treated by TACE”. World J Gastroenterol 2002; 8:658–662

[27] Forsberg, F., et al. "Clinical applications of ultrasound contrast agents."Ultrasonics,36.1 (1998): 695-701

[28] Goldberg, Barry B., Joel S. Raichlen, and Flemming Forsberg. Ultrasound contrast agents: basic principles and clinical applications. Informa Healthcare, 2001.

[29] Frinking, Peter JA, et al. "Ultrasound contrast imaging: current and new potential Methods." Ultrasound in medicine & biology 26.6 (2000): 965-975.

[30] De Jong, N., R. Cornet, and C. T. Lancee. "Higher harmonics of vibrating gas-filled microspheres. Part one: simulations." *Ultrasonics* 32.6 (1994): 447-453.

[31] Szabo, Thomas L. Diagnostic ultrasound imaging: inside out. Access Online via Elsevier, 2004.

[32] Faez, Telli, et al. "20 years of ultrasound contrast agent modeling." IEEE Transactions on Ultrasonics, Ferroelectrics and Frequency Control 60.1 (2013): 7-20.

[33] Hyde et al., “Comparison of Maximum Intensity Projection and digitally reconstructed projection for carotid artery stenosis measurement”, Med Phys 2007, 34:2968-2974

[34] Dave, Jaydev K., “Novel automated compensation algorithm for producing cumulative maximum intensity images from subharmonic ultrasound imaging of breast lesions”, idea.library.drexel.edu. Drexel University, Web 2015

[35] H. Zhuang et al. “Time-intensity curve parameters in colorectal tumors measured using double contrast-enhanced ultrasound: correlations with tumor angiogenesis”, The Association of coloproctology of Great Britain and Ireland, 14, 181-187, 2011

[36] Miller AP, Nanda NC, “Contrast echocardiography: now agents”, Ultrasound Med Biol. 30:425-435, 2004

[37] “Prescribing Information” DEFINITY®, Web May 30th, 2015

[38] ACUSON Sequoia™ C512 Echocardiography System Transducers, Web May 30th 2015.

[39] Sussane M. Stieger et al.,"Imaging of angiogenesis using Cadence™ contrst pulse sequencing and targeted contrast agents", Wiley InterScience, 2008

[40] Kono Y, Lucidarme O, Choi SH, et al. Contrast-enhanced ultrasound as a predictor of treatment efficacy within 2 weeks alter transarterial chemoembolization of hepatocellular carcinoma. J. Vasc. Interv. Radiol. 18:57-65, 2007.

APPENDIX A: RESULTS: PARAMETRIC IMAGES

APPENDIX A.1: PATIENT 01

Pre- treatment

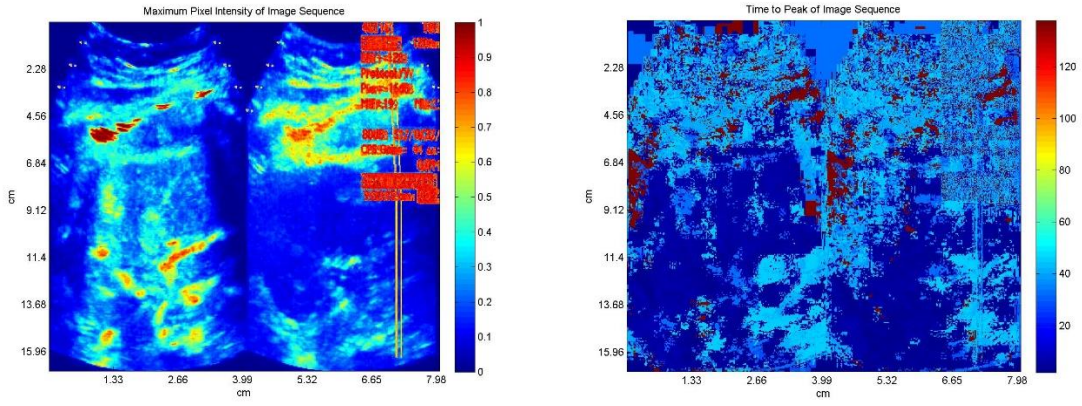

(a) **(b)**

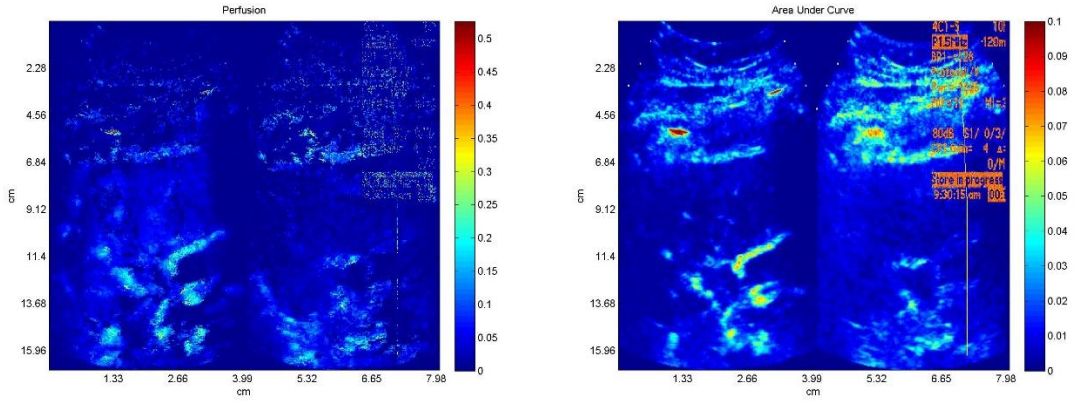

(c) **(d)**

a) Maximum Pixel Intensity of sequence, b) Time to peak of Sequence, c) Perfusion, d) Area under Curve

2 weeks post TACE

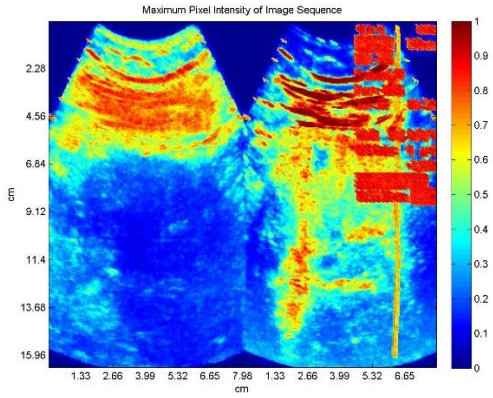

(a)

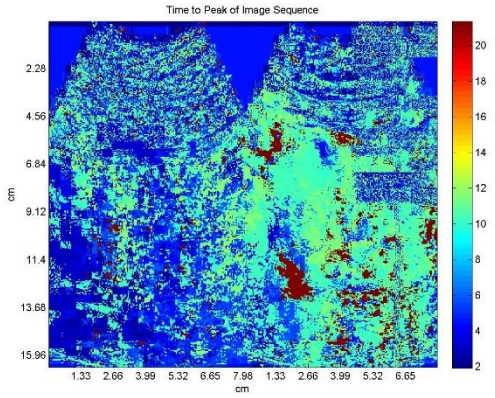

(b)

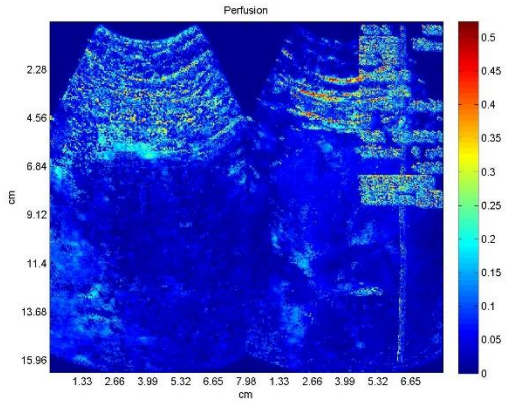

(c)

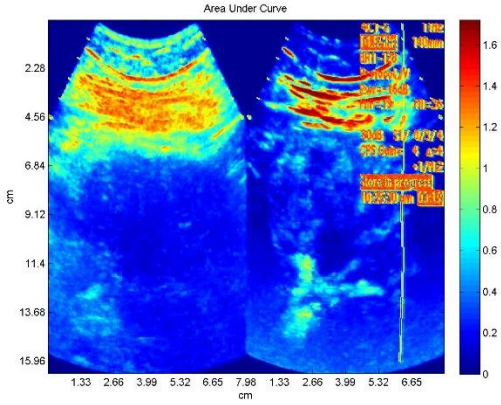

(d)

a) Maximum Pixel Intensity of sequence, b) Time to peak of Sequence, c) Perfusion, d) Area under Curve

4 weeks post TACE

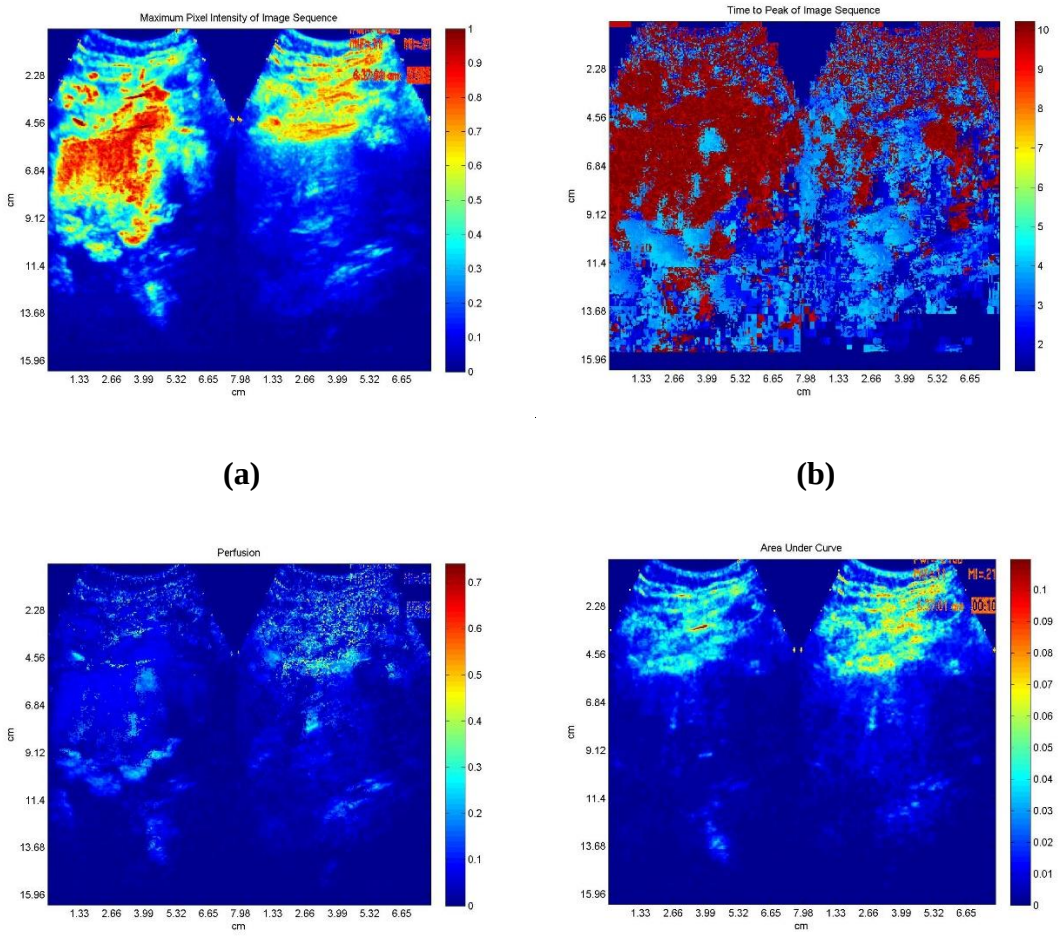

(a) **(b)**

(c) **(d)**

a) Maximum Pixel Intensity of sequence, b) Time to peak of Sequence, c) Perfusion, d) Area under Curve

APPENDIX A.2: PATIENT 02

Pre-treatment

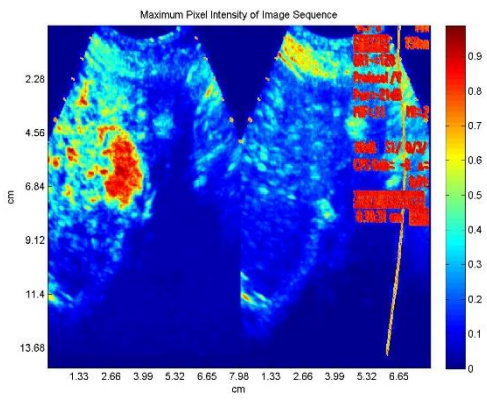

(a)

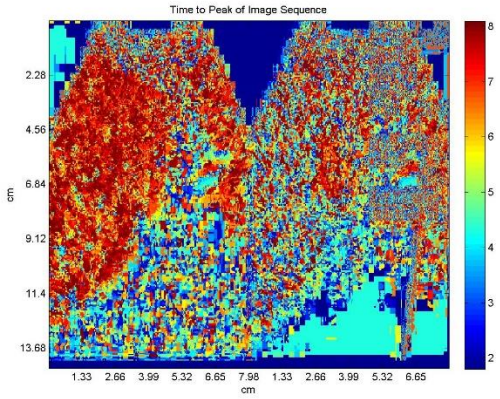

(b)

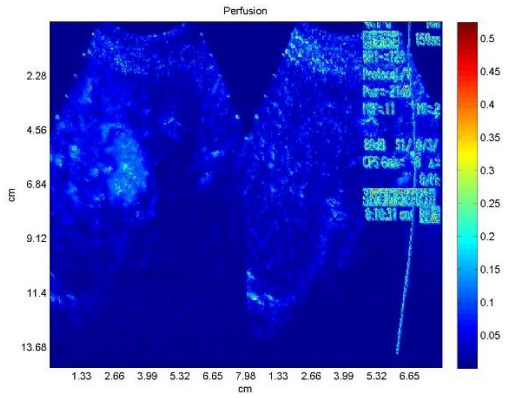

(c)

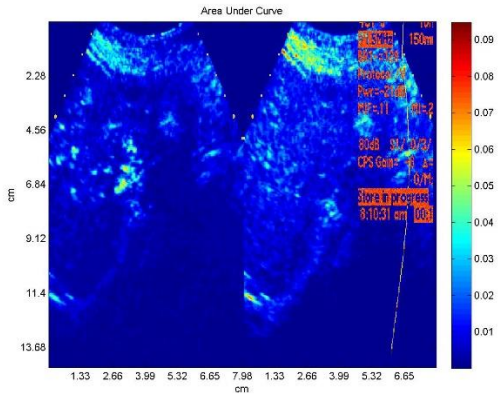

(d)

a) Maximum Pixel Intensity of sequence, b) Time to peak of Sequence, c) Perfusion, d) Area under Curve

2 weeks post TACE

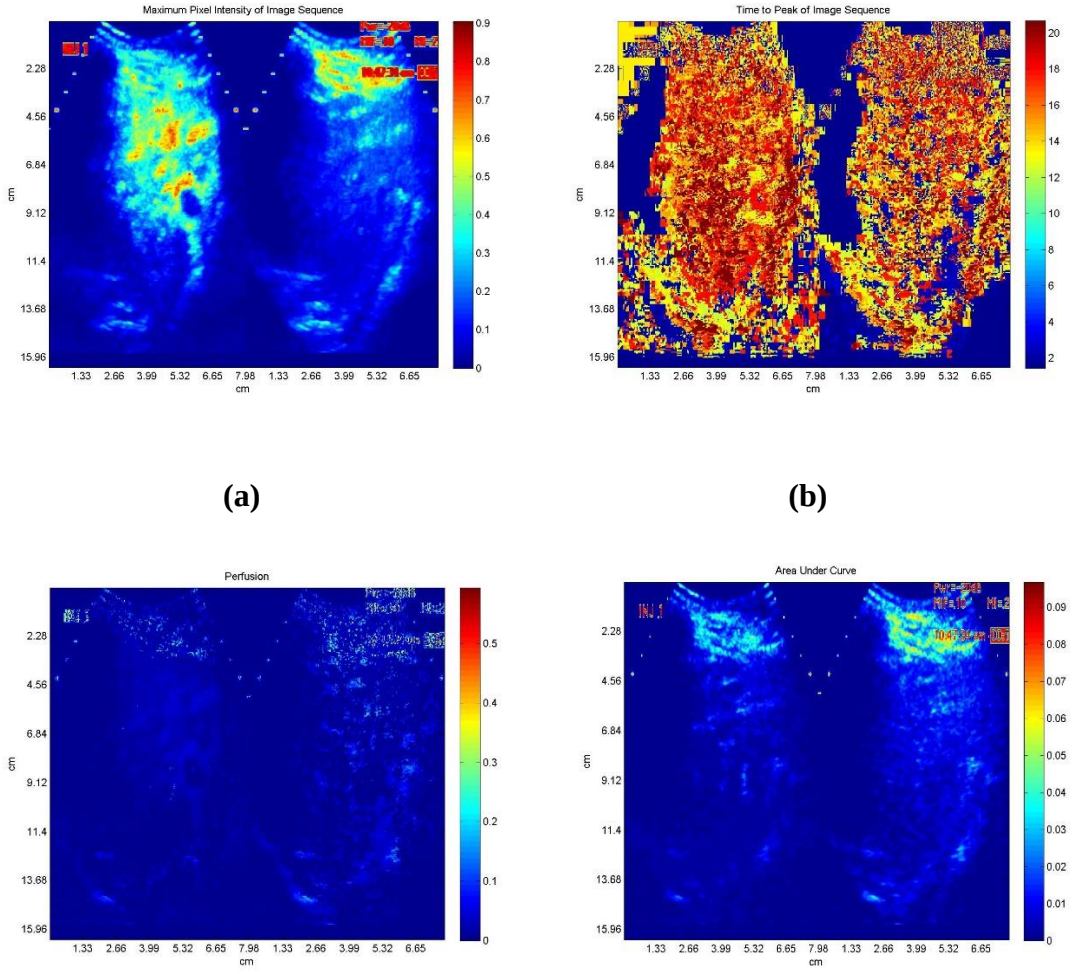

(a) **(b)**

(c) **(d)**

a) Maximum Pixel Intensity of sequence, b) Time to peak of Sequence, c) Perfusion, d) Area under Curve

4 weeks post TACE

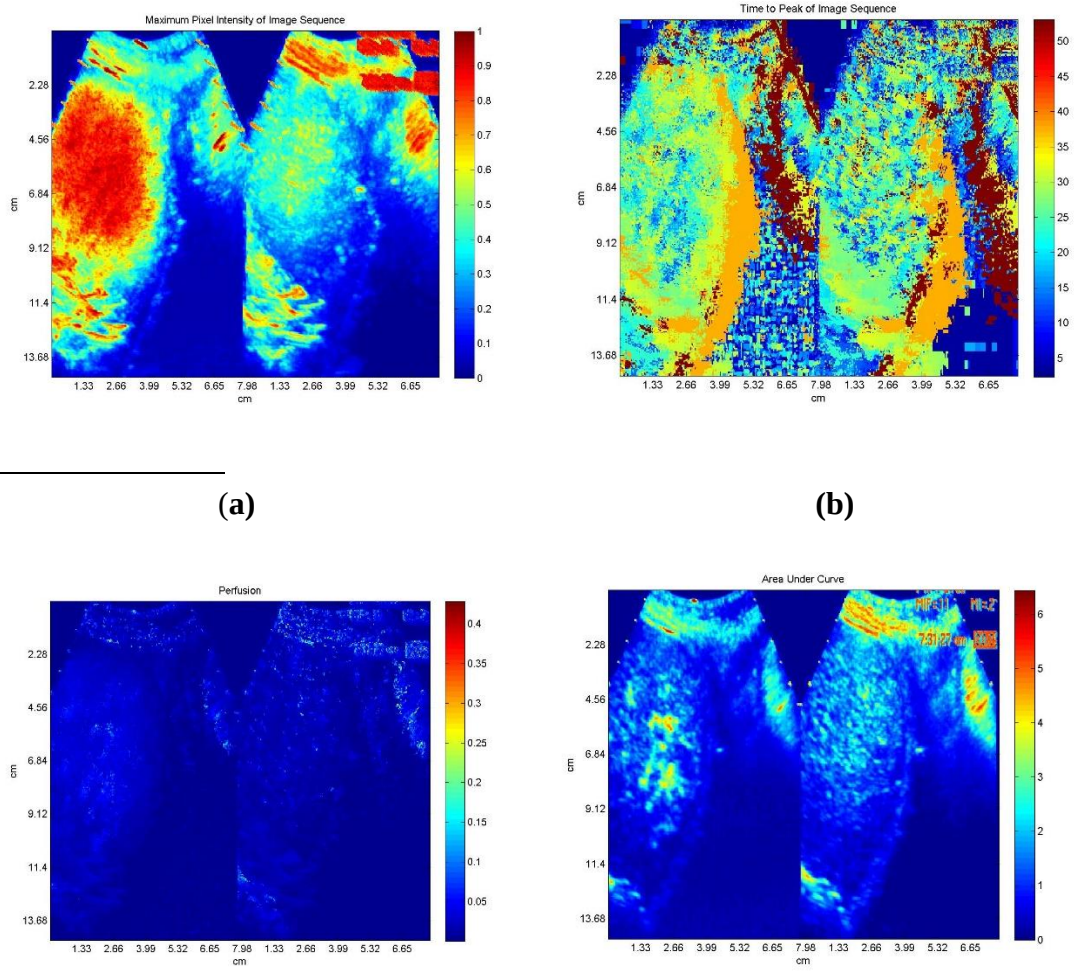

(a) **(b)**

(c) **(d)**

a) Maximum Pixel Intensity of sequence, b) Time to peak of Sequence, c) Perfusion, d) Area under Curve

APPENDIX A.3: PATIENT 05

Pre-treatment

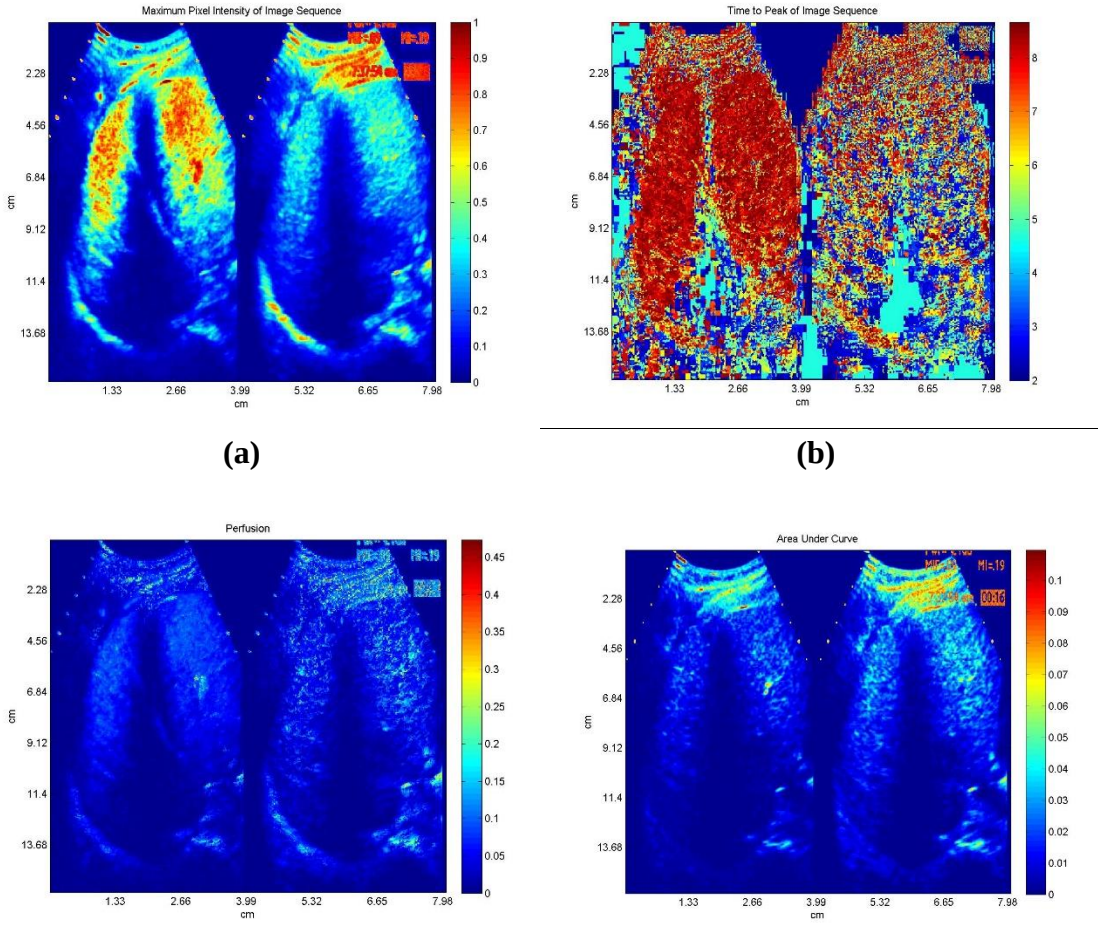

(a) **(b)**

(c) **(d)**

a) Maximum Pixel Intensity of sequence, b) Time to peak of Sequence, c) Perfusion, d) Area under Curve

2 weeks post TACE

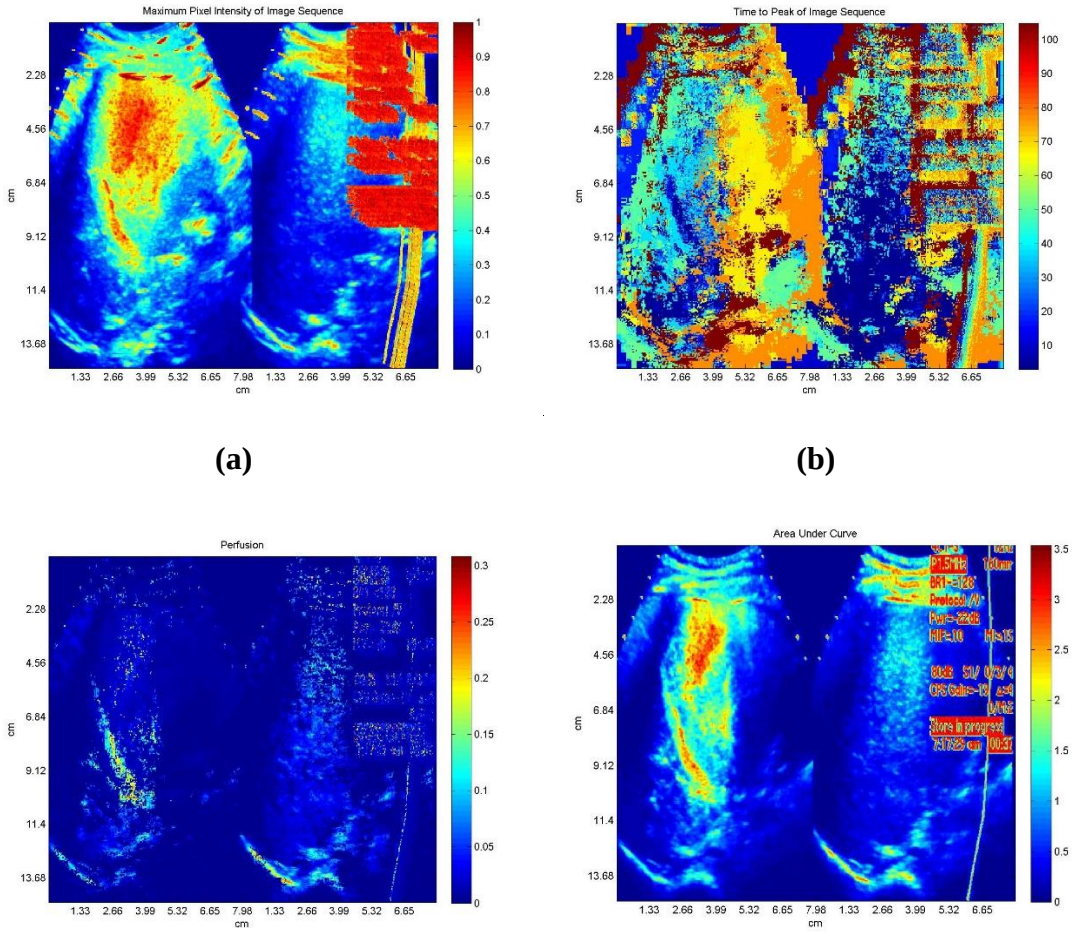

(a) **(b)**

(c) **(d)**

a) Maximum Pixel Intensity of sequence, b) Time to peak of Sequence, c) Perfusion, d) Area under Curve

4 weeks post TACE

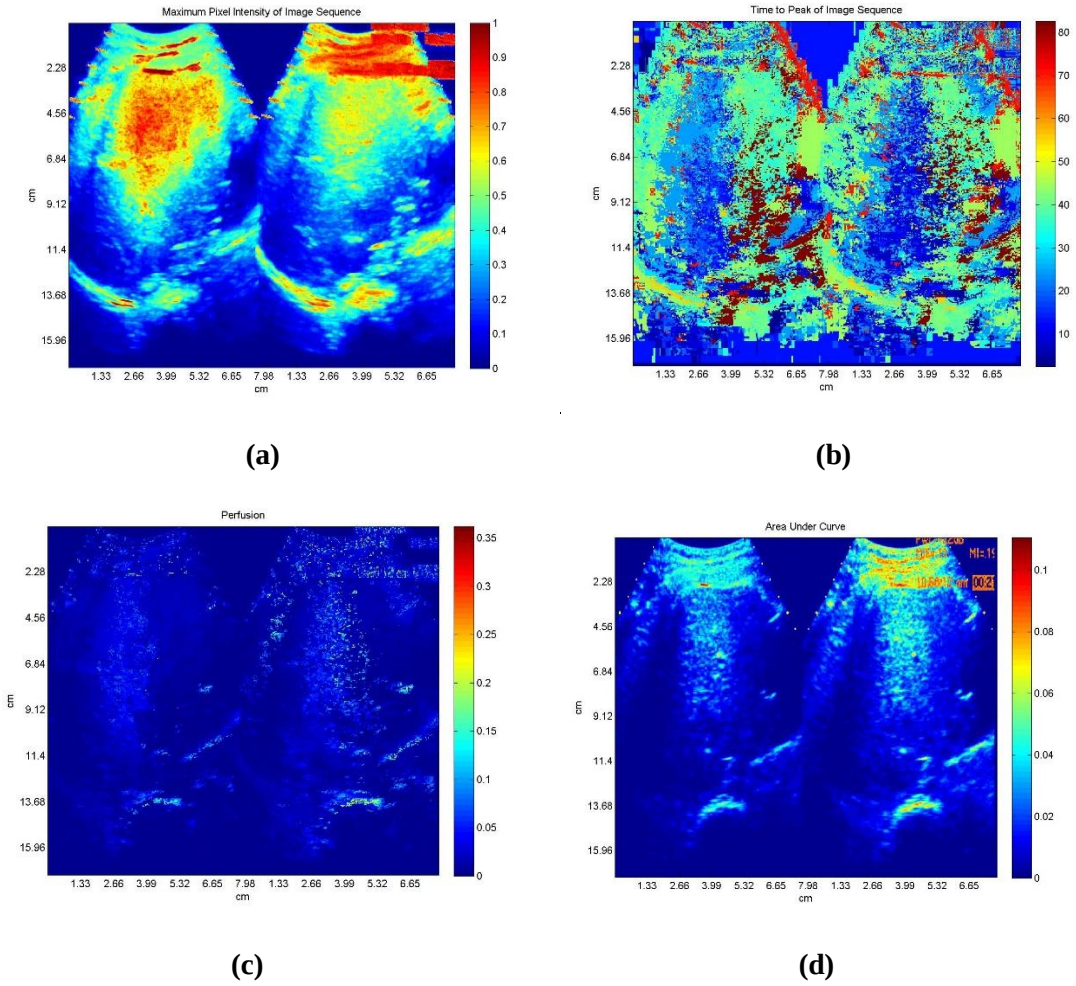

(a) **(b)**

(c) **(d)**

a) Maximum Pixel Intensity of sequence, b) Time to peak of Sequence, c) Perfusion, d) Area under Curve

APPENDIX A.4: PATIENT 06

Pre-treatment

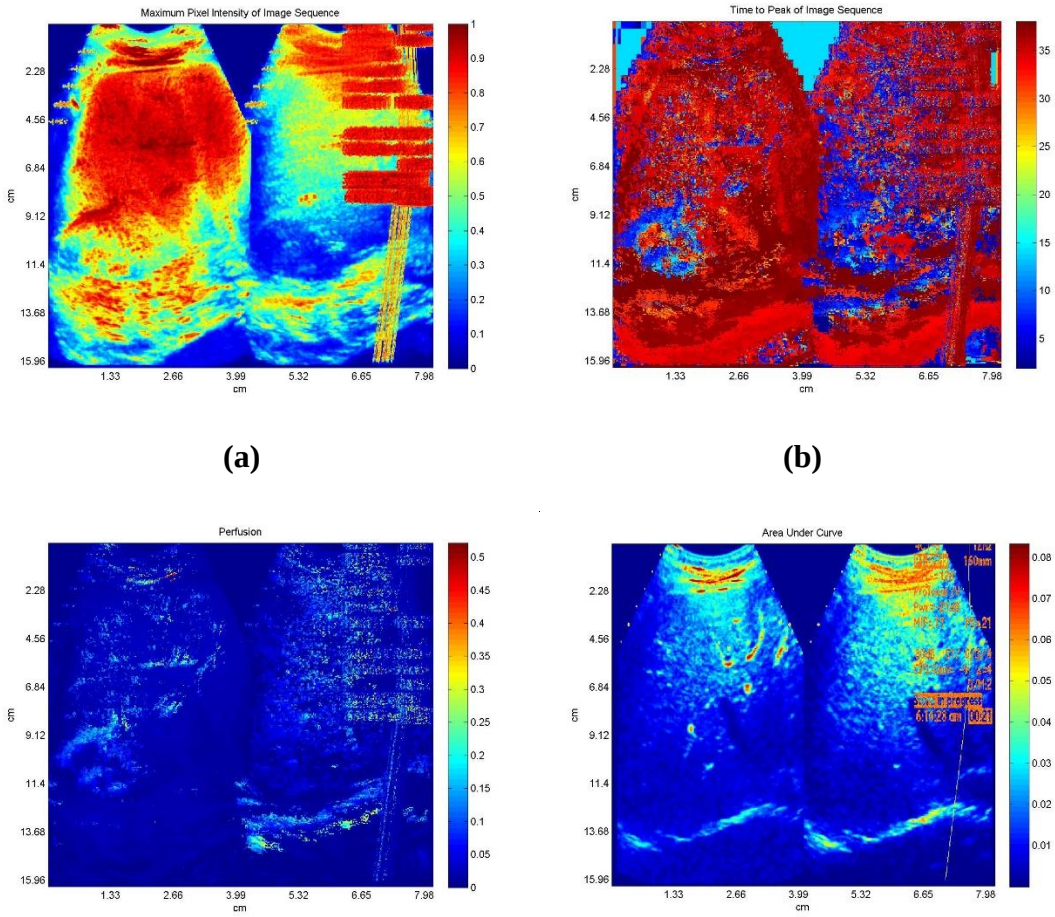

(a) **(b)**

(c) **(d)**

a) Maximum Pixel Intensity of sequence, b) Time to peak of Sequence, c) Perfusion, d) Area under Curve

4 weeks post TACE

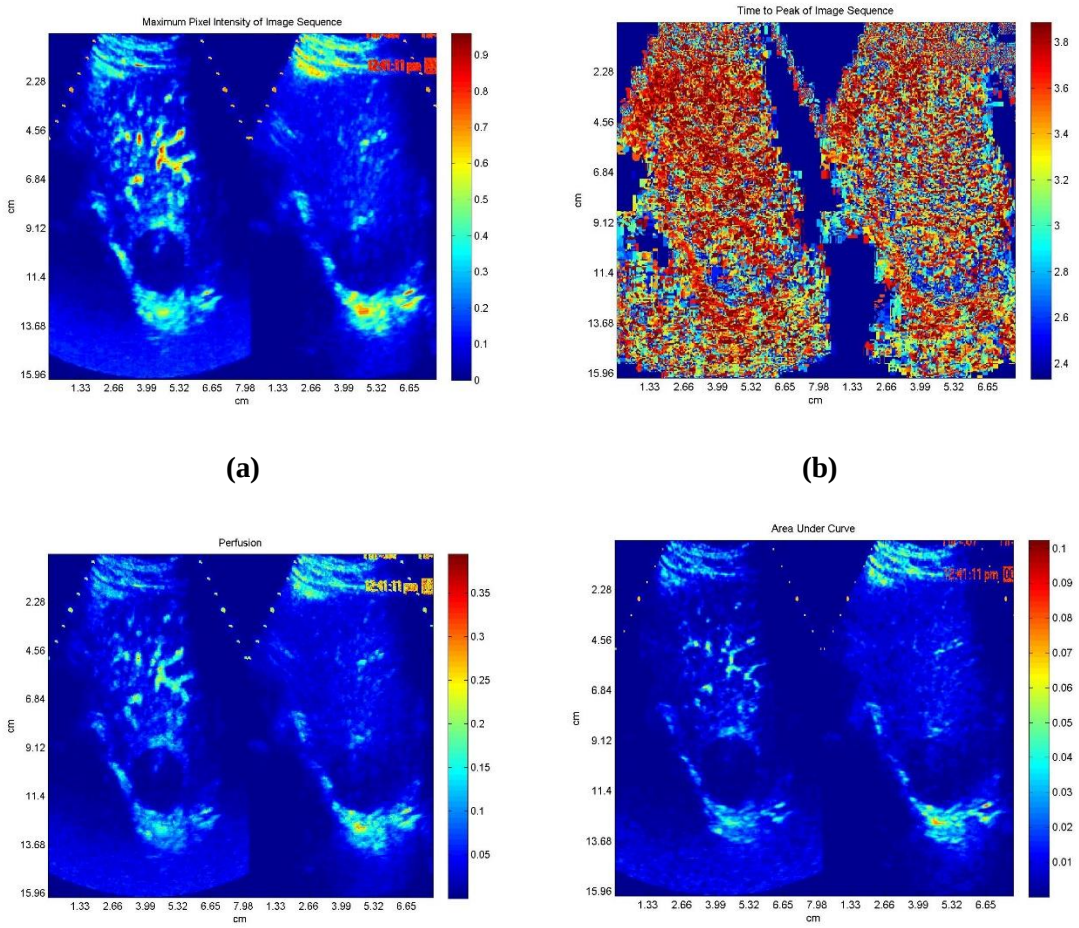

(a) **(b)**

(c) **(d)**

a) Maximum Pixel Intensity of sequence, b) Time to peak of Sequence, c) Perfusion, d) Area under Curve

APPENDIX A.5: PATIENT 07

Pre-treatment

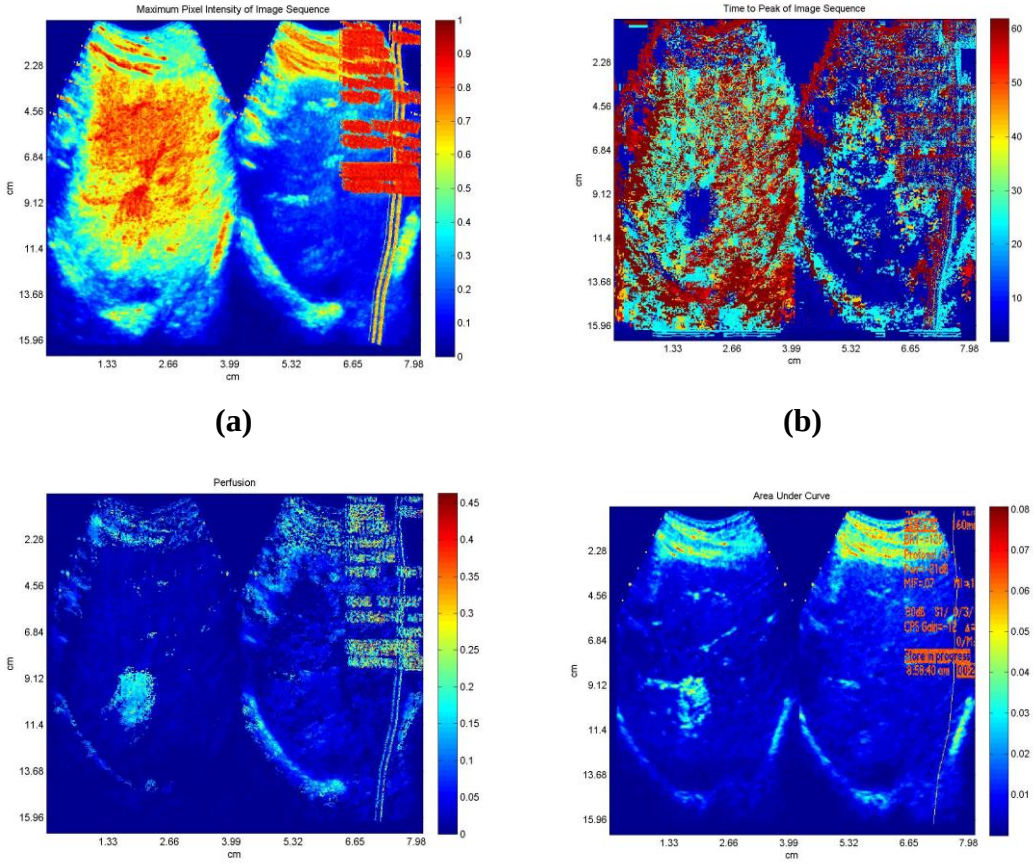

(a) **(b)**

(c) **(d)**

a) Maximum Pixel Intensity of sequence, b) Time to peak of Sequence, c) Perfusion, d) Area under Curve

2 weeks post TACE

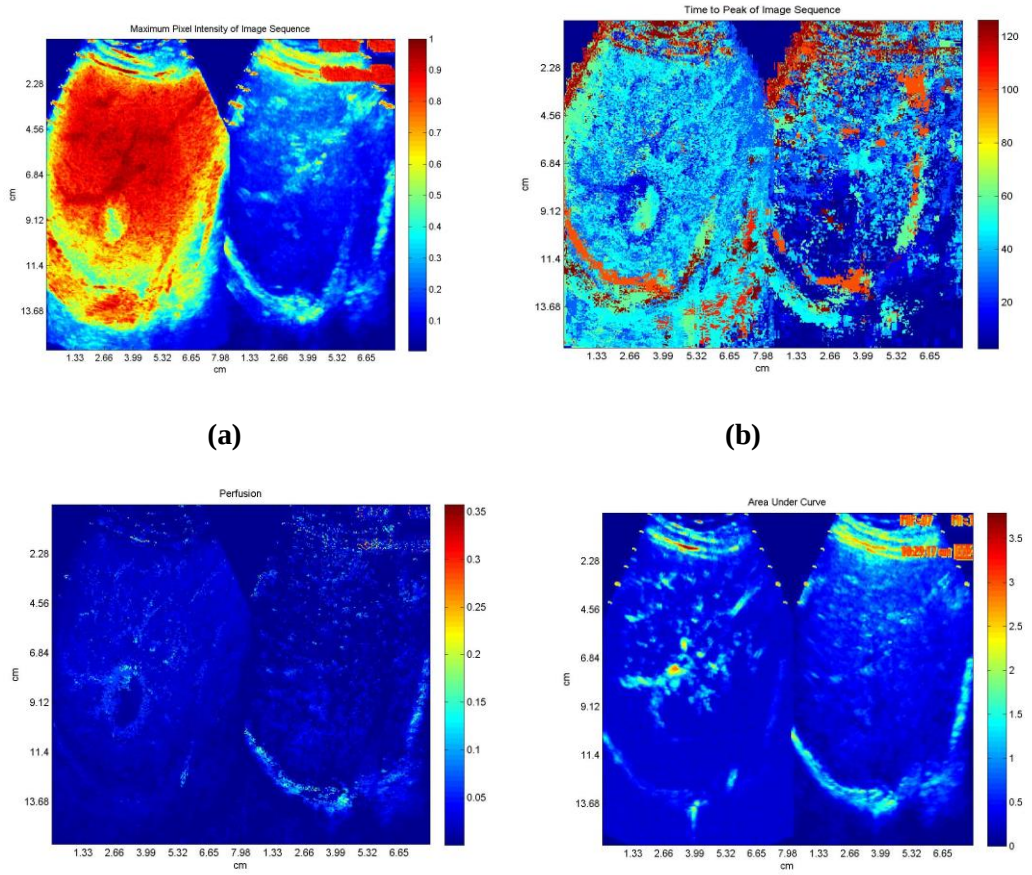

(a) **(b)**

(c) **(d)**

a) Maximum Pixel Intensity of sequence, b) Time to peak of Sequence, c) Perfusion, d) Area under Curve

4 weeks post TACE

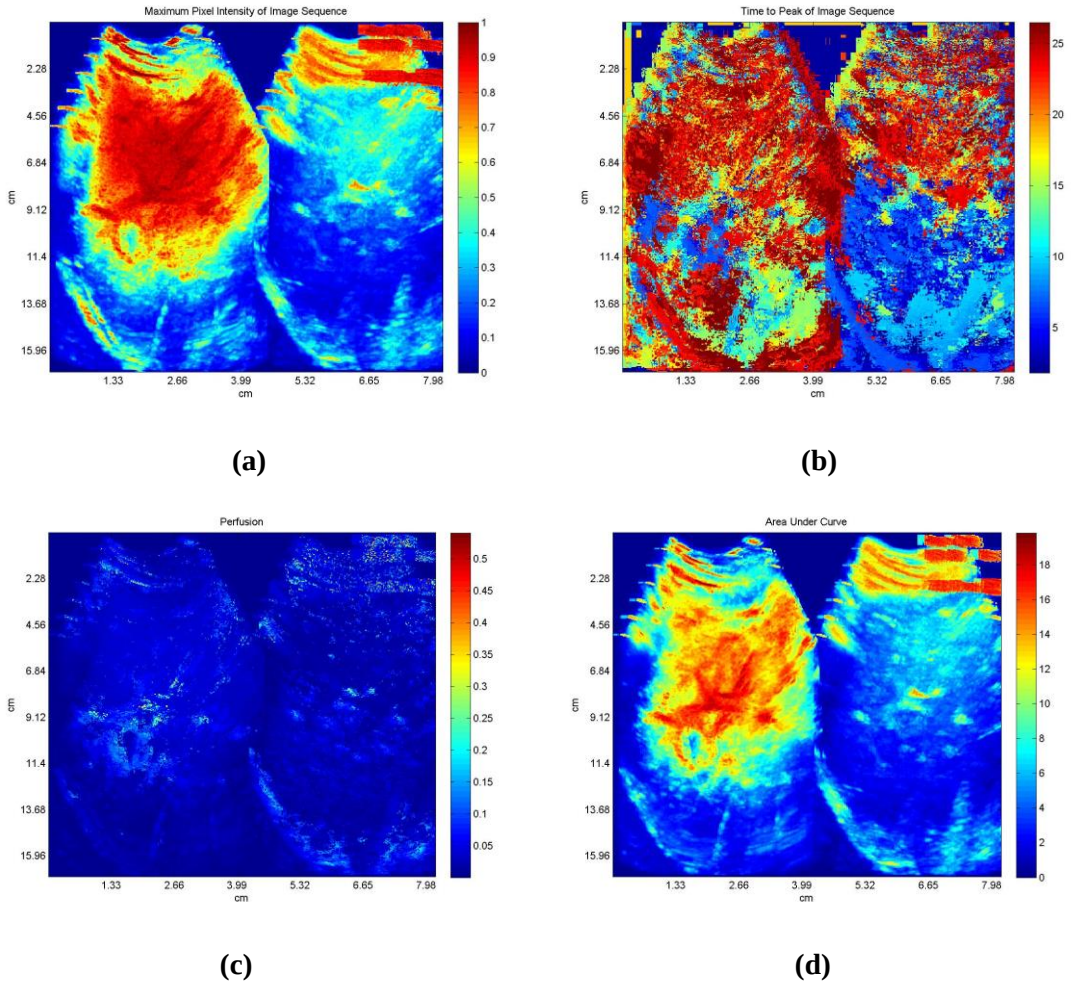

(a) **(b)**

(c) **(d)**

a) Maximum Pixel Intensity of sequence, b) Time to peak of Sequence, c) Perfusion, d) Area under Curve

APPENDIX A.6: PATIENT 08

Pre-treatment

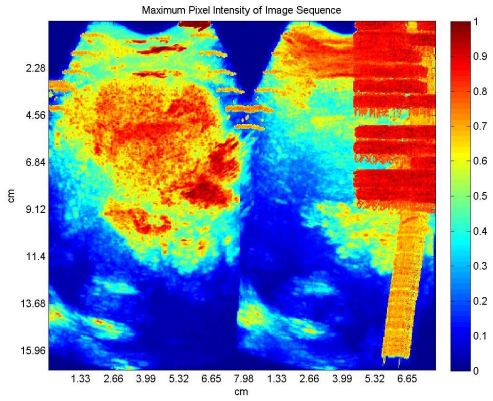

(a)

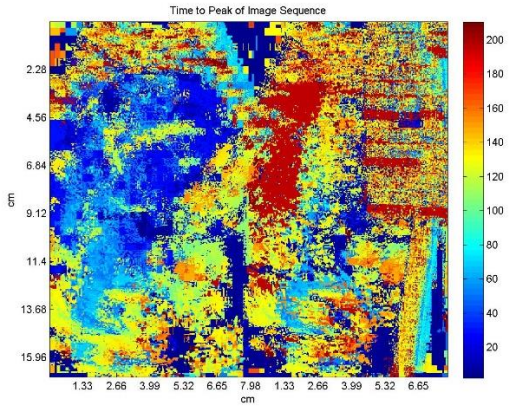

(b)

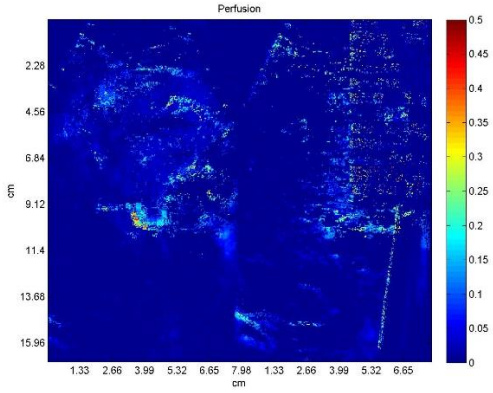

(c)

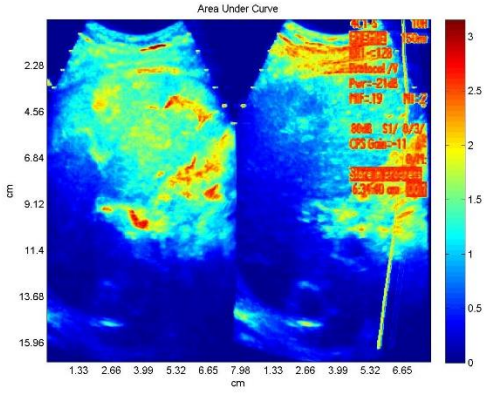

(d)

a) Maximum Pixel Intensity of sequence, b) Time to peak of Sequence, c) Perfusion, d) Area under Curve

2 Weeks post TACE

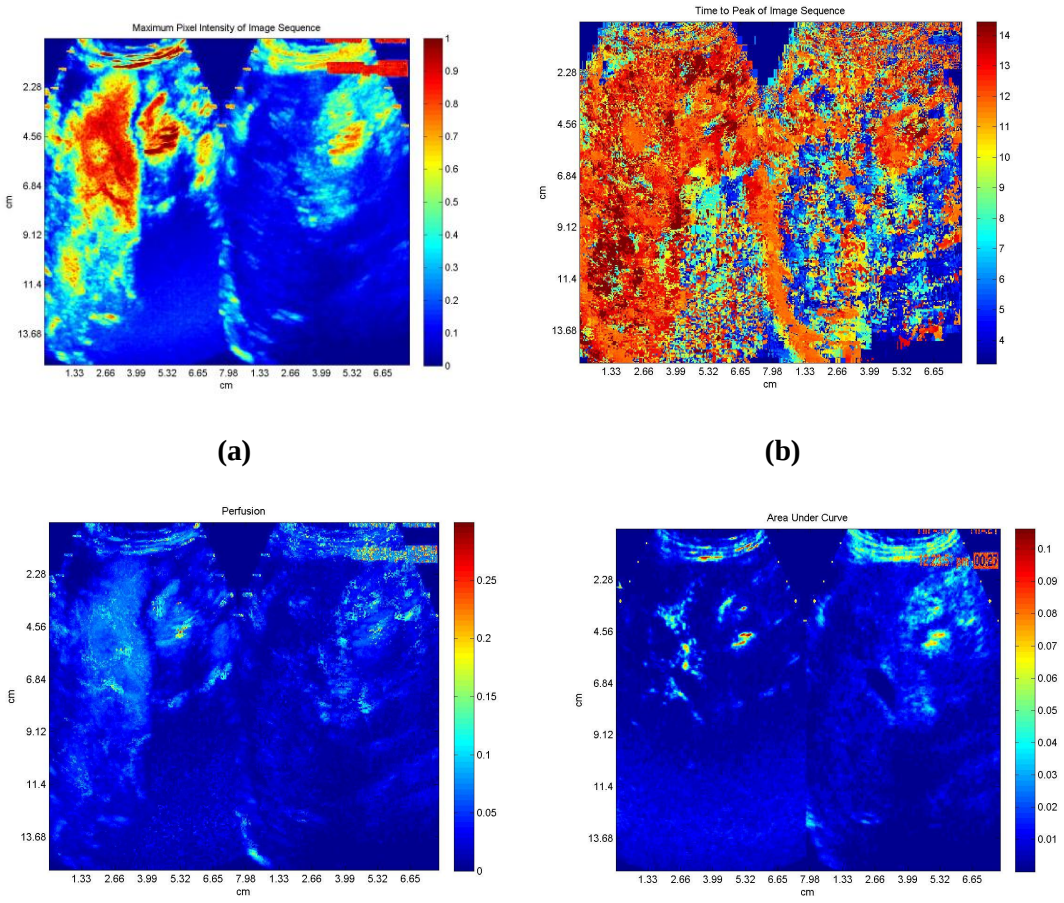

(a) **(b)**

(c) **(d)**

a) Maximum Pixel Intensity of sequence, b) Time to peak of Sequence, c) Perfusion, d) Area under Curve

4 weeks post TACE

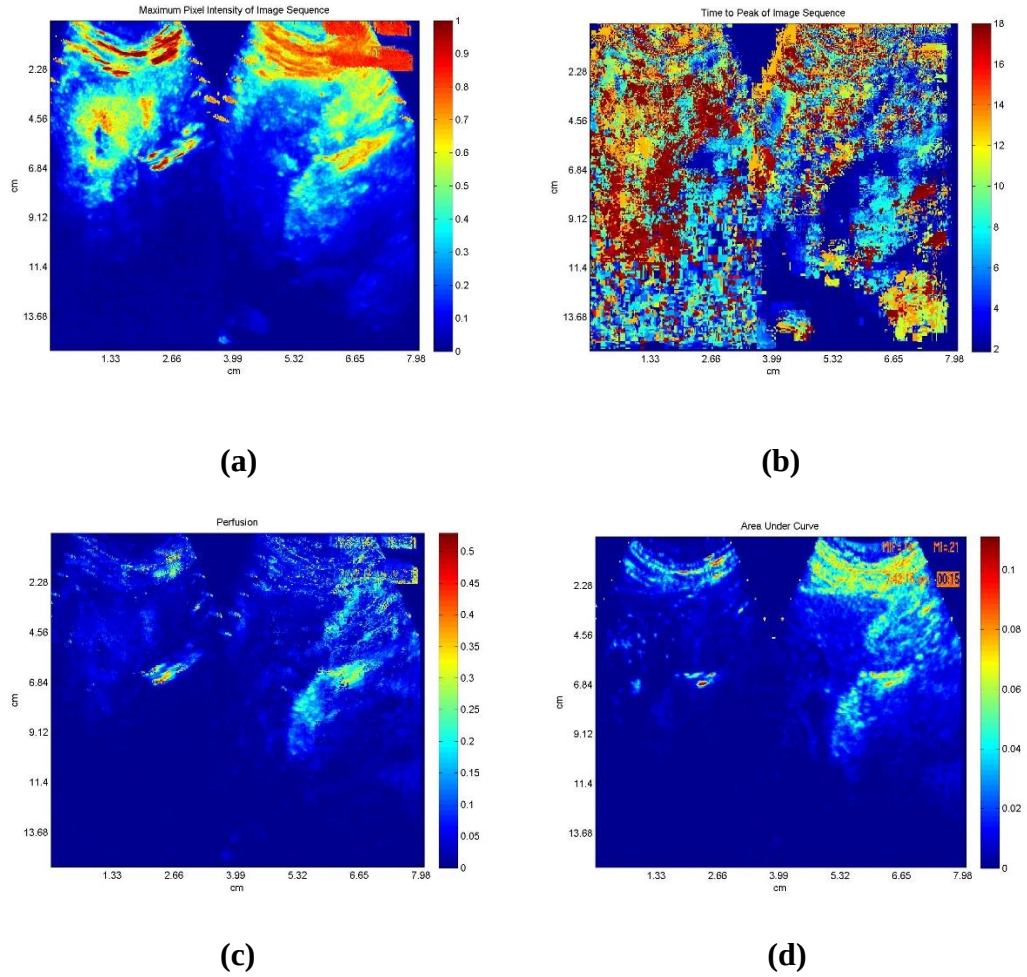

(a) **(b)**

(c) **(d)**

a) Maximum Pixel Intensity of sequence, b) Time to peak of Sequence, c) Perfusion, d) Area under Curve

APPENDIX A.7: PATIENT 10

Pre-treatment

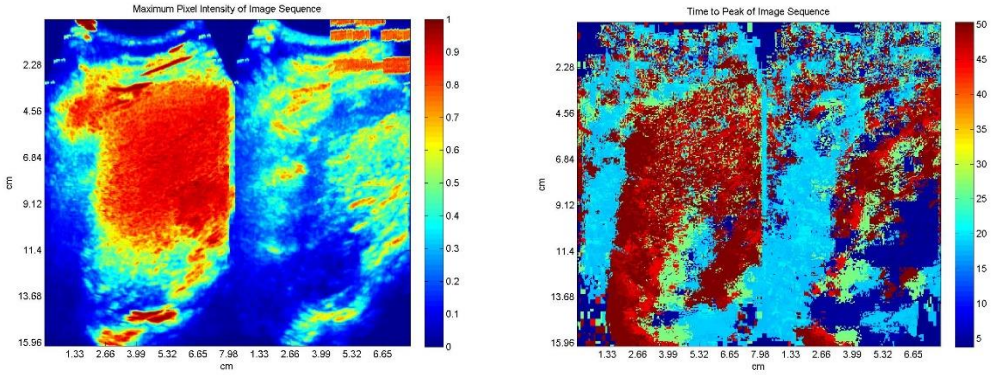

(a) **(b)**

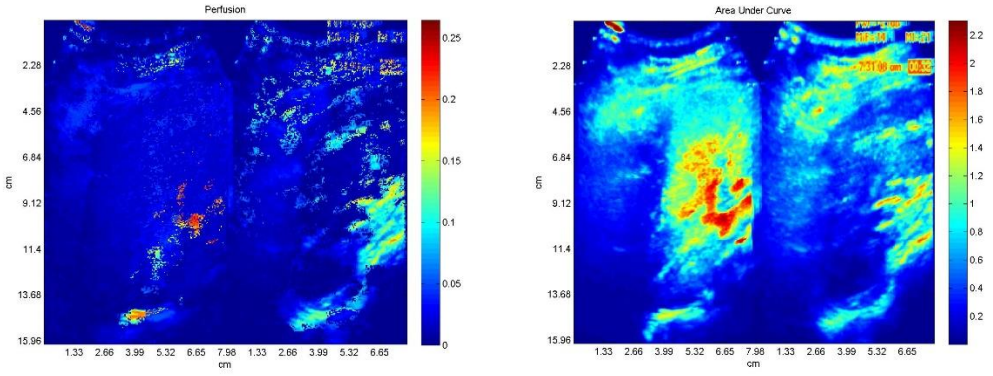

(c) **(d)**

a) Maximum Pixel Intensity of sequence, b) Time to peak of Sequence, c) Perfusion, d) Area under Curve

2 weeks post TACE

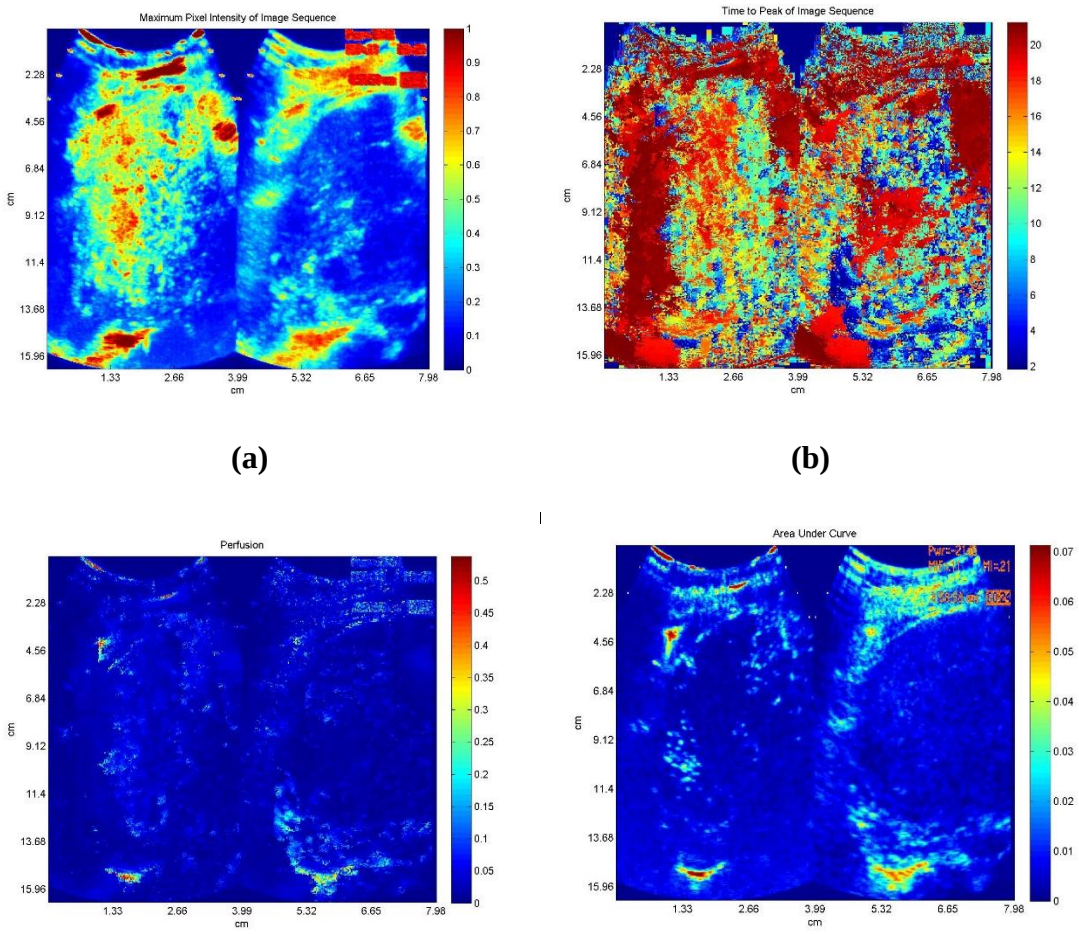

(a) **(b)**

(c) **(d)**

a) Maximum Pixel Intensity of sequence, b) Time to peak of Sequence, c) Perfusion, d) Area under Curve

4 weeks post TACE

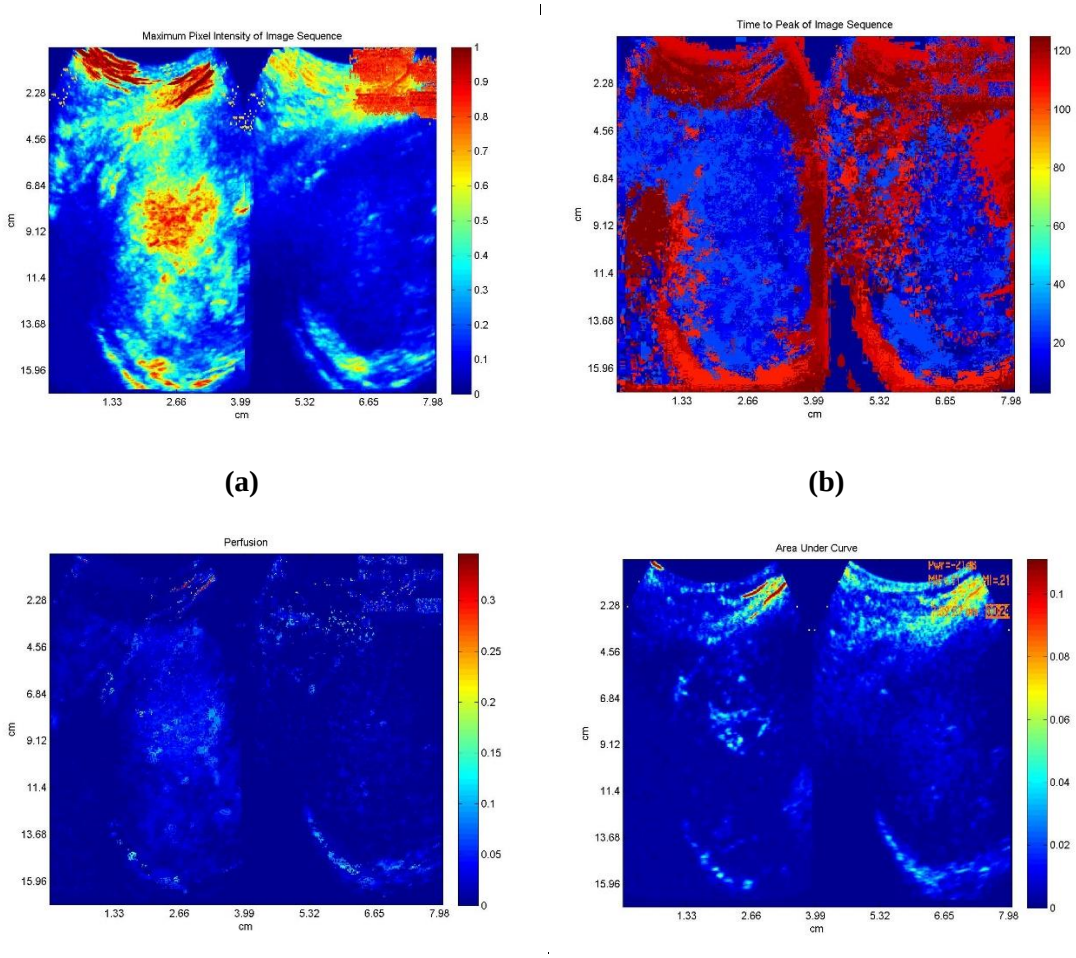

(a) **(b)**

(c) **(d)**

a) Maximum Pixel Intensity of sequence, b) Time to peak of Sequence, c) Perfusion, d) Area under Curve

APPENDIX A.8: PATIENT 11 Lesion 01

Pre-treatment

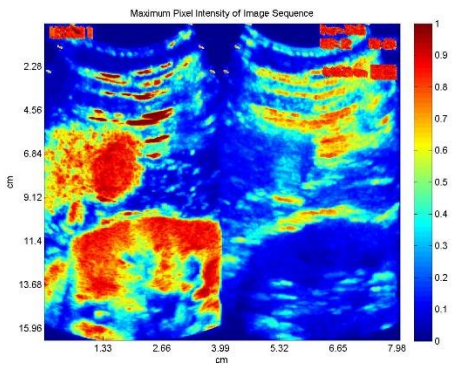

(a)

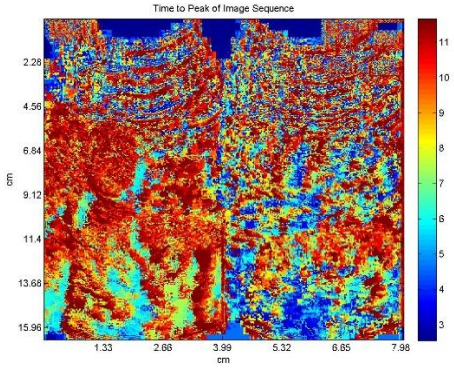

(b)

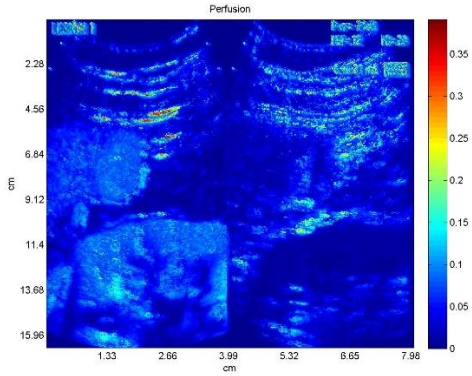

(c)

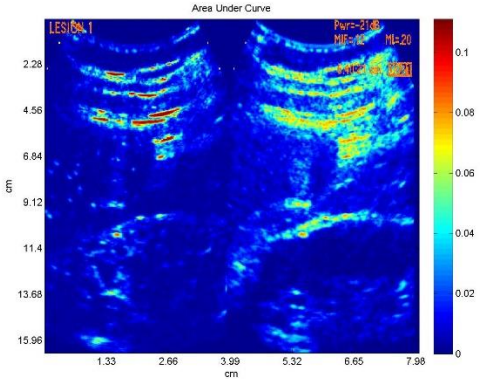

(d)

a) Maximum Pixel Intensity of sequence, b) Time to peak of Sequence, c) Perfusion, d) Area under Curve

2 weeks post TACE

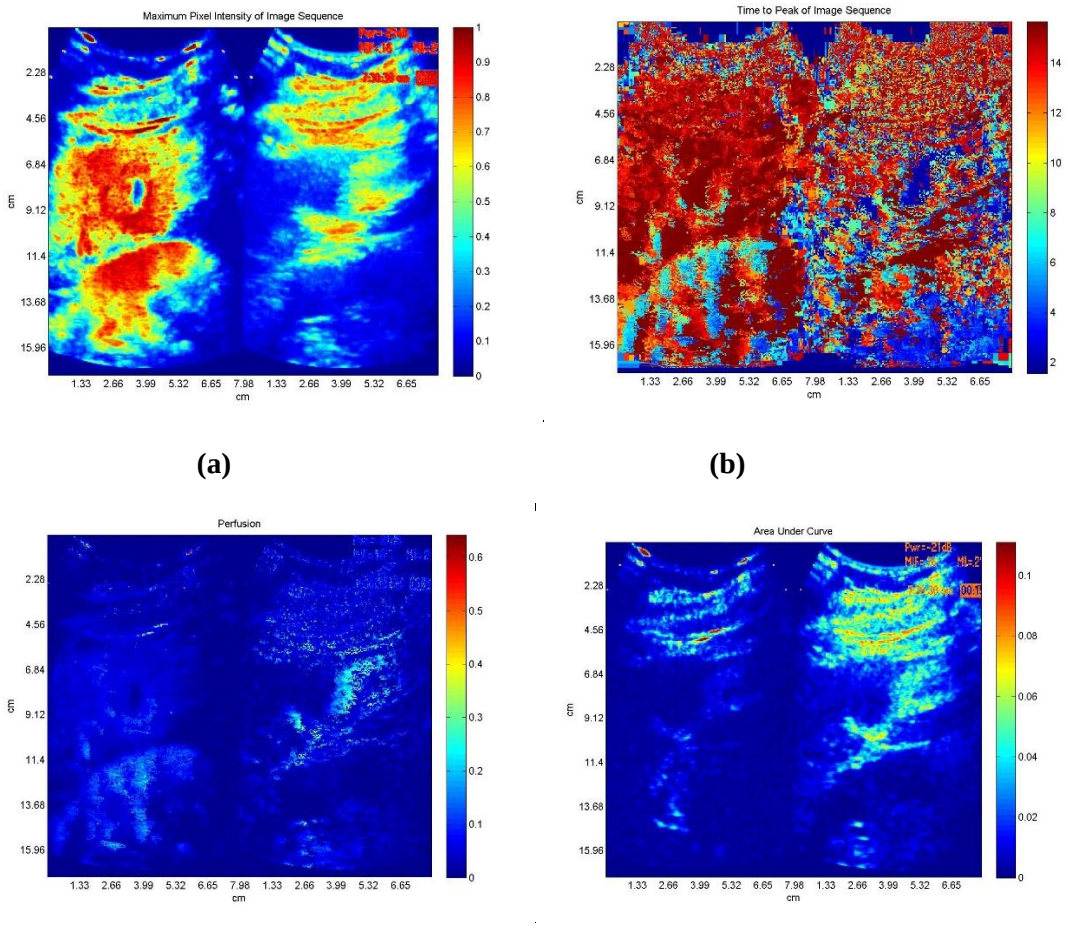

(a) **(b)**

(c) **(d)**

a) Maximum Pixel Intensity of sequence, b) Time to peak of Sequence, c) Perfusion, d) Area under Curve

4 weeks post TACE

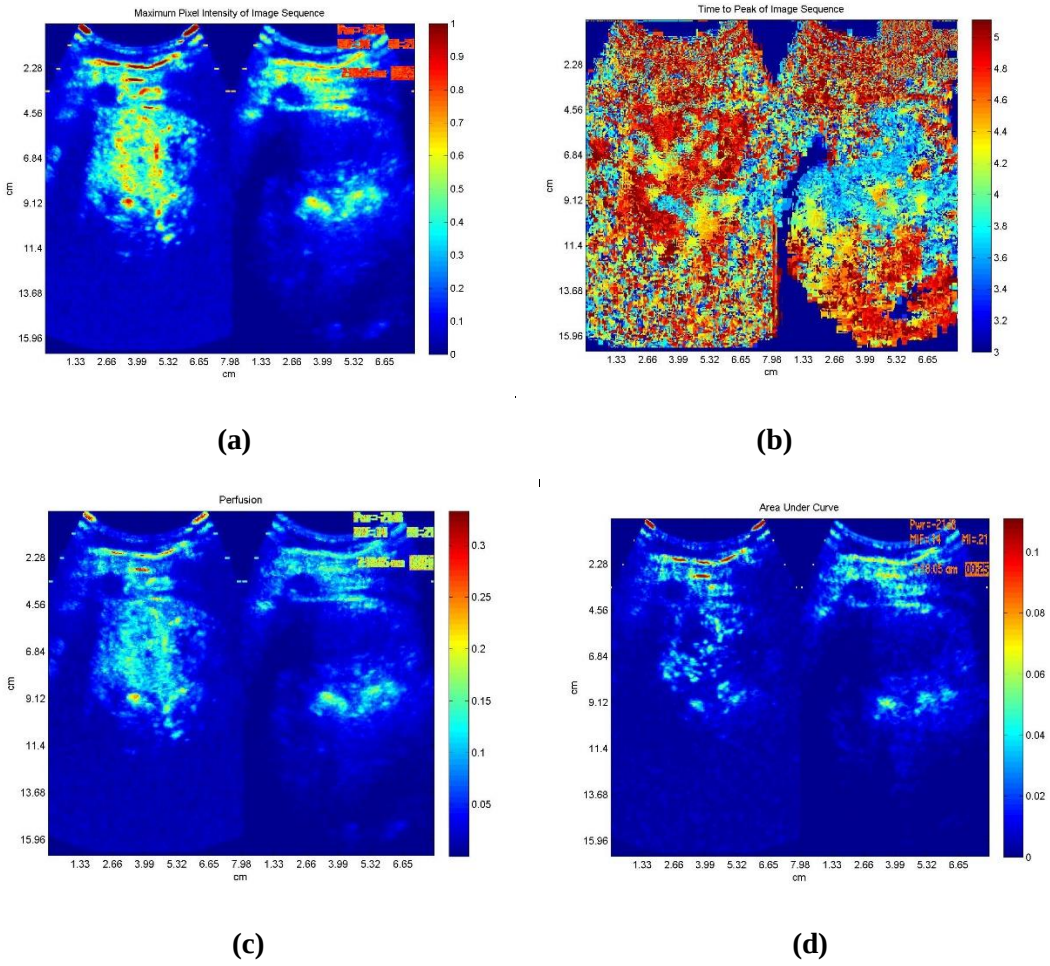

(a) **(b)**

(c) **(d)**

a) Maximum Pixel Intensity of sequence, b) Time to peak of Sequence, c) Perfusion, d) Area under Curve

APPENDIX A.9: PATIENT 11 Lesion 02

Pre-treatment

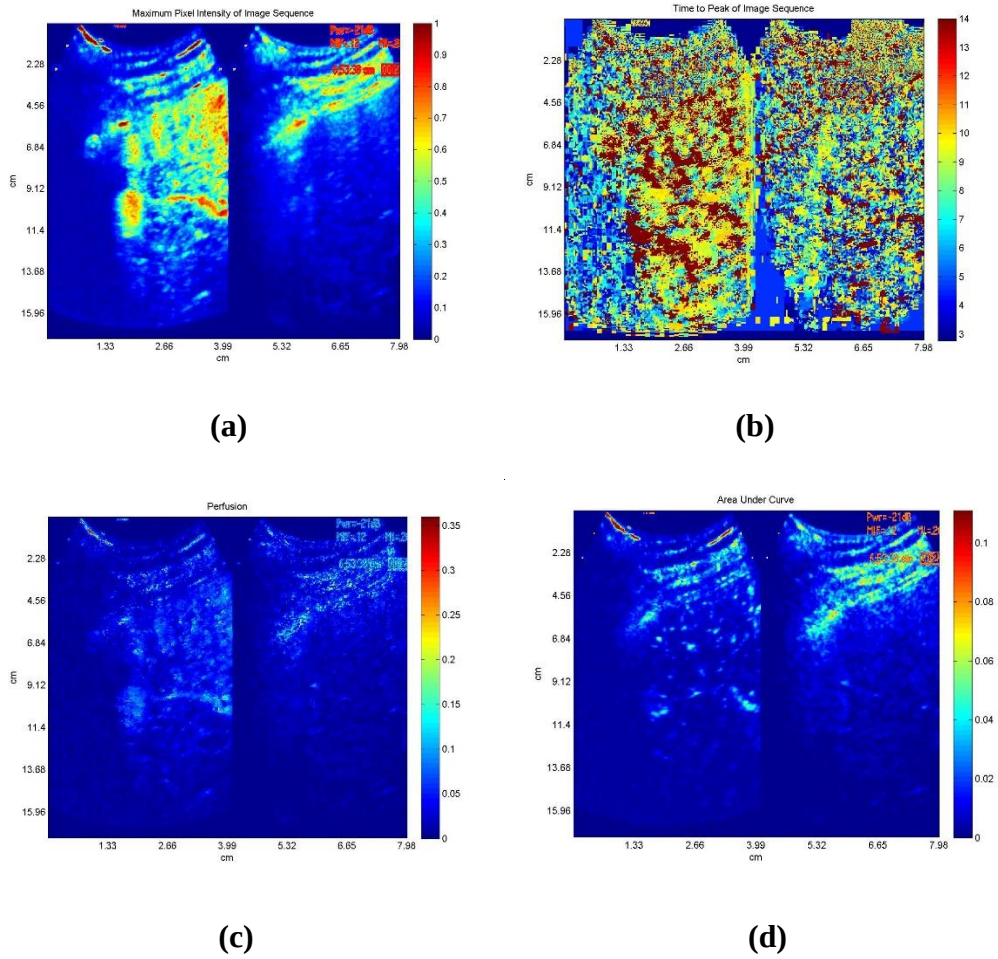

(a) **(b)**

(c) **(d)**

a) Maximum Pixel Intensity of sequence, b) Time to peak of Sequence, c) Perfusion, d) Area under Curve

2 weeks post TACE

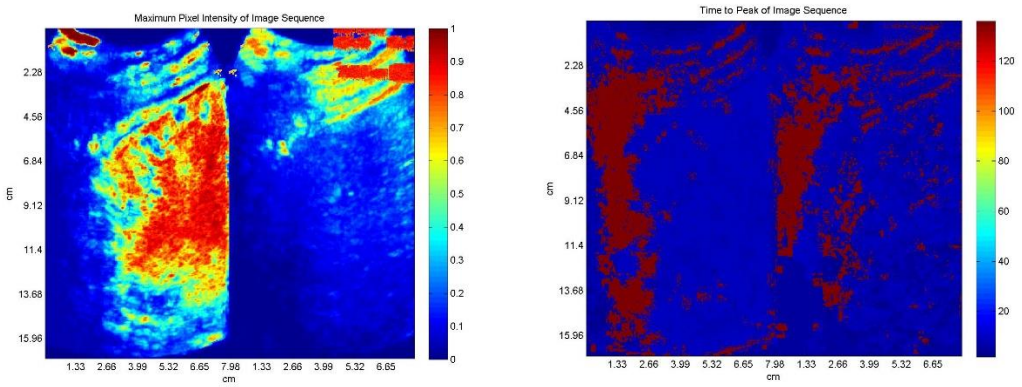

(a) **(b)**

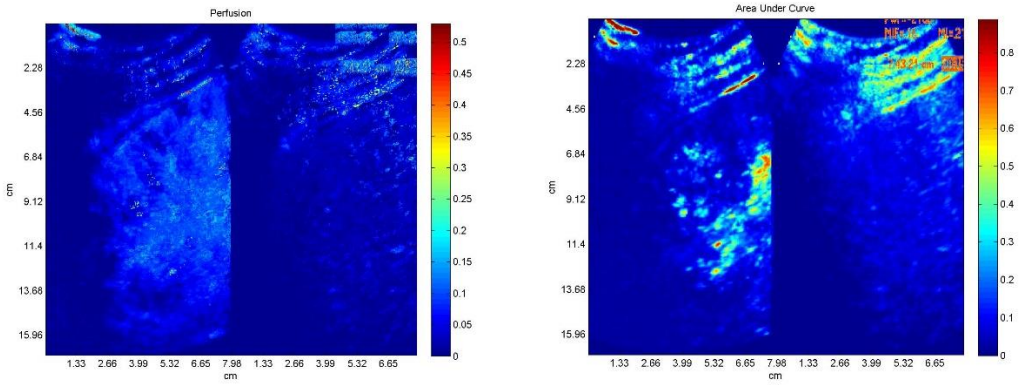

(c) **(d)**

a) Maximum Pixel Intensity of sequence, b) Time to peak of Sequence, c) Perfusion, d) Area under Curve

4 weeks post TACE

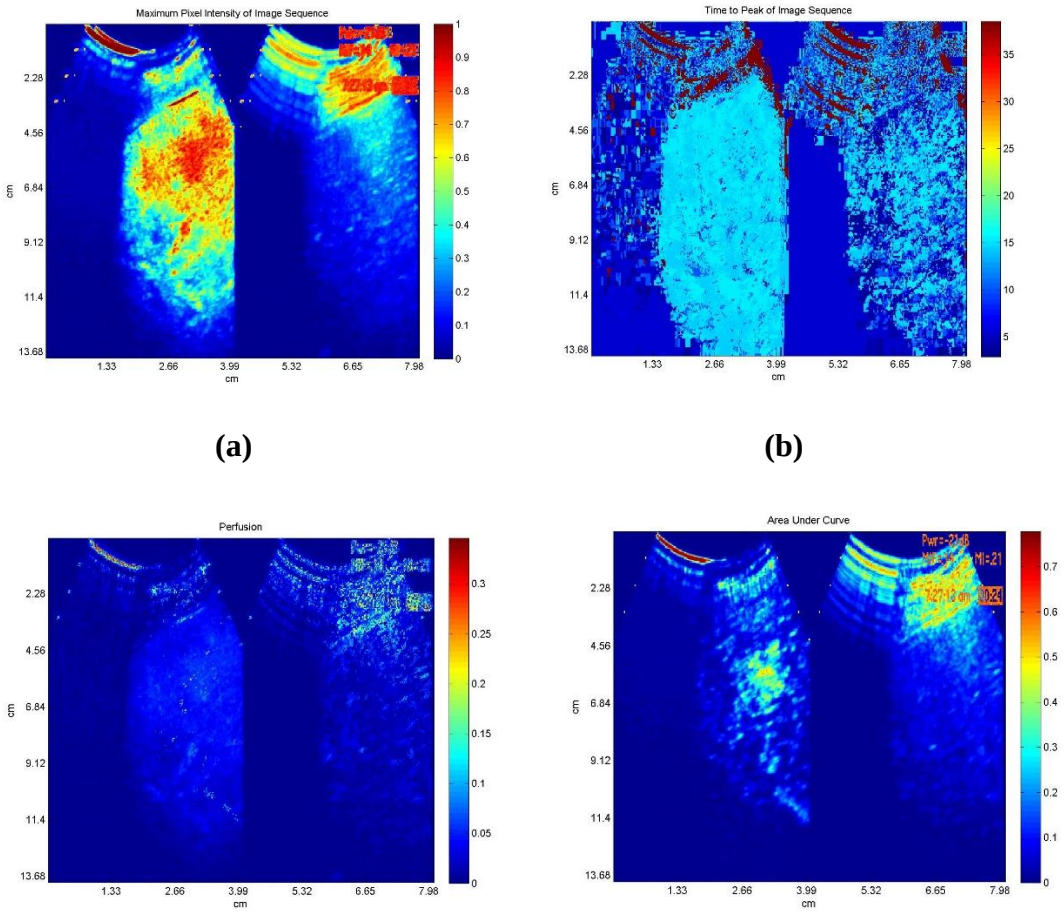

(a) **(b)**

(c) **(d)**

a) Maximum Pixel Intensity of sequence, b) Time to peak of Sequence, c) Perfusion, d) Area under Curve

APPENDIX A.10: PATIENT 14

Pre-treatment

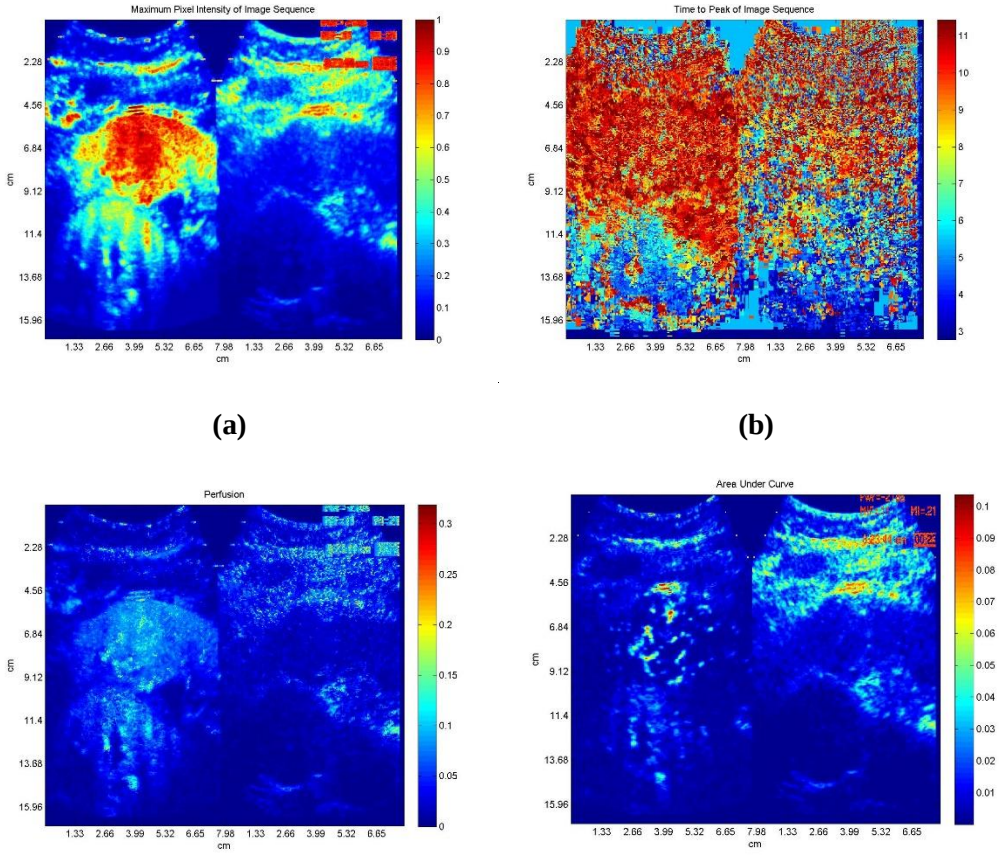

(a) **(b)**

(c) **(d)**

a) Maximum Pixel Intensity of sequence, b) Time to peak of Sequence, c) Perfusion, d) Area under Curve

2 weeks post TACE

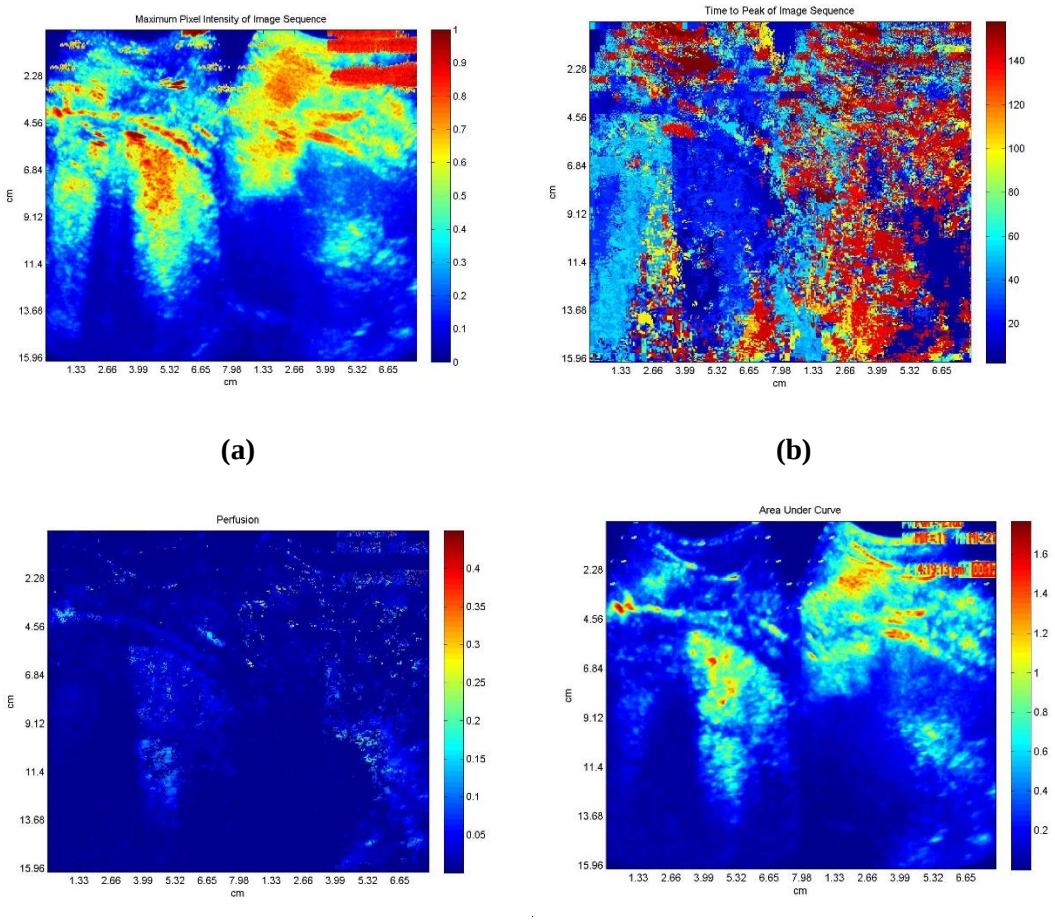

(a) **(b)**

(c) **(d)**

a) Maximum Pixel Intensity of sequence, b) Time to peak of Sequence, c) Perfusion, d) Area under Curve

4 weeks post TACE

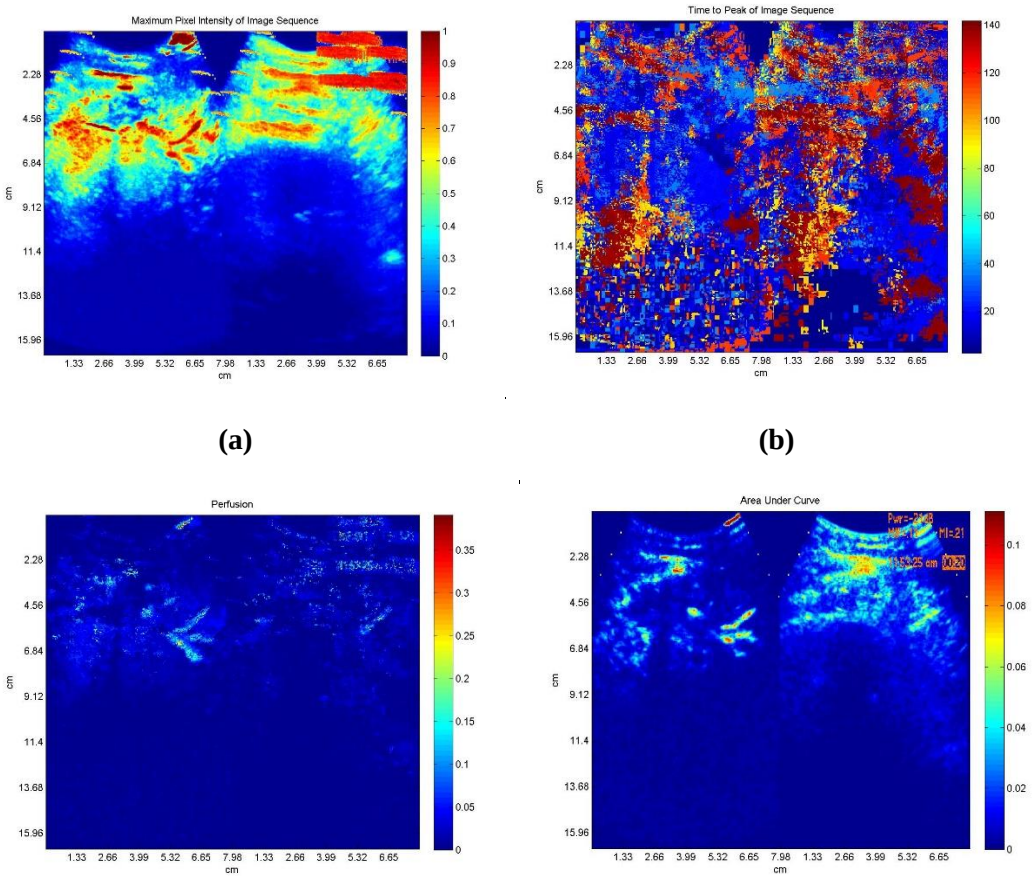

(a) **(b)**

(c) **(d)**

a) Maximum Pixel Intensity of sequence, b) Time to peak of Sequence, c) Perfusion, d) Area under Curve

APPENDIX B: Program Code

APPENDIX B.1: Motion Compensation Code

```
%This code has been developed by Dr. Jaydev K. Dave and his team at
%Ultrasound laboratory (Thomas Jefferson University)
clear all;
close all;
iptsetpref('ImshowBorder','tight');

%% Build image file list
TotalNumberofFrames=input('Enter Total Number of Frames in File List ---->');
[filename, pathname] = uigetfile('*.*','Select FIRST image file...');
cd(pathname);
filechar = double(filename);

t=1:TotalNumberofFrames;

loc1=find(filechar==48);
head=filename(1:loc1(2));

loc2=find(filechar==46);
tail=filename(loc2:end);

numimages=1;

% create file list for first 99 frames
for i=1:99
   numimages=numimages+1;
   if i-1<10
      fname=[head num2str(0) num2str(i-1) tail];
   else
      fname=[head num2str(i-1) tail];
   end
   filelist{numimages}=fname;
end

%  %add frames 100-999
head=filename(1:loc1(1));

for i=101:TotalNumberofFrames;
   numimages=numimages+1;
   if i-1<10
      fname=[head num2str(0) num2str(i-1) tail];
   else
      fname=[head num2str(i-1) tail];
   end
   filelist{numimages}=fname;
end
filelist = filelist';

%% Reading the first image!!
img11=imread(filelist{2});
```

```
%% Converting the image into suitable form
img11=im2double(rgb2gray(img11));

%% Selecting the required size of the image- Ignoring labels at the side
figure(1)
imshow(img11)
[tc,tr]=ginput(1);
[bc,br]=ginput(1);
tc=round(tc);
tr=round(tr);
br=round(br);
bc=round(bc);
img1=img11(tr:br,tc:bc);
[ori_rows,ori_cols]=size(img1);

%% For the User to select the kernel
figure(1)
subplot(2,1,1)
imshow(img1)
title('First Image in the series')
[topcolumn,toprow]=ginput(1);
[bottomcolumn,bottomrow]=ginput(1);
topcolumn=round(topcolumn);
toprow=round(toprow);
bottomrow=round(bottomrow);
bottomcolumn=round(bottomcolumn);

%% Making the kernel
kernel=img1(toprow:bottomrow,topcolumn:bottomcolumn);
figure(1)
subplot(2,1,2)
imshow(kernel)
title('kernel')
[kernelrows,kernelcolumns]=size(kernel);

%% Creating the final padded image on which the result will be pasted
finalrows=ori_rows+ori_rows;
finalcols=ori_cols+ori_cols;
final=zeros(finalrows,finalcols);
startrow=round((ori_rows)/2);
startcol=round((ori_cols)/2);
endrow=round((3*ori_rows/2));
endcol=round((3*ori_cols/2));

%% Preparing the Final image with the first image which will be used as reference
final(startrow:endrow-1,startcol:endcol-1)=img1;
figure(2)
imshow(final)

%% Calculating the number of total iterations required
numberofiterations_rows=ori_rows-kernelrows+1;
numberofiterations_cols=ori_cols-kernelcolumns+1;
number=numberofiterations_rows*numberofiterations_cols;
```

```
%% Change Made
alpha_matrix=zeros(numimages,1);

%% Reading the next images from the sequences
for k=2:numimages

   %% Reading the first image
   img22=imread(filelist{k});

   %% Converting the image into suitable form
   img22=im2double(rgb2gray(img22));

   %% Selecting the required size of the image- Ignoring labels at the side
   img2=img22(tr:br,tc:bc);

   %% Creating the array to store the result
   store=zeros(number,3);
   counter=0;

   %% SAD and storing the Result
   for i=1:numberofiterations_rows
      for j=1:numberofiterations_cols
         counter=counter+1;
         temp=abs(img2(i:i+kernelrows-1,j:j+kernelcolumns-1)-kernel);
         tempsum=sum(sum(temp));
         store(counter,:)=[i,j,tempsum];
      end
   end

   %% Finding the best match and calculating the displacement with respect
   %% to the first image
   minimumerr=min(store(:,3));
   SAD_mean=mean(store(:,3));
   MSAD=minimumerr;
   alpha_image=(SAD_mean-MSAD)/SAD_mean
   alpha_matrix(k)=alpha_image;
   if alpha_matrix(k)>=0.63
   loc=find(store(:,3)==minimumerr);
   matchrow=store(loc,1);
   matchcol=store(loc,2);
   displacement_row=toprow-matchrow;
   displacement_col=topcolumn-matchcol;

   %% Calculating the place where the next image has to be pasted with displacement
   newstartrow=startrow+displacement_row;
   newstartcol=startcol+displacement_col;
   newendrow=newstartrow+ori_rows;
   newendcol=newstartcol+ori_cols;
   for i=newstartrow:newendrow-1
      for j=newstartcol:newendcol-1
         ii= (i-displacement_row)-startrow+1;
         jj=(j-displacement_col)-startcol+1;
         if final(i,j)<img2(ii,jj)
```

```
            final(i,j)=img2(ii,jj);
        else
        end
    end
  end
  figure(3)
  imshow(final)
  text(225,100,['Image number being added : ', num2str(k)],'BackgroundColor',[.7 .9 .7])
%   if alpha_matrix(k)>=0.69
  saveas(gcf,strcat('Image_added',num2str(k),'.jpg'));
 end
 end
% end
figure(4)
imshow(final)
text(225,100,['Final Image!! Images Iterated : ', num2str(k)],'BackgroundColor',[.7 .9 .7])
finalf=final(startrow:endrow-1,startcol:endcol-1);
newnf=zeros(size(img11));
for i=1:434
  for j=1:532
    if i>=tr && i<=br && j>=tc && j<=bc
      newnf(i,j)=finalf(i-tr+1,j-tc+1);
    else
      newnf(i,j)=img11(i,j);
    end
  end
end

figure(5)
imshow(newnf)
```

APPENDIX B.2: Parametric Imaging Code

```
clear all;
close all;
FPS=input('Frames per second---->');
LeadTime=input('Enter Lead Time------->');
dT=1/FPS;

% to select folder path
[filename, pathname] = uigetfile('*.*','Select FIRST image file...');
cd(pathname);
filechar = double(filename);

%make a list of files with jpg extension and extract the frame number
from
%the file name
files=dir('*.jpg');
for i=1:numel(files)
    numberstr=regexp(files(i).name,'(\d*).jpg','tokens');
    numberstr=numberstr{1};
    number(i)=str2double(numberstr);
end
number=sort(number);%to sort the file numbers in ascending order
%to make a file list, this is the head and tail of the file name
loc1=find(filechar==48);
head1=filename(1:loc1(3));
head2=filename(1:loc1(2));
head3=filename(1:loc1(1));
loc2=find(filechar==46);
tail=filename(loc2:end);

numimages=0;

% create file list for all the frames
for i=1:max(size(number));
    numimages=numimages+1;
    if number(i)<10
        fname=[head1 num2str(number(i)) tail];

     elseif number(i)<100

        fname=[head2 num2str(number(i)) tail];
    else

        fname=[head3 num2str(number(i)) tail];
    end

    filelist{numimages}=fname;
end
%% to select the required size of the images
%reading the first image of the filelist
img1=imread(filelist{1});
%converting it to a suitable form
img1=im2double(rgb2gray(img1));
```

```
%selecting required size of the image
imshow(img1)
figure(1)
imshow(img1)
[tc,tr]=ginput(1);
[bc,br]=ginput(1);
tc=round(tc);
tr=round(tr);
br=round(br);
bc=round(bc);
imgtemp=img1(tr:br,tc:bc);
%% to read the next images in the file list and selecting the required
size
for j=1:max(size(filelist));
    j
    img22=imread(filelist{j});
    img22=im2double(rgb2gray(img22));
    img2=img22(tr:br,tc:bc);
    img(:,:,j)=img2;
end

%% Calculating the parameters
% Run through array one pixel at a time and determine at which peak
(3'rd dimension) highest intensity occurs

MatrixDem = size(img);
% Move through each row
for Row = 1:MatrixDem(1);
    % Move through each column
  for Column = 1:MatrixDem(2);
%calculate maximal intensity for pixel and determine frame number
[C,I]=max(img(Row,Column,:));
I1= number(I);%number(I) takes in the actual frame number from the
image file name
TimeToPeakFrames(Row,Column) = I1;
TimeToPeak(Row,Column) = (TimeToPeakFrames(Row,Column)+ LeadTime)/FPS;
MaxPeak(Row,Column) = C;
end
end
% calculate Perfusion rate
for Row = 1:MatrixDem(1);
  for Column = 1:MatrixDem(2);
Perfusion(Row,Column)=MaxPeak(Row,Column)/TimeToPeak(Row,Column);
  end
end

% Run though image sequence and calculate area under curve for each
pixel
for Row = 1:MatrixDem(1);
  for Column = 1:MatrixDem(2);
AreaUnderCurve(Row,Column)=sum(img(Row,Column,1:I)*dT);
  end
end

% Save data sets in folder with stored frames
save TimeToPeak
```

```
save MaxPeak
save Perfusion
save AreaUnderCurve

% Check results by examining images
figure(2)
imagesc(MaxPeak)
title('Maximum Pixel Intensity of Image Sequence')
colorbar
saveas(gcf,'max.jpg');

figure(3)
imagesc(TimeToPeak)
title('Time to Peak of Image Sequence')
colorbar
saveas(gcf,'ttp.jpg');

figure(4)
imagesc(Perfusion,[0 0.003])
title('Perfusion')
colorbar
saveas(gcf,'per.jpg');

figure(5)
imagesc(AreaUnderCurve)
title('Area Under Curve')
colorbar
saveas(gcf,'auc.jpg');

save figure2
save figure3
save figure4
save figure5
%% Evaluate all 4 parameters in a selected ROI
%Select Tumor Region of Interest
Frames=input('Frames ='); %this is to selected the frame that will be
displayed to select the ROI
image=img(:,:,Frames);
figure(6)
imshow(image);
title(['Select Tumor ROI'])
h=imfreehand
pos=getPosition(h);
BW=createMask(h);
s = regionprops(BW, 'Centroid');
center_x = s.Centroid(1) %acquire X position of the center mass
center_y = s.Centroid(2) %acquire Y position of the center mass
%use ginput to get the coordinates of the midpoint of the image
[m1 m2]=ginput(1);
%[r1 r2]=ginput(1);
[j l]=size(image);
d=abs(l-center_x);
p=abs(m1-center_x);
rowsToShift = 0;
columnsToShift = round(d+p);%round(l-(2*d));% round(d+p);
% BW2 = imtranslate(BW, [rowsToShift columnsToShift]);
```

```
BW2 = circshift(BW, [rowsToShift columnsToShift]);
figure(7)

imshow(BW2);
%Determine Size of ROI's
ROI=MaxPeak(BW2);
% ROI=MaxPeak(h)
V1Size=size(ROI);
V1=V1Size(1)*V1Size(2);
%Set data set ROI's
AreaUnderCurveROI=AreaUnderCurve(BW2);
MaxPeakROI=MaxPeak(BW2);
TimeToPeakROI=TimeToPeak(BW2);
PerfusionROI=Perfusion(BW2);

% Calculate 4 parameter values in ROI
Max=sum(sum(MaxPeakROI,1));
TTP=sum(sum(TimeToPeakROI,1));
Per=sum(sum(PerfusionROI,1));
AUC=sum(sum(AreaUnderCurveROI,1));

% Normalize values by number of ROI pixels
AUC=AUC/V1;
Max=Max/V1;
TTP=TTP/V1;
Per=Per/V1;

% Write Results
Max=[Max]
TTP=[TTP]
PER=[Per]
AUC=[AUC]
```

Appendix C: Copyright Permission

Minakshi Mohanty
Department of Biomedical Engineering
Drexel University
Philadelphia, PA 19104

25th June, 2015

Dr. Jaydev K. Dave ✓
Thomas Jefferson University
Philadelphia, PA 19107

Dear Dr. Dave,

I am requesting permission to reprint a portion of the following work:

J. Dave, Novel Automated Motion Compensation Algorithm for Producing Cumulative Maximum Intensity Images from Subharmonic Ultrasound Imaging of Breast Lesions (2008),", idea.library.drexel.edu. Drexel University, Web 2015,

- *Figure 3.3: Schematic of MIP algorithm to produce MIP image (page 24)*
- *Figure 4.17: Flowchart of the algorithm (page 62)*
- *Appendix D.1: Program code: working with no threshold (page 93-96)*

This request is for permission to include the above content as part of the following dissertation that I am preparing:

M. Mohanty, Parametric Contrast Enhanced Ultrasound Evaluation of Transarterial Chemoembolization, Master's Thesis, Drexel University, (2015)

This request is for a non-exclusive, irrevocable and royalty-free permission.

I would greatly appreciate your permission. If you agree with the terms as described above, please sign the letter where indicated below.

Sincerely,

Minakshi Mohanty

Permission is hereby granted by:

Signature: Jaydev Dave

Name & Title: JAYDEV DAVE, ASSISTANT PROFESSOR OF RADIOLOGY - THOMAS JEFFERSON UNIVERSITY

Date: JUNE 25, 2015

Appendix D: List of software used

1. **Matlab R2013a (The Mathworks Inc., Natick WA)**

   Purpose: To process ultrasound data, perform motion compensation and parametric imaging

   License: Drexel University

2. **SPSS Statistics 23 (IBM, Armonk, NY)**

   Purpose: To perform statistical analysis

   License: Drexel University

3. **Microsoft Office 2013 (Microsoft Corporation, Redmond, WA)**

   Purpose: For publishing, data handling and presentations.

   License: Drexel University

4. **Video to JPG Converter v.5.0.23 build 320 (DVDVideoSoft Ltd, New Zealand)**

   Purpose: For converting CEUS data into individual JPG frames

   License: Open Source

5. **Advanced Renamer Version 3.66 (Kim Jensen, Copenhagen, Denmark)**

   Purpose: For naming JPG files

   License: Open Source